ABSTRACT

Title of Document: NUCLEAR SPECKLE LOCALIZATION OF RNA BINDING MOTIF PROTEIN 5: AN IMMEDIATE EARLY GENE UP-REGULATED BY VASCULAR ENDOTHELIAL GROWTH FACTOR.

Janhavi Gupta, Doctor of Philosophy, 2006

Directed By: Dr. Ibrahim Ades,
Department of Cell Biology and Molecular Genetics

Angiogenesis is a fundamental process playing an important role in various pathological and physiological conditions including organ development and tumor metastasis. Blood vessels are primarily composed of endothelial cells. These cells are mostly quiescent in adults, but can be stimulated by an excess of pro-angiogenic factors. One specific pro-angiogenic factor, VEGF-A (specifically $VEGF_{165}$) plays a key role in a variety of pathological and physiological conditions. However, the molecular and cellular mechanisms by which VEGF-A regulates the complex fundamental process of blood vessel formation is unknown. This study was undertaken to identify the immediate early genes (IEGs) induced by VEGF-A, a hitherto uncharted research avenue. Differential screening of a suppression subtractive hybridization cDNA library potentially enriched in the IEGs induced by VEGF-A, led to the identification of 17 IEG transcripts. Surprisingly, this new putative VEGF-A response gene set consisted of transcripts with diverse functions,

including those of various transcription factors such as ATF3, EGR2 and IER2, growth factors, enzymes and novel genes.

RNA Binding Motif protein 5 (RBM5) was the only putative tumor suppressor gene and differential apoptotic regulator identified in this new putative VEGF-A response gene set. This dissertation further focuses on the then novel multi-modular protein RBM5, whose up-regulation by VEGF-A seemed paradoxical. Correct localization of any protein is not only essential for its function but can also provide vital clues about its potential cellular role. Although, RBM5 was previously shown to be localized in the nucleus, its subnuclear localization was not defined. Localization of RBM5 in nuclear speckles was determined using enhanced green fluorescent protein (EGFP) fusion constructs and colocalization studies. Based on these results it can be hypothesized that RBM5 may function in pre-mRNA metabolism. Additionally, site-directed mutagenesis and colocalization studies confirmed that nuclear localization of RBM5 is mediated by only the C-terminal bipartite NLS, absent in all RBM5 splice variants.

NUCLEAR SPECKLE LOCALIZATION OF RNA BINDING MOTIF PROTEIN 5: AN IMMEDIATE EARLY GENE UP-REGULATED BY VASCULAR ENDOTHELIAL GROWTH FACTOR.

By

Janhavi Gupta.

Dissertation submitted to the Faculty of the Graduate School of the
University of Maryland, College Park, in partial fulfillment
of the requirements for the degree of
Doctor of Philosophy
2006

Advisory Committee:
Dr. Ibrahim Ades, Chair
Dr. Jeffery DeStefano
Dr. William Higgins
Dr. Wenxia Song
Dr. Stephen Wolniak

DEDICATION

This dissertation is dedicated to my family.

ACKNOWLEDGEMENTS

I would like to thank Dr. Ibrahim Ades for his advice throughout my graduate career and forever challenging me to think outside the box. I would also like to thank all the members of my advisory committee: Dr. Stephen Wolniak, Dr. Wenxia Song, Dr. Jeffery DeStefano and Dr. William Higgins for their continual guidance and valuable suggestions shaping my research. I am especially grateful to Dr. Robert Brown for tremendous patience, answering all my queries and teaching me many skills that I know today.

A special thanks to Hamp Edwards who taught me the essentials of insect cell culture techniques and to Dr. Kiledjian (Rutgers University) and Dr. Cameron (Pennsylvania State University) for sharing plasmids.

I am especially grateful to my Mom, Dad, Dwijen and my extended family for their unwavering love and support. Lastly this dissertation would have been impossible without the love and understanding of my best friend and husband, Akash. Thank you for cheering me up when things seemed to go downhill and never letting me give-up.

TABLE OF CONTENTS

LIST OF TABLES

LIST OF FIGURES

LIST OF ABBREVIATIONS

HUVEC	human umbilical vein endothelial cells
ECs	endothelial cells
bFGF	basic fibroblast growth factor
EGF	epidermal growth factor
VEGF	vascular endothelial growth factor
KDR/Flk-1/VEGFR2	kinase insert domain receptor/fetal liver kinase-1/ vascular endothelial growth factor receptor 2
Flt-1/VEGFR1	*fms* related tyrosine kinase-1/vascular endothelial growth factor receptor 1
IEG	immediate early gene
MAPK	mitogen activated kinase
PKC	protein kinase C
PKB	protein kinase B (Akt)
FCS	fetal calf serum
MCS	multiple cloning site
X-gal	5-Bromo-4-chloro-3indolyl-β-D-galactoside
IPTG	isopropyl-β-D-thiogalactopyranoside
PBS	phosphate buffered saline
CIP	calf intestinal phosphatase
BSA	bovine serum albumin
MOPS	3-(*N*-morpholino) propanesulfonic acid
DEPC	diethyl pyrocarbonate

RBM5	RNA binding motif protein 5
NLS	nuclear localization signal
EGFP	enhanced green fluorescent protein
DAPI	4', 6-diamidino-2-phenylindole, dihydrochloride
EDTA	ethylenediaminetetraacetic acid
DIC	differential interference contrast
ROI	region of interest
PFU	plaque forming units
MOI	multiplicity of infection
HRP	horseradish peroxidase
SELEX	systemic evolution of ligands by exponential enrichment
SNAAP	specific nucleic acids associated with proteins
RRM	RNA recognition motif
RBP	RNA binding protein
AcNPV	*Autographa californica* nuclear polyhedrosis virus
GST	glutathione S-transferase
bp	basepair
kDa	kilo Dalton
PAGE	polyacrylamide gel electrophoresis

PART I

CHAPTER 1

ANGIOGENESIS

GENERAL INTRODUCTION

Angiogenesis is defined as the process by which capillaries sprout from pre-existing vasculature or blood vessels (Ferrara,1999). It is a fundamental process occurring in various physiological conditions such as wound healing, placental development, embryonic development and organ formation. It also plays a key role in a number of pathological conditions including diabetic retinopathy, psoriasis, age-related macular degeneration and rheumatoid arthritis (Carmeliet and Collen. 1999; Dvorak et al., 1999; Ferrara,1999). Moreover, the growth of tumors and development of metastases depends on the *de novo* formation of blood vessels, that is neovascularization or angiogenesis (Carmeliet and Jain, 2000). Blood vessel walls (vascular wall) are chiefly composed of endothelial cells (tunica intima) and mural smooth muscle cells, also known as pericytes (tunica media). The endothelial cells (ECs) line the entire interior surface of the vascular wall forming a continuous monolayer of cells (figure 1). Both arteries and veins have an additional outermost layer composed of collagen fibers and fibroblast cells (tunica adventitia) imparting rigidity to the blood vessels. Capillaries are solely comprised of endothelial cells

supported by a basement membrane and lack the two outermost layers tunica media and tunica adventitia present in larger blood vessels.

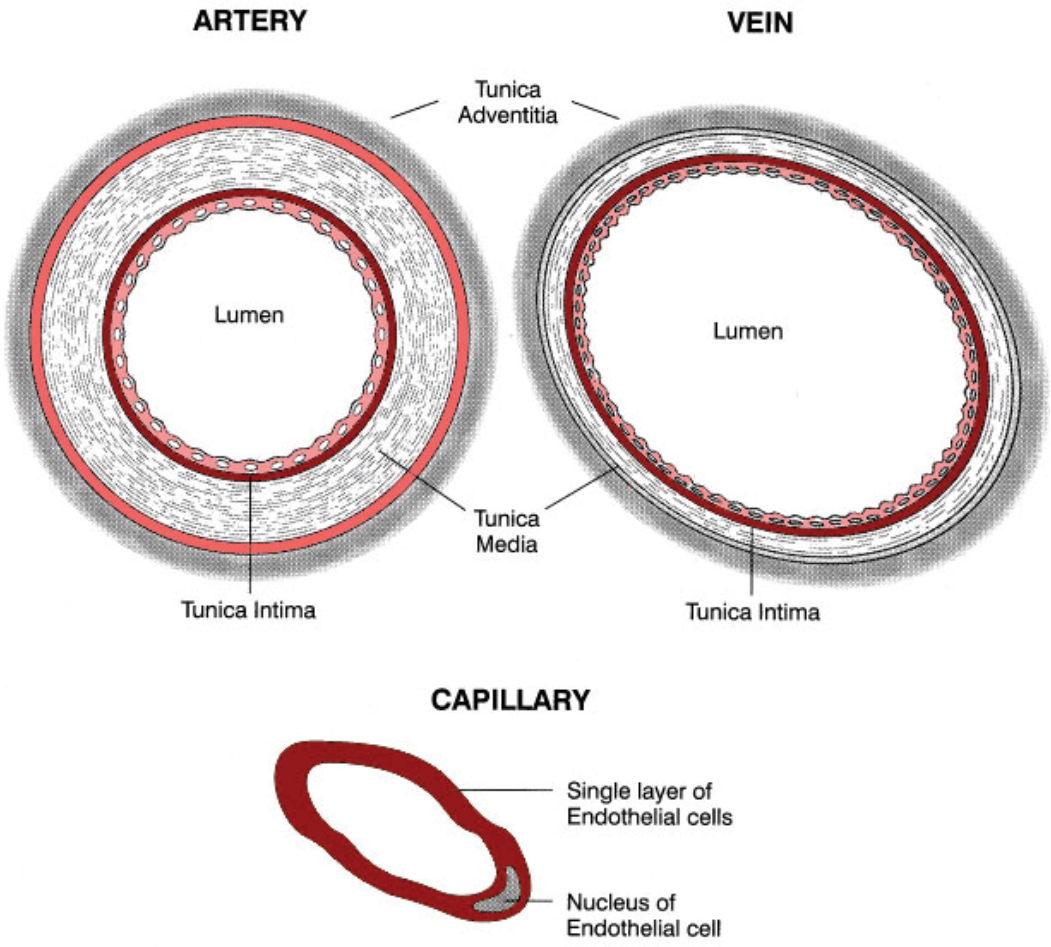

Figure 1: Structure of blood vessels. Endothelial cells form the innermost layer (tunica intima) of blood vessels followed by a layer of smooth muscle cells (tunica media) and collagen fibers (tunica adventitia). The two outermost layers confer rigidity to the vascular wall and are absent in capillaries. Capillaries are composed of a single layer of endothelial cells supported by a basement membrane (not shown). This image was obtained from the website: www.nurse-prescriber.co.uk/.../pp109.jpg

Endothelial cells are normally quiescent in the adults, but are metabolically active and have a remarkable ability to proliferate and migrate to form new vessels (Ferrara, 1999; Yancopoulos et al., 2000). In addition to angiogenesis, vascular endothelium plays a key role in various physiological functions such as inflammation, coagulation, control of hemostasis and thrombosis and also functions in the regulation of vascular permeability, macromolecular transport and vascular wall structure (Dvorak et al., 1999; Sato, 2001a). Vascular endothelium also contributes to vascular tone by releasing potent vasodilators and vasoconstrictors. The continuous release of NO (nitric oxide) by the vascular endothelium relaxes the smooth muscle cells and ensures vessel patency (Dvorak et al., 1999; Sato, 2001a).

Angiogenesis is a complex phenomenon that involves multiple steps of migration, proliferation, differentiation, and morphogenesis of endothelial cells. The six sequential steps thought to occur in the process of angiogenesis are: 1) vascular destabilization by the detachment of pericytes 2) degradation of the extracellular matrix by endothelial proteases such as MMPs (matrix metalloproteinases) and/or urokinase 3) endothelial cell migration 4) proliferation of endothelial cells 5) formation of tube like structure by endothelial cells and finally 6) vascular stabilization by reattachment of the pericytes (Sato, 2001a).

Since the vascular endothelial cells line the inner surface of the blood vessel, they have long been considered to be the key component of angiogenesis (Veikkola et al., 2000). A number of molecules are expressed in ECs following stimulation by angiogenic growth factors, leading to the final outcome of angiogenesis. Thus, the transcriptional regulation of gene expression in ECs has become an important issue

for understanding the key molecular mechanisms involved in the regulation of angiogenesis.

The process of angiogenesis is tightly regulated by a balance between pro-angiogenic and anti-angiogenic factors (table 1). Nearly twenty different angiogenic factors have been recognized so far, a few of which are: angiopoietin-1, bFGF (basic fibroblast growth factor), ephrins and VEGF (vascular endothelial growth factor) (Gale and Yancopoulos, 1999).

Angiogenic Growth Factors	**Anti-Angiogenic Growth Factors**
Angiogenin	Angiostatin (plasminogen fragment)
Angiopoietin-1	Antiangiogenic antithrombin III (aaATIII)
Del-1	Canstatin
Fibroblast growth factors (FGF): acidic/basic	Cartilage-derived inhibitor (CDI)
Follistatin	Endostatin (collagen XVIII fragment)
Granulocyte colony-stimulating factor (G-CSF)	Fibronectin fragment
Hepatocyte growth factor (HGF)	Gro-beta
Interleukin-8 (IL-8)	Heparinases
Leptin	Heparin hexasaccharide fragment
Midkine	Human chorionic gonadotropin (hCG)
Placental growth factor	Interferon alpha/beta/gamma
Platelet-derived endothelial cell growth factor (PD-ECGF)	Interferon inducible protein (IP-10)
Platelet-derived growth factor-BB (PDGF-BB)	Interleukin-12 (IL-12)
Pleiotrophin (PTN)	
Proliferin	Kringle 5 (plasminogen fragment)
Transforming growth factor-alpha and beta (TGF-α/β)	Metalloproteinase inhibitors (TIMPs)
Tumor necrosis factor-alpha (TNF-alpha)	Pigment epithelial-derived factor (PEDF)
Vascular endothelial growth factor (VEGF)	Platelet factor-4 (PF4)
Wnt/Norrin	Thrombospondin-1
	Tumstatin

Table 1: List of some of the pro-angiogenic and naturally occurring anti-angiogenic discovered so far. This table was adapted from the angiogenesis foundation website: www.angio.org/understanding/understanding.html and other references (Ribatti et al., 2002; Ferrara, 2005; Masckauchán and Kitajewski, 2006).

VASCULOGENESIS AND ANGIOGENESIS

Among all these diverse physiological functions performed by the vascular endothelium, angiogenesis is an important process, it being crucial both in normal development and reproduction. In the vertebrate embryo, the vascular system is the first functional organ that develops. Blood vessels in the entire body are formed by two distinct but related processes, vasculogenesis and angiogenesis (Carmeliet and Collen. 1999; Gale and Yancopoulos, 1999). Vasculogenesis is the first step in the process of vascular development followed by angiogenesis. In vasculogenesis the extraembryonic mesodermal cells, also known as hemangioblasts, aggregate and form islands in the yolk sac, where they subsequently differentiate to form an external layer of endothelial cells (ECs) and an inner core of blood cells. The outer ECs form the primary vascular plexus. Similarly, the intraembryonic mesodermal hemangioblasts and/or angioblasts in the proximal lateral mesoderm differentiate into ECs to form the dorsal aorta. Subsequently, in the process of angiogenesis, neo-vessels are generated from the primary vascular plexus and become distributed throughout the entire body to form a complex network of blood vessels (figure 2). The final stage of the vascular development involves the differentiation of mesenchymal cells into pericytes which surround the blood vessels making them mature and stable (Carmeliet and Collen. 1999; Saaristo et al., 2000; Yancopoulos et al., 2000; Sato, 2001b).

In comparison to the embryo, blood vessels in adults are already stabilized. Sprouting of any new blood vessels (angiogenesis) is stabilized by the surrounding pericytes (arteriogenesis). Arterial networks are connected by extensive re-modeling

of existing vessels in a phenomenon known as collateral growth (Carmeliet, 2004). In adults, physiological angiogenesis occurs during wound healing and in the female reproductive cycle (Ferrara, 1999; Carmeliet and Jain, 2000). Pathological angiogenesis can occur either due to enhanced neovascularization, characteristic of rheumatoid arthritis, psoriasis, diabetic retinopathy, tumor development and metastases, or due to insufficient vascular proliferation common in myocardial and limb ischemia (Carmeliet and Jain, 2000).

REGULATORS OF ANGIOGENESIS

Three different receptor tyrosine kinase systems specific for the vascular endothelium, the ephrins, the angiopoietin-Tie system and the VEGF/VEGFR system have been implicated so far in angiogenesis. All of these systems play a varied role in the development of vascular system (Davis and Yancopoulos, 1999; Gale and Yancopoulos, 1999; Carmeliet and Jain, 2000; Dodelet and Pasquale, 2000). VEGF not only acts as a specific mitogen of the vascular endothelial cells, but also is the most potent inducer of vascular permeability known so far. The VEGF/VEGFR system also seems to be critical for the earliest stages of vasculogenesis and continues to play a vital role during the subsequent angiogenesis. The angiopoietin-Tie system and the ephrin system act in the later stages of angiogenesis but unlike VEGF, they do not promote mitogenic response in ECs (Gale and Yancopoulos, 1999). Differentiation of blood vessels into either arteries or veins is governed by the ephrin

system (Saaristo et al., 2000). The angiopoietin-Tie and the ephrin receptor tyrosine kinase systems are discussed in brief below followed by an in depth review of the VEGF/VEGFR system - the primary focus of this dissertation.

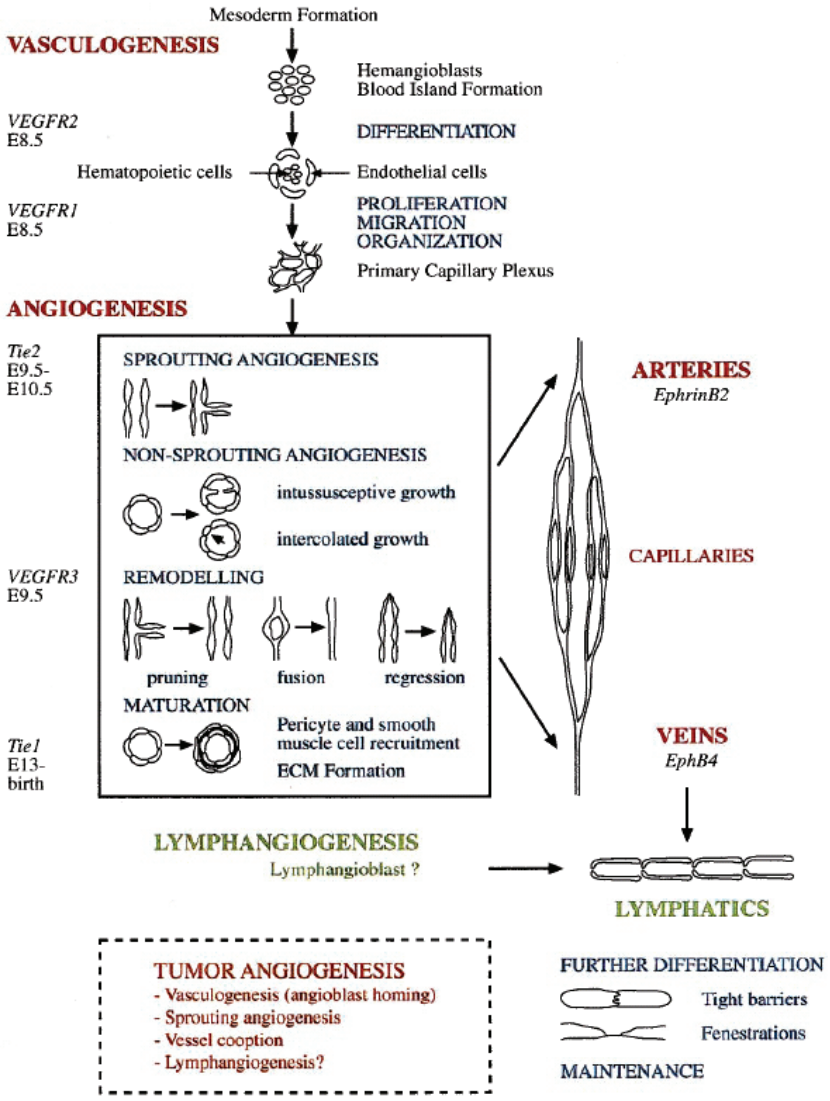

Figure 2: Steps involved in the formation of blood vessel during embryogenesis. The three important steps are thought to be vasculogenesis, angiogenesis and vascular remodeling. Also represented in this diagram are the various receptor tyrosine kinase systems involved – Tie/angiopoietins, Eph/ephrins and VEGFR/VEGF. Lethality caused due to absence of individual functional receptor tyrosine kinase system is represented as respective embryonic days. This figure was adapted from Saaristo et al., 2000.

THE ANGIOPOIETIN-TIE SYSTEM

Angiopoietins were the second family of growth factors discovered after VEGF which, similar to VEGF, displayed a very high specificity for the vascular endothelium. The specificity of the angiopoietins is due to the restricted distribution of their tyrosine kinase receptors, Tie1 and Tie2 on the vascular endothelial cells. Both Tie1/2 receptors display an identical domain structure consisting of a cytosolic split tyrosine kinase domain and extracellular fibronectin III, EGF-like (epidermal growth factor like) and immunoglobulin domains (figure 3). There are four members in the angiopoietin family, all of which bind to the Tie2 receptor and have a similar architecture consisting of coiled-coil fibrinogen domains (Davis and Yancopoulos, 1999; Koh et al., 2002). The angiopoietins were the prototype of a vertebrate growth factor family consisting of both receptor activators and blockers (figure 3) (Gale and Yancopoulos, 1999). In this system, Angiopoietin-1 (Ang-1, incorporated in the ECM) and Angiopoietin-2 (Ang-2, secreted) are the best characterized examples of an activator/agonist and an inhibitor/antagonist, respectively (Davis and Yancopoulos, 1999; Partanen and Dumont, 1999; Eklund and Olsen, 2006).

In vitro analysis has revealed that Ang-1 does not elicit any mitogenic response or induce any tubule formation in cultured endothelial cells similar to VEGF-A (the founding member of the VEGF growth factor family), but does promote endothelial cell sprouting and maintains structural integrity of blood vessels (Reiss et al., 2005). Ang-1 seems to act in a coordinated and complementary fashion along with VEGF in the development of vasculature (Partanen and Dumont, 1999).

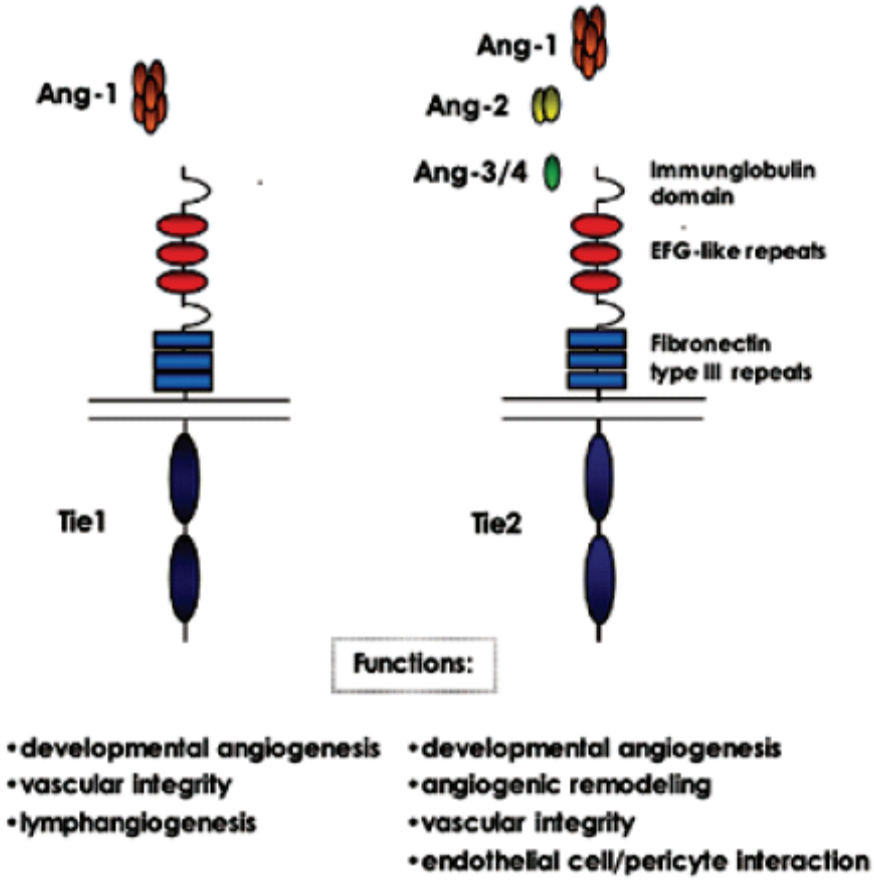

Figure 3: Differential functions and binding properties of the two angiopoietin receptors Tie1 and Tie2 are illustrated. The domain structure of the two receptors is identical and contains extracellular immunoglobulin domain, EGF-like repeats and fibronectin type III repeats along with a split cytosolic tyrosine kinase domain. Unlike Ang-2, Ang-1 can induce receptor phosphorylation leading to initiation of signaling cascades. Function of Ang-3 and Ang-4 are not yet well defined. This picture was adapted from Reiss et al., 2005.

In vivo analysis indicated that mouse embryos lacking either Ang-1 or Tie2 have normal early vascular development resulting in the formation of primitive vasculature. However, further remodeling and stabilization of the vasculature in Ang-1 or Tie2 deficient mouse embryos is severely perturbed (table 2). This is thought to result from the disturbed interaction between the ECs and the smooth muscle cells underlying them (Davis and Yancopoulos, 1999; Gale and Yancopoulos, 1999).

Shortly after the cloning and characterization of Ang-1, Maisonpierre et al. in 1997 discovered Ang-2. Ang-2 was found to bind to the Tie2 receptor like Ang-1, but could not activate it similar to Ang-1. Transgenic overexpression of Ang-2 during embryogenesis leads to a lethal phenotype similar to that seen in embryos lacking either Ang-1/Tie2 (Gale and Yancopoulos, 1999). Thus, Ang-2 was the first known naturally occurring antagonist of a receptor tyrosine kinase. Unlike Ang-1, which is constitutively expressed in the adult, Ang-2 is highly expressed only at sites of vascular remodeling allowing the vessels to revert to a more plastic and an unstable state (Davis and Yancopoulos, 1999; Gale and Yancopoulos, 1999; Partanen and Dumont, 1999). Recent studies present a more complicated context dependent action of Ang-2. It is now known that Ang-2 can either result in growth or regression depending on the presence or absence of VEGF in the microenvironment, respectively (Reiss et al., 2005). Functions of both Ang-3 and Ang-4 ligands are not yet clearly defined. However, preliminary studies suggest that Ang-3 and Ang-4 might have antagonistic and agonist functions, respectively. Although a clear role of Tie1 is still unclear, recent studies implicate Tie1/Ang-1 in lymphangiogenesis and

maintenance of endothelial cells in quiescent stage (Reiss et al., 2005; Eklund and Olsen, 2006).

Gene knockout	Time of death	Stage of vessel development	Causes of lethality
VEGF-A (+/-)	E11.5	vasculogenesis/ (angiogenesis)	Reduced red blood cells; defective heart and aorta formation; defective vessel connectivity; defective sprouting
VEGF-A (-/-)	E10.5	vasculogenesis	Absent dorsal aorta; defective endothelial cell development
VEGFR1	E8.5-E9.5	vasculogenesis	Failure of endothelial cell formation
VEGFR2	E8.5-E9.5	vasculogenesis	Excess endothelial cells form abnormal vessel structures entering vessel lumens
VEGFR3	E10.5-E12	vasculogenesis	Defective vessel remodeling and organization; irregular large vessels with defective lumens
Ang-1	E10.5	angiogenesis	Defective vessel remodeling and organization; and sprouting; heart trabeculation defects
Ang-2	E12.5-P1	maturity	Poor vessel integrity, edema, and hemorrhage
Tie1	E13.5-P1	maturity	Poor vessel integrity, edema, and hemorrhage
Tie2	E10.5	angiogenesis	Defective vessel remodeling organization, and sprouting; heart trabeculation defects
Ephrin-B2/EphB4	E10.5	vasculogenesis/ angiogenesis	Some defective vessel primordial; defective vessel remodeling, organization, and sprouting; heart trabeculation defects
EphB2/EphB3	E10.5 (~30%)	vasculogenesis/ angiogenesis	Some defective vessel primordial; defective vessel remodeling, organization, and sprouting; heart trabeculation defects
EphA2	Viable	-	-

Table 2: Gene knockout studies in mice from the VEGFR/VEGF, Tie2/Ang-1, and Eph/ephrins families exhibiting a variety of embryonic defects in vascular development. Knockouts of VEGF and its receptors yielded defects in the early process of vasculogenesis and hence the mutants tend to die at early stages of development. In contrast, to these results the Tie2 and Ang-1 knockout embryos die at later stages with normal vasculogenesis but abnormal angiogenesis. This table was obtained from Gale and Yancopoulos, 1999.

THE EPHRIN SYSTEM

The ephrin receptors (Erythropoietin-producing human hepatocellular carcinoma) and their ligands, the ephrins (Eph family receptor interacting proteins), are the largest subfamily of receptor tyrosine kinases and consist of 16 distinct members (Gale and Yancopoulos, 1999; Heroult et al., 2006). Ephrins were initially identified as neuronal guidance molecules but have since been implicated in arterio-venous differentiation and tumorigenesis (Heroult et al., 2006). Unlike other receptor tyrosine kinase ligands, the ephrins do not function as typical soluble ligands, but have to be membrane bound to activate their receptors. Multimerization of the ligands by membrane attachment seems to be necessary to activate the receptors on adjacent cells, whereas the monomeric soluble forms act like antagonists. All known ephrins are tethered to the cells in which they are expressed (Dodelet and Pasquale, 2000; Cheng et al., 2002). The ephrin receptors (Eph) are divided into two families A and B representing the nature of GPI-anchored (glycosylphosphatidyl inositol) peripheral membrane or transmembrane ligands, respectively (figure 4A). Anomalous to this generalization is EphA4 receptor which can bind to ligands from both families (figure 4B). There are ten members of EphA family of receptors binding to six ephrin-A ligands compared to six EphB receptors binding to three ephrin-B ligands (Brantley-Sieders et al., 2004; Heroult et al., 2006). EphA10 a novel member of ephrin receptors was recently described by Aasheim et al. in 2005.

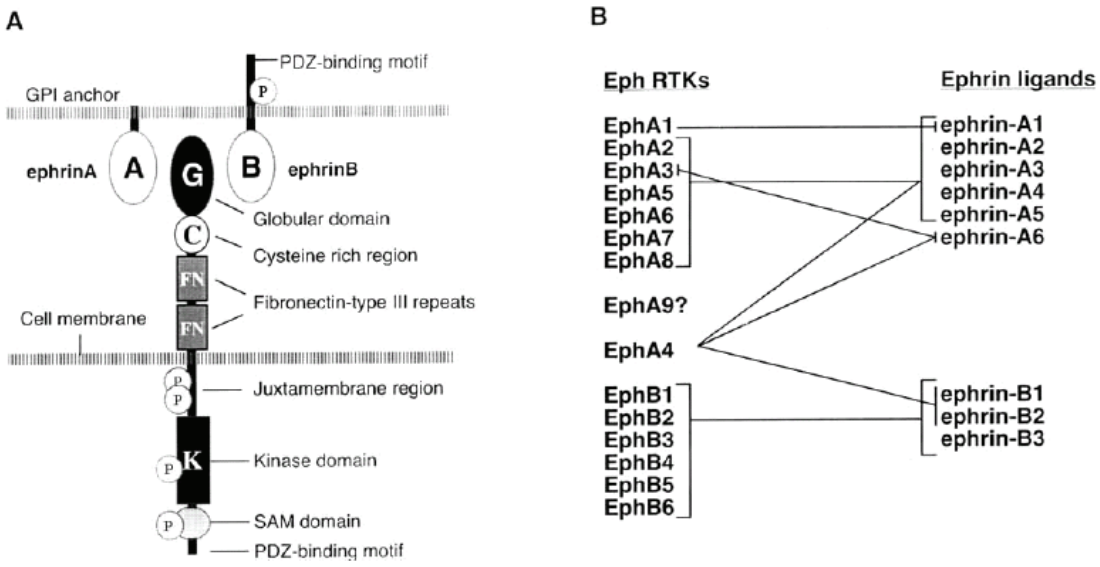

Figure 4: The structure of ephrin ligands and receptors (A). Glycosylated ephrin receptors are single transmembrane spanning domain proteins with an immunoglobulin-like domain on the extracellular side interacting with the respective ephrin ligands. The intracellular region of the Eph receptors contains a kinase domain along with SAM and PDZ domains. Eph receptors are classified into two families A and B depending on the GPI-anchor or transmembrane nature of the ephrin ligands (B). In addition to the nine Eph receptors, a new member EphA10 has been recently reported. This figure was adapted from Brantley-Sieders et al., 2004.

The Eph receptors are glycosylated and contain multiple domains (figure 4A). The extra-cellular immunoglobulin-like repeats interact with the ephrin ligands resulting in signaling through the intracellular domains. Phosphorylation of multiple tyrosine residues present in the juxtamembrane region, kinase domain and SAM (sterile-α-motif) domain can initiate 'forward' signaling cascades by binding of SH2/SH3 (**S**rc-**H**omology-**2/3**) domain containing proteins. The PDZ domain (**P**SD-95 post synaptic density protein, **D**iscs large, **Z**ona occludens tight junction protein) can bind to other PDZ domain containing proteins resulting in a scaffold for further assembly of multiple-protein signaling complexes (Brantley-Sieders et al., 2004; Vearing and Lackmann, 2005; Heroult et al., 2006). Conversely, interaction between Eph receptors and ephrin ligands leads to 'reverse' signaling due to oligomerisation of ephrin ligands (Lu et al., 2001; Vearing and Lackmann, 2005).

As mentioned before, action of the Eph family members has been implicated in important processes such as neural guidance. Gene knockout studies have suggested that the ephrins play a vital role in vascular development too (Gale and Yancopoulos, 1999; Dodelet and Pasquale, 2000; Heroult et al., 2006). Ephrins cannot induce potent mitogenic responses from endothelial cells, but do induce sprouting *in vivo*, similar to that observed using either VEGF or angiopoietin. Also, since the ephrins cannot activate their receptors unless they are membrane-bound, the ephrin/Eph interactions are restricted to the sites of direct cell-cell contact (Cheng et al., 2002).

Venous endothelium expresses both EphB3 and EphB4 receptors in addition to the ephrin-B ligand, whereas the arterial endothelium expresses both ephrin-B1 and

ephrin-B2 besides the expression of the EphB3 receptor at few sites (Adams and Klein, 2000; Cheng et al., 2002). Mouse embryos lacking either ephrin-B2 or its receptor EphB4 showed severe defects in the vascular remodeling both in arterial and venous domains (table 2) (Gale and Yancopoulos, 1999; Heroult et al., 2006). It is hypothesized that these defects arise from the bi-directional signaling mediated by the reciprocal expression of ephrin-B2 and EphB4 occurring between arterial and venous vascular beds during embryonic angiogenesis (Dodelet and Pasquale, 2000; Cheng et al., 2002). Thus, the differential expression of ephrin-B2/EphB4, critical for normal development of vasculature seems to be partially genetically programmed in arterial and venous endothelium. Sprouting, another aspect of angiogenesis responsible for in growth of vessels in previously avascular areas of embryos does not occur in ephrin-B2 knockout animals (table 2). Although a clear model of the function of ephrins in vascular development and angiogenesis has not yet emerged, it is hypothesized that antagonistic functions of EphB4 and ephrin-B2 mediate the arterio-venous differentiation (Dodelet and Pasquale, 2000; Cheng et al., 2002; Heroult et al., 2006).

THE VEGF-VEGFR SYSTEM

VEGF is a potent inducer of vasculogenesis and angiogenesis, but it is different from other endothelial growth factors in its ability to selectively stimulate the endothelial cells (ED_{50} 2-10 pM for micro- and macrovascular endothelial cells) derived from arteries, veins and lymphatics (Ferrara and Davis-Smyth, 1997). Connolly et al. first

discovered VEGF independently as vascular permeability growth factor in 1989. Molecular cloning of the genes encoding both these proteins revealed that these two proteins were the same, encoded by a single gene located on chromosome 6p21.3. VEGF belongs to the VEGF-PDGF (platelet derived growth factor) supergene family (Yancopoulos et al., 2000). The proteins in this family (cysteine knot growth factor family) have precisely spaced 8 cysteine residues, conserved in the 100 amino acid VEGF homology domain, and all these products function as antiparallel disulfide linked homodimers (Karkkainen and Petrova, 2000; Veikkola et al., 2000).

In humans, VEGF or VEGF-A (was discovered first) has nine isoforms, which are 121, 145, 148, 162, 165b, 165, 183, 189 and 206 amino acid proteins based on alternative splicing of the VEGF gene that is organized in eight exons (figure 5). Of these nine isoforms, $VEGF_{121}$, $VEGF_{165}$ and $VEGF_{189}$ are preferentially made in various VEGF-producing cells, including endothelial cells. However, the mechanism governing the levels of various VEGF isoforms produced is unknown (Takahashi and Shibuya, 2005). $VEGF_{165}$ is the major form and functions as a homodimeric glycoprotein of 46 kDa (Ferrara and Davis-Smyth, 1997). In contrast to $VEGF_{165}$, $VEGF_{165}$b is an endogenously produced inhibitor, which binds to VEGFR2 with an equal affinity but cannot activate it (figure 5) (Takahashi and Shibuya, 2005). $VEGF_{121}$ which lacks exons 6 and 7, is a weakly acidic polypeptide and does not bind to heparan sulfate proteoglycans unlike $VEGF_{165}$ (Ferrara and Davis-Smyth, 1997).

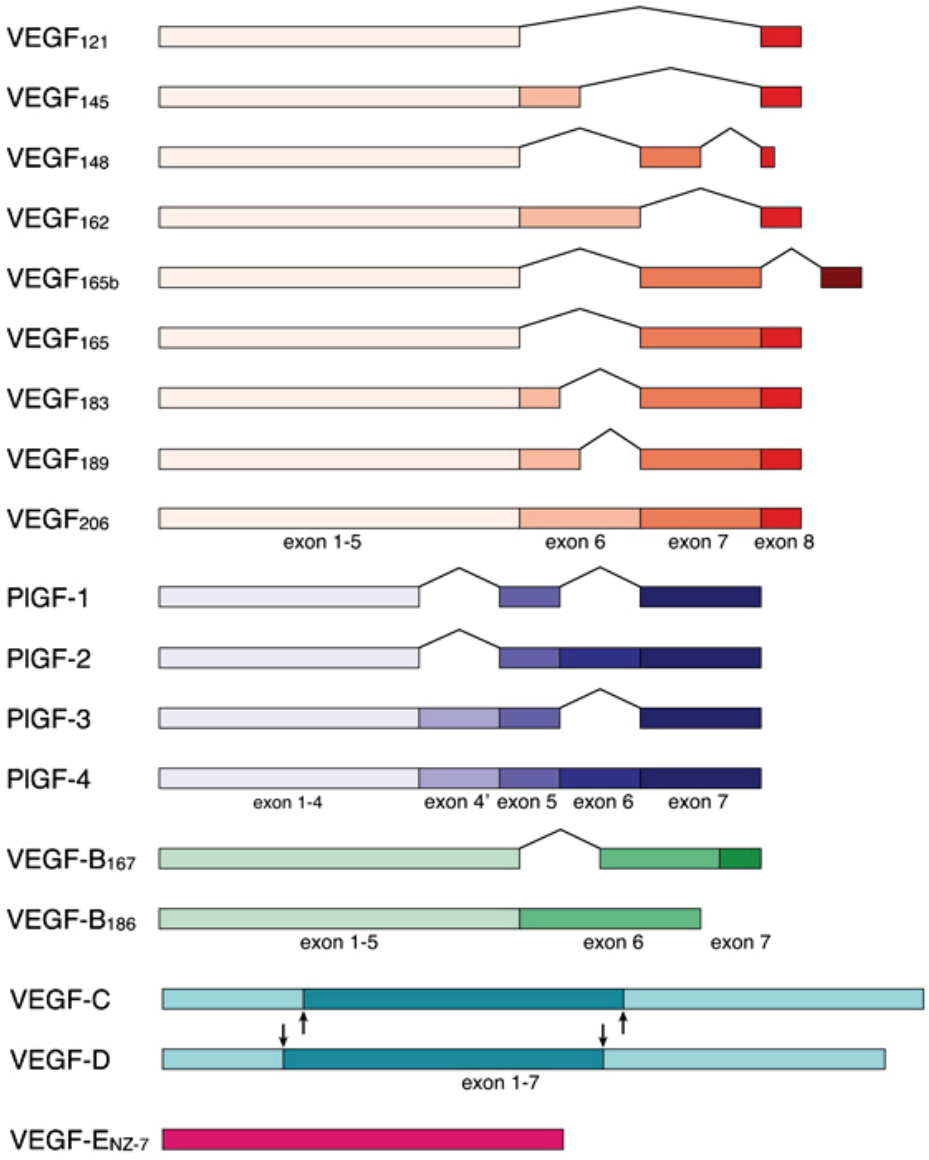

Figure 5: Comparison of structures of VEGF-A subfamily and other VEGF homologues. Sites of proteolytic cleavage in VEGF-C and VEGF-D are denoted by arrows. VEGF-E_{NZ-7} is a viral homologue encoded in the genome of Orf virus and binds with high affinity to VEGFR2/KDR. Regions colored with matching colors are identical as represented in the figure. This figure was adapted from Takahashi and Shibuya, 2005.

Poltorak et al. in 1997 demonstrated that another isoform of VEGF, $VEGF_{145}$, that induces angiogenesis in mouse skin, is secreted as an approximately 41 kDa homodimer. $VEGF_{145}$ also inhibits binding by $VEGF_{165}$ to the KDR/Flk-1 receptor in cultured endothelial cells (Poltorak et al., 1997). In contrast, $VEGF_{189}$ and $VEGF_{206}$ are much more basic (due to exon 6 sequence) and therefore have a greater binding affinity to heparan sulfate proteoglycans than VEGF-A ($VEGF_{165}$) itself (figure 5) (Ferrara and Davis-Smyth, 1997; Ferrara, 1999). Similar to $VEGF_{189}$, but unlike $VEGF_{165}$, $VEGF_{145}$ binds efficiently to the extracellular matrix (ECM) by a mechanism that is not dependent on ECM-associated heparan sulfates (Eriksson and Alitalo, 1999; Neufeld et al., 1999).

Regulation of VEGF gene expression

The spatial and temporal control of the concentration of VEGF is of extreme importance since it is potent activator of the vascular endothelium. Disruption of both VEGF alleles in mice leads to a complete absence of vasculature (table 2). Disruption of only one allele in mice leads to embryonic lethality due to severe abnormalities in the development of vasculature (table 2) (Gale and Yancopoulos, 1999 Neufeld et al., 1999, Yancopoulos et al., 2000). Some of the factors that up-regulate VEGF gene expression are low pO_2, various cytokines such as EGF (epidermal growth factor), TGF-ß (transforming growth factor-beta) and KGF (keratinocyte growth factor) (Ferrara, 2005). Various cell transforming events such as mutation of p53 and VHL tumor suppressor genes and oncogenic mutations such

as in ras and bcl-2 also result in the induction of VEGF gene expression (Ferrara and Davis-Smyth, 1997; Ferrara, 1999; Jośko and Mazurek, 2004).

VEGF homologues

At least five different homologues of VEGF, PlGF (placental growth factor), VEGF-B, VEGF-C, VEGF-D and VEGF-E have been discovered to date (figure 5) (Olofsson et al., 1996; Carmeliet and Collen, 1999; Eriksson and Alitalo, 1999; Clauss, 2000). Recent gene knockout studies in mice have indicated that the absence of PlGF causes deficiencies in adult vascular remodeling (Takahashi and Shibuya, 2005). Whereas, mice lacking VEGF-B are normal and fertile but have hearts which are reduced in size, indicating that VEGF-B may be important in coronary vascularization and growth (Yancopoulos et al., 2000). Transgenic overexpression of VEGF-C, which selectively binds to lymphatic specific VEGFR3, leads to lymphatic hyperplasia. The normal physiological role of VEGF-D however, remains to be elucidated (Carmeliet and Jain, 2000; Yancopoulos et al., 2000).

Selective binding of VEGF and its homologues to three different tyrosine kinase receptors VEGFR1-3 help in the fine-tuning and control of angiogenesis (figure 6). VEGF-B and PlGF both can bind to VEGFR1, whereas VEGF-A can interact with both VEGFR1 and VEGFR2. VEGF-C and VEGF-D bind both VEGFR2 and VEGFR3 and the viral homologue VEGF-E binds and activates only VEGFR2 (Eriksson and Alitalo, 1999; Shibuya and Claesson-Welsh, 2006). In addition to the VEGFRs, neuropilin-1, a transmembrane protein implicated in the regulation of axonal guidance in neurons also acts as a co-receptor for VEGF-B,

PlGF-2, VEGF-E and $VEGF_{165}$ (Neufeld et al., 1999; Clauss, 2000). In addition to being an endothelial growth factor, VEGF also targets monocytes, retinal epithelial cells astrocytes, tumor derived cell lines, hematopoietic progenitor cells, trophoblasts and neuronal cells (Clauss, 2000).

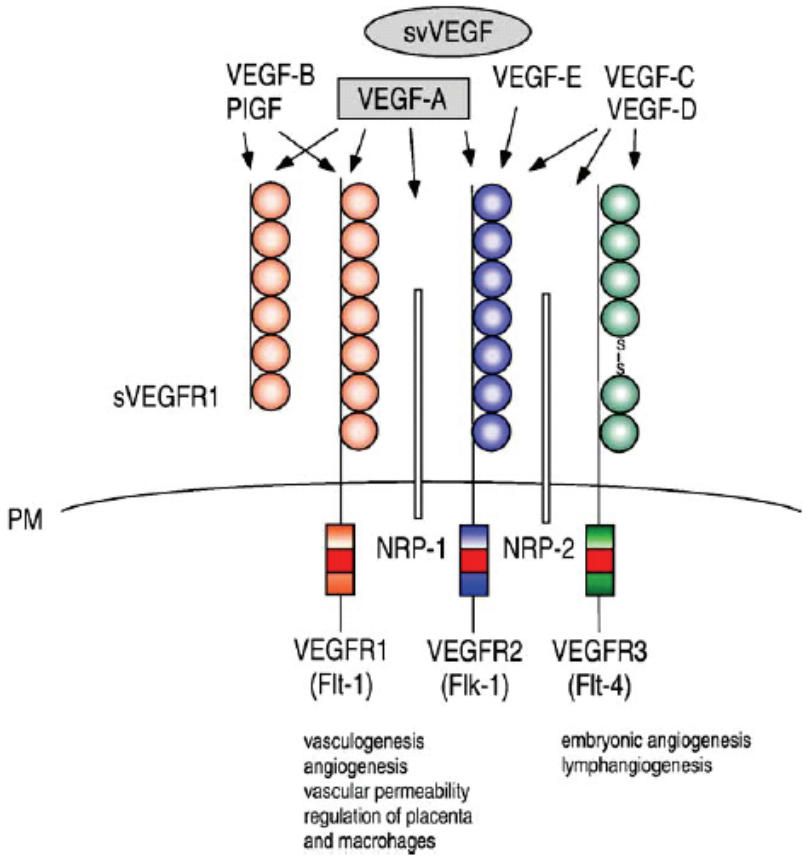

Figure 6: Differential binding of various VEGF homologues to three VEGFRs along with the two neuropilin co-receptors. All VEGF receptors have a characteristic split tyrosine kinase domains and seven extracellular immunoglobulin repeats. VEGFR1 is also found in soluble form denoted as sVEGFR1. VEGFR2 is the primary receptor eliciting the signaling cascades mediating downstream effects of vasculogenesis, angiogenesis and vascular permeability. VEGFR3 is mainly found in lymphatic endothelial cells and plays an important role in lymphangiogenesis and embryonic angiogenesis. This figure was adapted from Shibuya and Claesson-Welsh, 2006.

VEGF receptors

The VEGFR family includes three receptors VEGFR1 (Flt-1), VEGFR2 (Flk-1), and VEGFR3 (Flt-4) all belonging to the platelet derived growth factor receptor subfamily of receptor tyrosine kinases (Taipale et al., 1999; Karkkainen and Petrova, 2000; Robinson et al., 2000; Yancopoulos et al., 2000; Shibuya, 2001). The receptors share a common characteristic of having seven extracellular immunoglobulin homology domains along with a single transmembrane domain and a split tyrosine kinase domain at the cytoplasmic end (Shibuya, 2001).

Of all the receptor tyrosine kinases recruited by VEGF, binding and activation by VEGF-A to VEGFR1 and VEGFR2 are most intensely studied. The function of these two receptors in vascular development and the recruitment of individual signal transduction cascades are discussed below in detail. However, the understanding about the manner in which signal transduction cascades induced by VEGF affect the corresponding stimulation of vessel growth is still incomplete.

VEGFR1/Flt-1 (*fms*-like protein tyrosine kinase) and signaling

VEGFR1/Flt-1 has the highest affinity to $VEGF_{165}$, with a K_d of approximately 16-114 pM (Zachary and Gliki, 2001). Although, VEGFR1 is a transmembrane glycoprotein of 180 kDa, its mRNA can be spliced to produce a shorter soluble protein consisting only the first six extracellular immunoglobulin domains (Ferrara, 1999). This soluble sFlt-1/sVEGFR1 has the capability to bind VEGF with high affinity (K_d 10-20 pM) and is able to inhibit VEGF induced angiogenesis (Ferrara and Davis-Smyth, 1997; Mukhopadhyay et al., 2004). Thus,

sVEGFR1 may function as a physiological negative regulator of VEGF action either by acting as a decoy receptor or by suppressing signaling through VEGFR2. This idea is further strengthened by the fact that mice engineered for loss of VEGFR1 (E8.5-9.0) show an excess formation of abnormally coalescing endothelial cells, whereas mice engineered to express a truncated form of VEGFR1 (lacking tyrosine kinase domain) appear to be normal (table 2) (Gale and Yancopoulos, 1999; Carmeliet and Jain, 2000). Additionally, domain swapping experiments between VEGFR1 and VEGFR2 conducted by Gille et al. in 2000 have demonstrated that a short ANGG motif unique to the intracellular juxtamembrane VEGFR1 domain has the ability to inhibit VEGFR2 mediated signaling and cell migration (Gille et al., 2000; Zachary and Gliki, 2001). Also, VEGFR1 is the only receptor expressed in monocytes mediating both tissue factor production and monocyte chemotaxis (Heil et al., 2000). Additionally, VEGFR1 induces expression of metalloproteinase and mediates production of urokinase and plasminogen activator inhibitor in smooth muscle cells (Ferrara and Davis-Smyth, 1997). VEGFR1 expression is up-regulated by hypoxia via HIF-1 (hypoxia inducible factor-1) binding site upstream of its coding sequence (Breier, 2000).

Even though signaling through VEGFR1 is weak and does not appear to be important for the biological activities such as proliferation and migration of endothelial cells, it is essential for normal vascular development as seen from the gene knockout studies (table 2). Cunningham et al. in 1995 using yeast two hybrid system assays demonstrated that VEGFR1 associates with the p85 subunit of PI3K (phosphatidylinositol 3'–kinase), but so far this has not been shown to have any

relevance with respect to any biological activity. Several adaptors of the Src family such as Fyn and Yes have also been shown to be phosphorylated due to VEGF/VEGFR1 interaction (Zachary and Gliki, 2001). Recent studies have shown that signaling cascades emerging from VEGFR1 as a result of stimulation by VEGF-A or PlGF are different. This difference might arise due to varied intracellular receptor confirmation or may be governed by neuropilin or heparan sulfate proteoglycan co-receptors mediating the availability of tyrosine residues for kinases (Shibuya and Claesson-Welsh, 2006).

VEGFR2/KDR (kinase insert domain)/Flk-1 (fetal like kinase-1) and signaling

VEGFR2 is a transmembrane protein of 230 kDa and has no splice variants unlike VEGFR1 (Veikkola et al., 2000). As compared to VEGFR1, KDR/VEGFR2 has a lower affinity to VEGF in the range of 0.4-1 nM (Zachary and Gliki, 2001). Unlike VEGFR1, VEGFR2 is indirectly regulated by hypoxia via increased concentration of VEGF, which in turn induces VEGFR2 gene expression (Ferrara and Davis-Smyth, 1997; Ferrara, 1999). Activation of VEGFR2 in the absence of VEGFR1 in porcine aortic endothelial cells lacking in endogenous VEGF receptors leads to a mitogenic response. Consistent with this *in vitro* action, VEGF and VEGFR2 are critical for the earliest stages in vasculogenesis (Yancopoulos et al., 2000). Mice engineered to lack either VEGF (VEGF-A) or VEGFR2 have very few endothelial and primitive hematopoietic cells and develop an abnormal vasculature, where major vessel tubes fail to develop in appreciable numbers leading to early embryo lethality (table 2) (Gale and Yancopoulos, 1999; Zachary and Gliki, 2001).

Some of the biological functions elicited via VEGFR2 are release of tissue factor, chemotaxis, proliferation and sprouting of cultured endothelial cells *in vitro* and angiogenesis *in vivo* (Zachary, 1998; Kliche and Waltenberger, 2001). Corresponding to this, targeted inactivation of VEGFR2 using blocking antibodies leads to disruption of tumor angiogenesis and prevents DNA synthesis in response to VEGF (Ferrara, 1999; Carmeliet and Jain, 2000).

Since VEGFR2/KDR is the major transducing receptor, many research groups have been focusing on this aspect. Overexpression of VEGFR2 and its subsequent activation by VEGF in endothelial cells leads to a rapid recruitment of adaptor proteins such as VRAP, Shc, Nck and Grb2 along with protein tyrosine phosphatases such as SHP-1 and SHP-2 (figure 7) (Wu et al., 2000; Kliche and Waltenberger, 2001; Zachary and Gliki, 2001). The yeast two-hybrid assay and RT-PCR analysis in conjunction with RNase protection assays also implicate recruitment of Sck (an Shc homologue), HCPTPA (a low molecular weight protein tyrosine phosphatase similar to SHP-1 and SHP-2) and a new SH2-containing proline rich adaptor protein, which binds constitutively to PLCγ (phospholipase C gamma) and PI3K (figure 7) (Huang et al., 1999; Gelinas et al., 2002; Ratcliffe et al., 2002). Cell proliferation subsequent to VEGF-A/VEGFR2 interaction via activation of ERK1/2 (p42/44 MAP kinase) cascade has also been demonstrated in various endothelial cells such as BMEC (bovine microvascular ECs) and PAE (porcine aortic ECs) (Yu and Sato, 1999; Gille et al., 2001). Activation of Ras and also various isoforms of PKC (protein kinase C) via the PLCγ pathway and subsequent increased intracellular Ca^{2+} levels has also been reported (Meadows at al., 2001). VEGF stimulates the release nitric oxide via

increased synthesis of eNOS (endothelial nitric oxide synthase). The activation of eNOS can be carried out either by increased intracellular Ca^{2+} concentration due to IP3 or in a Ca^{2+}-independent manner through the activation of Akt/PKB serine/threonine kinase (figure 7) (Gelinas et al., 2002). Migration responses in endothelial cells are mediated through the increased production of NO and also due to tyrosine phosphorylation of FAK (mediated by Hsp90) and paxillin subsequent to VEGF stimulation (Zachary and Gliki, 2001). The stress activated p38 MAPK and its downstream effector HSP27 (F-actin polymerizing factor) have been shown to be essential for VEGF induced motility responses and actin reorganization (figure 7) (Matsumoto and Claesson-Welsh, 2001).

In addition to proliferation and migration responses induced in endothelial cells, VEGF also prevents apoptosis induced due to serum starvation or through TNFα, thereby protecting and increasing survival of endothelial cells. Signal transduction cascades emerging from VEGF/VEGFR2 interaction are responsible for conferring this protection (Schlessinger, 2000). This cell survival signal is transduced via the PI3K-Akt/PKB, which then leads to the up-regulation of anti-apoptotic proteins such as survivin, XIAP and Bcl-2, and inhibition of pro-apoptotic proteins such as BAD, FKHR1 and caspase-9 (figure 7) (Gerber et al., 1998; Veikkola et al., 2000; Matsumoto and Claesson-Welsh, 2001; Zachary and Gliki, 2001 Karkkainen et al., 2002; Shibuya and Claesson-Welsh, 2006). Other key components involved in this cell survival process are β-catenin, VE-cadherin (endothelial adherens junction protein) and $\alpha_v b_3$ integrin expressed on angiogenic endothelial cells (Matsumoto and Claesson-Welsh, 2001; Zachary and Gliki, 2001).

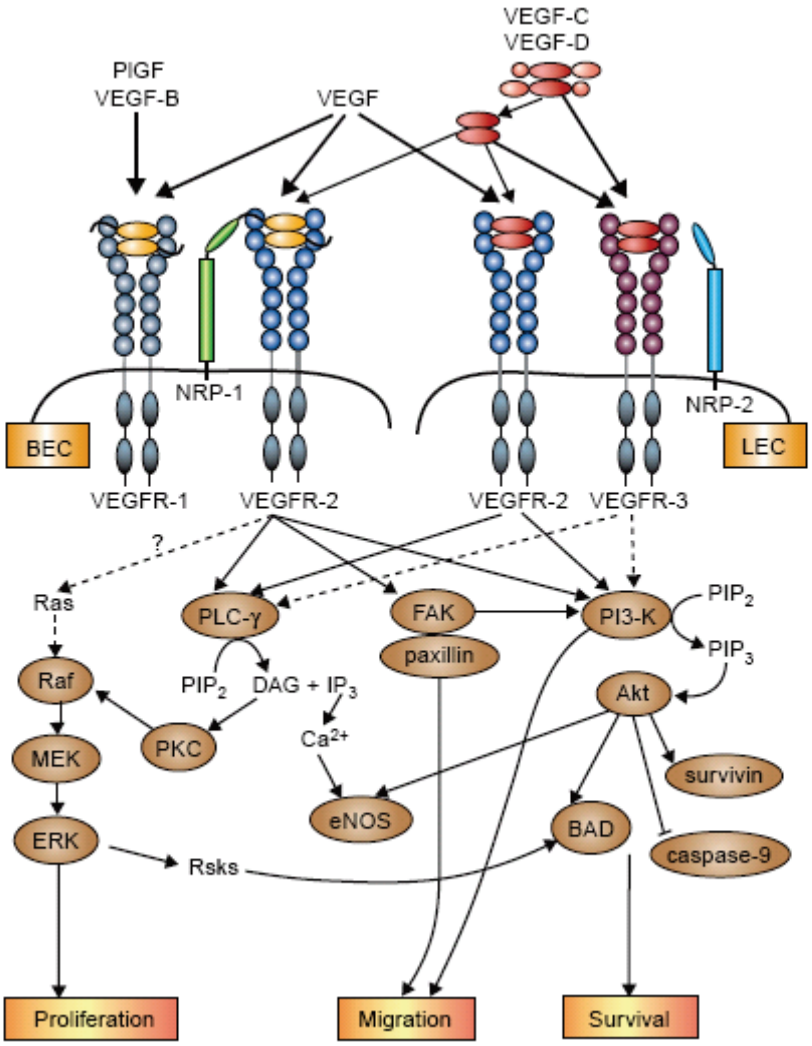

Figure 7: Signal transduction cascades emerging from various VEGFR on stimulation with various VEGF homologues in BEC (blood vascular endothelial cells) and LEC (lymphatic endothelial cells). The signal transduction cascades as a result of VEGF/VEGFR2 are stronger than those emerging from other VEGF/VEGFR systems. Detailed explanation of the VEGF/VEGFR2 pathway is given in the text along with the references cited. Final responses elicited by individual pathways as a result of VEGF-A/VEGFR2 are illustrated as boxes. This figure was adapted from Karkkainen et al., 2002.

The $VEGF_{165}$ (VEGF-A)/VEGFR2 response and migration of endothelial cells is further potentiated due to interaction with a co-receptor-neuropilin-1. Neuropilin-1 is not known to have any signal transducing ability since it possesses a short cytoplasmic tail. Indeed, cells with neuropilin-1 but no VEGFR2 fail to show any response to VEGF. Nevertheless gene disruption studies involving neuropilin-1 show that it is an important regulator of angiogenesis. Mouse embryos lacking neuropilin-1 die due to failure of development of cardiovascular system. Another co-receptor, neuropilin-2, similar to neuropilin-1 has also been discovered (Matsumoto and Claesson-Welsh, 2001).

VEGFR3/Flt-4 and signaling

To date very little is known about the signal transduction cascades induced via VEGFR3. However, VEGFR3 has been shown to be a component in the regulation of development and growth of lymphatic vasculature and also in the formation of primary cardiovascular network (table 2) (Clauss, 2000; Veikkola et al., 2000). VEGFR3 knockout mice die early in the development due to cardiovascular failure (Gale and Yancopoulos, 1999; Matsumoto and Claesson-Welsh, 2001). Both VEGF-C and VEGF-D ligands selectively activate VEGFR3 and are the key components involved in the regulation of lymphangiogenesis and angiogenesis. Activation of VEGFR3 subsequent to ligand stimulation leads to rapid tyrosine phosphorylation of Shc and activation of MAPK along with increased cell motility, actin reorganization and proliferation, similar to the VEGF-A/VEGFR2 response (Taipale et al., 1999). VEGFR3 is constitutively expressed on the lymphatic vessels later in development.

In addition to being a marker of the lymphatic vessels, recent studies have shown that VEGFR3 is also expressed in tumor blood vessels during the process of neovascularization (Taipale et al., 1999; Shibuya and Claesson-Welsh, 2006).

DISSERTATION OBJECTIVES

Angiogenesis is growth of blood vessels from pre-existing vasculature. This fundamental process plays an important role in various pathological and physiological conditions including tumor metastasis. Vascular endothelial growth factor (specifically VEGF-A or $VEGF_{165}$) has been found to be a primary factor, regulating angiogenesis and various functions of endothelial cells. Although much research has been done in the field of angiogenesis, there is a dearth of knowledge regarding genes mediating the various downstream pleiotropic effects seen in endothelial cells stimulated by VEGF-A and VEGFR2 interactions. This project was undertaken to identify genes, specifically the immediate early genes (IEGs) induced by VEGF-A. This dissertation is divided in three parts. Part I discusses the 17 IEGs discovered in this study induced by VEGF-A using suppression subtractive hybridization and differential screening techniques. Study of RNA binding protein 5 (RBM5), the only IEG with an implicated role as a tumor suppressor gene and an apoptotic regulator is addressed in Part II of this dissertation. Conclusions and future studies are discussed in Part III. A protocol for production of full-length RBM5 in insect cells for RNA binding studies, beyond the scope of this dissertation, is detailed in Appendix A.

Another aspect this dissertation attempts to address is the resolution of signal transduction mediators upstream of RBM5 emerging from the VEGF/VEGFR signal transduction cascades, by using pharmacological inhibitors and real time PCR (Appendix B).

CHAPTER 2

IDENTIFICATION OF IMMEDIATE EARLY GENES INDUCED BY VEGF

INTRODUCTION

Endothelial cells are usually quiescent unless stimulated by an angiogenic growth factor. As discussed in Chapter 1, VEGF-A ($VEGF_{165}$) plays a key role in angiogenesis since it not only acts as a specific mitogen of endothelial cells, but also is the most potent regulator of vascular permeability. Much of the effort has been focused on the characterization of the signal transduction cascade emerging from the two receptors VEGFR1 and VEGFR2, resulting from VEGF-A stimulation. At the beginning of this study, even though the entire signal transduction cascade emerging from the two receptors had been elucidated, there was scant information regarding the immediate early genes induced in endothelial cells through either of these receptors.

The induction of immediate early genes (IEGs) represents the first wave of cellular response to external stimuli and does not require *de novo* protein synthesis. This rapid and transient response of immediate early genes consequently orchestrates the downstream genomic response, which is unique for each stimuli or cell type. The immediate early gene response thus plays a critical role in translating diverse situations such as exposure to growth factors, stress or oxygen deprivation to a defined cellular response (Greenberg and Ziff, 1984; Lau and Nathans, 1986;

Edwards and Mahadevan, 1992). Only a few immediate early gene products induced by VEGF-A stimulation have been discovered so far. Some of the IEGs induced by VEGF cited in the literature are –CTGF, CYR61, COX2 and EGR1 (Babic et al., 1998; Suzuma et al., 2000, Abe and Sato, 2001; Sato, 2001b).

Although transcription factors belonging to NF-κB, Myc and AP-1 families such as c-*Fos* and c-*Jun* are most well known among the immediate early gene products, all IEGs are not transcription factors. More than 100 different immediate early gene products have been identified so far. The activation of a diverse set IEGs of which only a small subset may be overlapping as seen in different situations offer plasticity to the cells to respond to a variety of cell stimuli (Bravo, 1990). The level of IEGs in quiescent cells is very low, but is induced rapidly within 0.5 to 2 hours of cell stimulus. The IEGs are induced at the level of transcription and have a high turnover rate as expected since most of the immediate early gene products are responsible for the transition of cells from G0 to the G1 phase. Immediate early gene expression is further augmented in the presence of protein synthesis inhibitors such as cycloheximide and anisomycin along with mitogen, leading to an over accumulation of IEG transcripts (Efrat and Kaempfer, 1984; Greenberg et al., 1986; Lau and Nathans, 1986). This phenomenon known as 'superinduction' was first observed by Cochran et al. in 1983. They observed induction of two genes KC and JE within 1 hour of PDGF stimulation in presence of protein synthesis inhibitors in 3T3 cells.

Based on different studies it is proposed that superinduction may be due to a four prong effect elicited by protein synthesis inhibitors (Edwards and Mahadevan, 1992). Firstly, there is an enhancement of stability of the usually labile IEG mRNA.

This increased mRNA stability may in turn be governed by three effects: 1) degradation of labile mRNAases or, 2) inhibition of translation which is needed for maintaining the rapid mRNA turnover kinetics and 3) auto-repression mechanism exhibited by some transcription factors or lastly, the presence of protein synthesis inhibitors may lead to entrapment of mRNAs on polysomes thus shielding them from cytosolic ribonucleases (Cochran et al., 1983; Wilson and Treisman, 1988; Pontecorvi et al., 1988; Edwards and Mahadevan, 1992). Secondly, protein synthesis inhibitors such as cycloheximide or anisomysin by themselves can stimulate nuclear signaling leading to phosphorylation of pp33 and pp15 chromatin associated proteins (Mahadevan and Edwards, 1991). The third factor leading to superinduction may be due to loss of labile transcriptional repressors as suggested by Wall et al., in 1986 and Subramaniam et al., in 1989. Lastly, there is increased transcription in presence of protein synthesis inhibitors suggesting that protein synthesis is essential to shut off translation (Greenberg et al., 1986; Edwards and Mahadevan, 1992).

To derive a transcriptional set of IEGs unique to endothelial cells as a result of VEGF-A stimulation, the phenomenon of superinduction (to enrich IEG transcripts) along with suppression subtractive hybridization to exclusively select induced IEGs from other transcripts was used. Suppression subtractive hybridization (SSH) to generate cDNA libraries was first described by Diatchenko et al. in 1999. This technique relies upon a normalization step coupled with a subtraction step, resulting in the detection of even low copy number differentially expressed genes. Using this method, I identified a unique set of 17 IEGs induced by VEGF-A. It is possible that

each gene identified in this unique subset may be responsible for a significant part of the molecular signaling pathways leading to VEGF-A mediated angiogenesis.

MATERIALS AND METHODS

Cell culture and VEGF treatment

Pooled HUVEC cells (Cambrex Biosciences) between passage 4 and 5 were grown to 80-90% confluence in EGM (Appendix B) supplemented with 1 ng/ml basic fibroblast growth factor (Invitrogen) at 37°C in a 5% CO_2 incubator. Prior to VEGF-A stimulation, the cells were washed twice with 10 ml of EBM 0.5 (Appendix B) and consequently serum starved in 30 ml of EBM 0.5 for 18 hours. Subsequent to serum starvation the cells were treated with 10 ng/ml of VEGF-A and or 10 μg/ml of cycloheximide (CHX) for 0, 1 and 3 hrs. After growth factor stimulation, the cells were either harvested using ice cold 1 mM EDTA in phosphate buffered saline for replating or processed further for RNA isolation as mentioned below.

RNA isolation

HUVEC cells grown on 150 mm dishes (Corning) were stimulated with VEGF-A (10 ng/ml) for 0, 1 and 3 hours as stated in the above section. For RNA isolation, the cells were lysed directly on the plate using 3 ml of RNA Bee (Tel-Test) per dish (Chomczynski and Sacchi, 1987; Sambrook et al., 1989). RNA was further isolated according to the manufacturer's directions. Briefly, 0.6 ml of chloroform

was added and mixed by shaking the tube vigorously for 15 seconds. The tubes were incubated on ice for 5 minutes and further centrifuged for 15 minutes at 4ºC at 12,000g for phase separation. The upper clear aqueous phase was separated from the lower blue colored phenol phase and mixed with equal volumes of isopropanol. RNA was precipitated by centrifuging the tubes at 7,500g for 5 minutes. The RNA pellet was further washed in 2 ml of 75% ethanol and dissolved in either DEPC treated distilled water or TE buffer (Appendix B). RNA integrity was confirmed by measuring 260/280 absorbance ratio and by running a 5 µl aliquot on 1.2% formaldehyde agarose gel.

Construction of suppression subtractive hybridization cDNA library

A suppression subtractive hybridization (SSH) library was screened to identify differentially expressed genes in endothelial cells as a result of stimulation by VEGF-A ($VEGF_{165}$). The library had been constructed by Dr. Brown in our lab using PCR Select ^{TM} cDNA Subtraction Kit according to the manufacturer's instructions (Clontech Laboratories). Briefly, $polyA^+$ RNA was isolated using Oligotex kit (Qiagen) for subsequent cDNA preparation from HUVEC cells treated with 10 ng/ml VEGF-A and 10 µg/ml cycloheximide for 3 hours ('tester' cDNA pool) and untreated HUVEC cells ('driver' cDNA pool). Hybridization of excess driver cDNA to the tester cDNA pool resulted in a subtracted library of cDNAs potentially enriched in VEGF-A induced immediate early gene transcripts.

Differential screening of suppression subtractive hybridization cDNA library

Selection of recombinant clones - The subtracted transcripts (refer to the above section) were ligated into Sma1 digested pGEM®-3Zf(+) vector (Promega). Following transformation in DH5α cells (Promega), the cells were plated onto Luria-Bertani (LB) agar plates containing 100 µg/ml ampicillin, 80µg/ml X-gal (5-bromo-4-chloro-3-indolyl-beta-D-galactopyranoside) and 0.5mM IPTG (isopropyl-β-D-thiogalactopyranoside). After overnight incubation at 37°C the recombinant white colonies were identified by the blue/white screening and picked up randomly. Each selected recombinant colony was grown separately overnight at 37°C/200 rpm in 3 ml of LB broth containing 100 µg/ml of ampicillin. Plasmid DNA was isolated from each of the clones by performing boiling plasmid minipreps (Sambrook et al., 1989).

Preparation of dot blots - Each plasmid clone was mixed with equal amounts of 0.6N NaOH (9 µl each) and arrayed (dot blotted) in triplicates onto individual GeneScreen Plus® nylon membrane (NEN™ Life Science). The blots were air dried and subsequently neutralized in 0.5M Tris HCl (pH 7.5). After rinsing the blots thrice in distilled water, the plasmid DNA was crosslinked to the nylon membranes by a 15 second exposure to ultraviolet light.

Preparation of radiolabeled probe - Equal quantities (75 ng) of 'tester' and 'driver' cDNA were labeled in two separate reactions using Prime-a-Gene® Labeling System (Promega) according to manufacturer's directions. Briefly, the each cDNA pool dissolved in 4µl of TE was mixed with 10 µl of 5X labeling buffer (containing 26 A_{260} µ/ml random hexadeoxyribonucleotides) and 26 µl of distilled water. This

mixture was boiled for 5 minutes and cooled on ice. Each reaction was then assembled by adding the following components:

dNTPs (20 µM each of dGTP, dATP and dTTP)	2µl
BSA	2 µl
[α-^{32}P] dCTP (10 µCi/µl or 3,000 Ci/mmol)	5 µl
DNA Polymerase I, Large Klenow Fragment (5 u/µl)	1 µl

The labeling reactions were incubated further for 90 minutes at room temperature. The labeled cDNA (tester and driver pool) was precipitated by adding 0.2M EDTA (5 µl), 10M ammonium acetate (18 µl) and of ethanol (150 µl) on ice for 2 hours. The reaction was then centrifuged for 15 minutes and the pellet redissolved in 50 µl of TE buffer. An aliquot (1 µl) of each labeled tester and driver cDNA pool was further assayed for the amount of radioactivity incorporated by liquid scintillation. The labeled tester and driver cDNA (equal counts) were then boiled for 5 minutes with 500 µl of FSS and added to the blots which were processed as detailed in the next section. Approximately 50 ng of 'cocktail' containing cDNAs representing all the genes identified before from this library, was also labeled in a similar fashion and used to hybridize the third blot.

Membrane hybridization - The dot blots were pre-hybridized at 42ºC for 4 hours in 10 ml of 1:1 FSS:pre-hybridization (Appendix B) solution. After pre-hybridization the solution was replaced with 10 ml of 1:1 FSS:hybridization solution (Appendix B). The labeled probes were added to the individual blots and further incubated overnight at 42ºC for hybridization.

Washing protocol and exposure - After hybridization each of the three blots were washed as follows before exposing to phosphor screen (BioRad) for autoradiography:

100 ml 1X SSC/0.1%SDS for 10 minutes at room temperature

100 ml 0.2X SSC/0.1% SDS for 30 minutes at 42ºC X 3 times

The phosphor screen was scanned using Molecular Imager FX (BioRad) and images were processed using Quantity One software (BioRad).

Differential Screening - All autoradiography images were further processed with Adobe Photoshop software. All clones having at least twice the signal intensity on the tester cDNA probed blot as compared to the driver cDNA probed blot and none on the cocktail were selected. The selected clones representing potentially VEGF-A induced IEGs were handled as detailed below.

Isolation of inserts corresponding to IEGs potentially induced by VEGF-A

Plasmid preps - Each of the plasmid clones identified as potentially positive was selected and grown overnight in 100 ml of Terrific broth containing 100 µg/ml ampicillin at 37°C/200 rpm. Plasmid DNA was isolated by the alkaline lysis method (Sambrook et al., 1989). Purity of the isolated DNA was confirmed by measuring 260/280 absorbance ratio and by running 2 µg on 1% agarose gel.

Restriction digests of plasmids to isolate inserts - Two restriction enzymes pairs (EcoR I - Hind III and Sac I - BamH I), each corresponding to the T7 and SP6 MCS of pGEM®-3Zf(+) vector were used to splice out the inserts from each of the identified clones. The restriction digests were incubated at 37ºC for one hour and

then run on a 1% agarose gel. The enzyme pair giving the largest insert size was selected for each plasmid clone and the reaction was scaled up to yield 2 µg for each insert. The scaled up restriction digests were run in a 1% agarose gel and the inserts were purified using DEAE membrane and high salt solution extraction method (Sambrook et al., 1989).

Sequencing - All inserts isolated above were sequenced by the dye terminator sequencing method at our campus facility. BLAST search analysis was carried out to identify the IEGs. Up-regulation of some of the IEGs by VEGF-A was confirmed by Northern analysis as given below.

Northern analysis

Preparation of RNA samples - Total RNA (10-15 µg/well) dissolved in formamide in a final volume of 20 µl was mixed with 7 µl of formaldehyde, 4 µl of 5X formaldehyde RNA gel running buffer and 9 µl of DEPC treated distilled water in a microcentrifuge tube. The RNA was denatured by heating the samples to 65ºC for 10 minutes and then chilled on ice. Subsequently, 4 µl of RNA gel loading buffer along with 2 µl of 10 mg/ml ethidium bromide was added per 40 µl of the RNA samples. The RNA samples were loaded onto a pre-run 1.2% formaldehyde agarose gel and separated by electrophoresis at 90 volts (constant voltage) until the bromophenol blue dye migrated to the bottom 2/3rd of the gel. The gel was soaked in 150 ml distilled water twice for 15 minutes and in 150 ml 10X SSC for 30 minutes to remove all the formaldehyde. The RNA bands were seen by ultraviolet illumination and recorded using BioRad Imager and Quantity One Software.

Transfer of RNA to nylon membranes - The RNA from gel was transferred overnight to a GeneScreen Plus® nylon membrane (NEN™ Life Science) using capillary elution in an ascending flow of 10X SSC buffer (Sambrook et al., 1989). The nylon membrane was pried away from the gel and washed in 150 ml of 2X SSC for 10 minutes to remove any gel particles sticking to the membrane. The damp nylon membrane was then exposed to ultraviolet illumination for 15 seconds to crosslink the RNA and then dried under vacuum in between 2 sheets of 3MM paper at 80ºC for 2 hours.

Preparation of radiolabeled probe and membrane hybridization - Linear insert DNA (50 to 100 ng) labeled using Prime-a-Gene® Labeling System (Promega) was hybridized to RNA blots as detailed in the previous section.

Washing protocol and exposure - After hybridization the blots were washed as follows before exposing to phosphor screen (BioRad) for autoradiography:

100 ml 1X SSC/0.1%SDS for 10 minutes at room temperature

100 ml 0.1X SSC/0.1% SDS for 30 minutes at room temperature X2

100 ml 0.1X SSC/0.1% SDS for 30 minutes at 42ºC

The phosphor screen was scanned using Molecular Imager FX (BioRad) and images were processed using Quantity One software (BioRad) as mentioned before.

RESULTS AND DISCUSSION

Differential screening of cDNA library

Differential screening of 329 clones led to the identification of 21 new clones representing putative immediate early genes induced by VEGF-A (figure 8). Subsequent sequencing and BLAST search identified a new putative VEGF-A response gene set of 14 new genes (table 3) along with ZNEU1, IL-8 and RBM5 which were previously identified in our lab by Dr. Brown (Altschul et al., 1997). Interestingly, all of the inserts represented the 3' end of the identified genes and ranged from 200-500 base pairs in length.

Additionally, to root out any false positives, induction of IEGs was confirmed by Northern analysis using RNA isolated from endothelial cells stimulated with VEGF-A only (in the absence of cycloheximide). The probes used for Northern analysis were the same inserts sequenced to identify the genes as explained above. Up-regulation of all immediate early genes verified by Northern analysis were induced within 1 hour of VEGF-A stimulation and tapered off by the 3 hours time point. Equal loading of RNA for each time point was confirmed by gel analysis or by striping and re-probing the blots with GAPDH (glyceraldehyde-3-phosphate dehydrogenase) housekeeping gene. Up-regulation by VEGF-A could not be confirmed for EXOC4, DDIT3, MIDN, RGS3 and clone 648 due to lack of good probes for Northern analysis. Of all the positive clones analyzed it was found that clones representing ATF3 were the most prevalent.

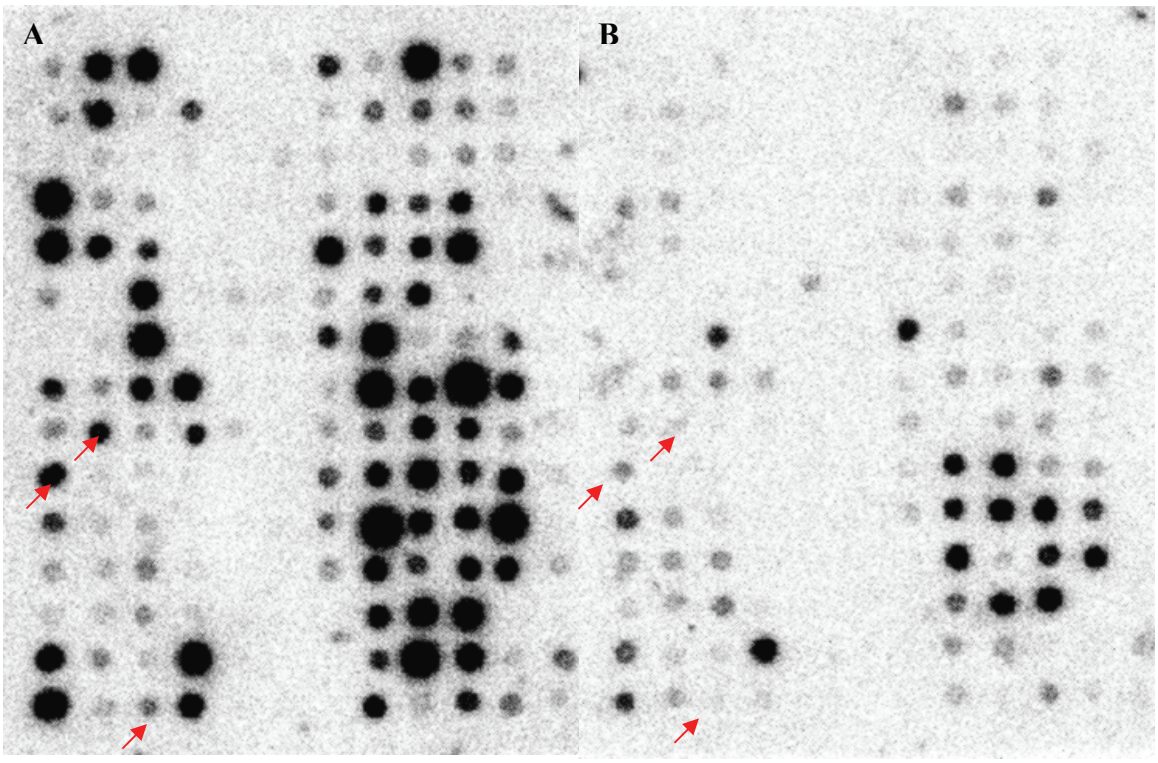

Figure 8: An autoradiograph showing differential screening of a cDNA library made by suppression subtractive hybridization method to isolate immediate early genes induced by VEGF-A in human umbilical vein endothelial cells. The dot blots represent 172 of the 329 clones arrayed in duplicates on A) forward probe hybridized and B) reverse probe hybridized blots. Both the membranes were probed with equal counts of [α-^{32}P] dCTP radioactivity as determined by liquid scintillation. Plasmid clones showing at least twice the signal on forward probe blot-A than on a reverse probed blot-B and on the cocktail probe blot (not shown) were selected and processed further as outlined in Materials and Methods section. This selection process was designed to eliminate repetitive selection of the cDNAs representing genes previously identified from this library. Arrows indicate some of the clones selected using this method.

	Gene	Induced by VEGF	Chromosome location	Gene Bank Gene ID/ Accession number	Gene Function
1.	ATF3	YES	1q32.3	467	Activating transcription factor 3, transcriptional repressor
2.	DDIT3	N/A	12q13.1	1649	DNA-damage-inducible transcript 3 encoding a bZip protein
3	EGR2	YES	10q21.1	1959	Early growth response 2, Cys2His2 zinc finger transcription factor
4.	FOSB/ GOS3	YES	19q13.32	2354	Leucine zipper /G0/G1 switch regulatory gene 3 protein
5.	PTGS2/ COX-2	YES	1q25.2	5743	Prostaglandin-endoperoxide synthase or cyclooxygenase 2
6.	CTGF	YES	6q23.1	1490	Connective tissue growth factor
7.	DUSP1/ CL100	YES	5q34	1843	Dual specificity phosphatase 1
8.	EXOC4	N/A	7q31	60412	Exocyst complex 4 or SEC8 protein
9.	RGS3/ RGP3	N/A	9q32	5998	Regulator of G protein signaling 3, a GTPase activating protein for g(ialpha) and g(qalpha)
10.	MIDN	N/A	19p13.3	90007	Midnolin (midbrain nucleolar protein)
11.	Clone 532	YES	12	AC009246	Homo sapiens DKFZp686D0473 cDNA
12.	Clone 648	N/A	1p36.12	AK027830	Homo sapiens, highly similar to GENE 33 polypeptide
13.	FOS	YES	14q24.3	AF111167	Leucine zipper /jun dimerization protein
14.	IER2/ ETR101	YES	19p13.13	9592	Immediate early response 2 (transcription factor)
15.	ZNEU1/ EGFL7	YES	9q34.3	353156	Vascular endothelial –statin
16.	IL8	YES	4q13-q21	3576	Interleukin 8, CXC chemokine
17.	RBM5/ LUCA15	YES	3p21.3	10181	Putative tumor suppressor gene and apoptosis regulator

Table 3: List of immediate early genes identified by differential screening of the cDNA library created by suppression subtractive hybridization. Most of the genes identified in this new putative VEGF-A response gene set have been confirmed to be induced either by Northern analysis in this study or have been cited in the literature.

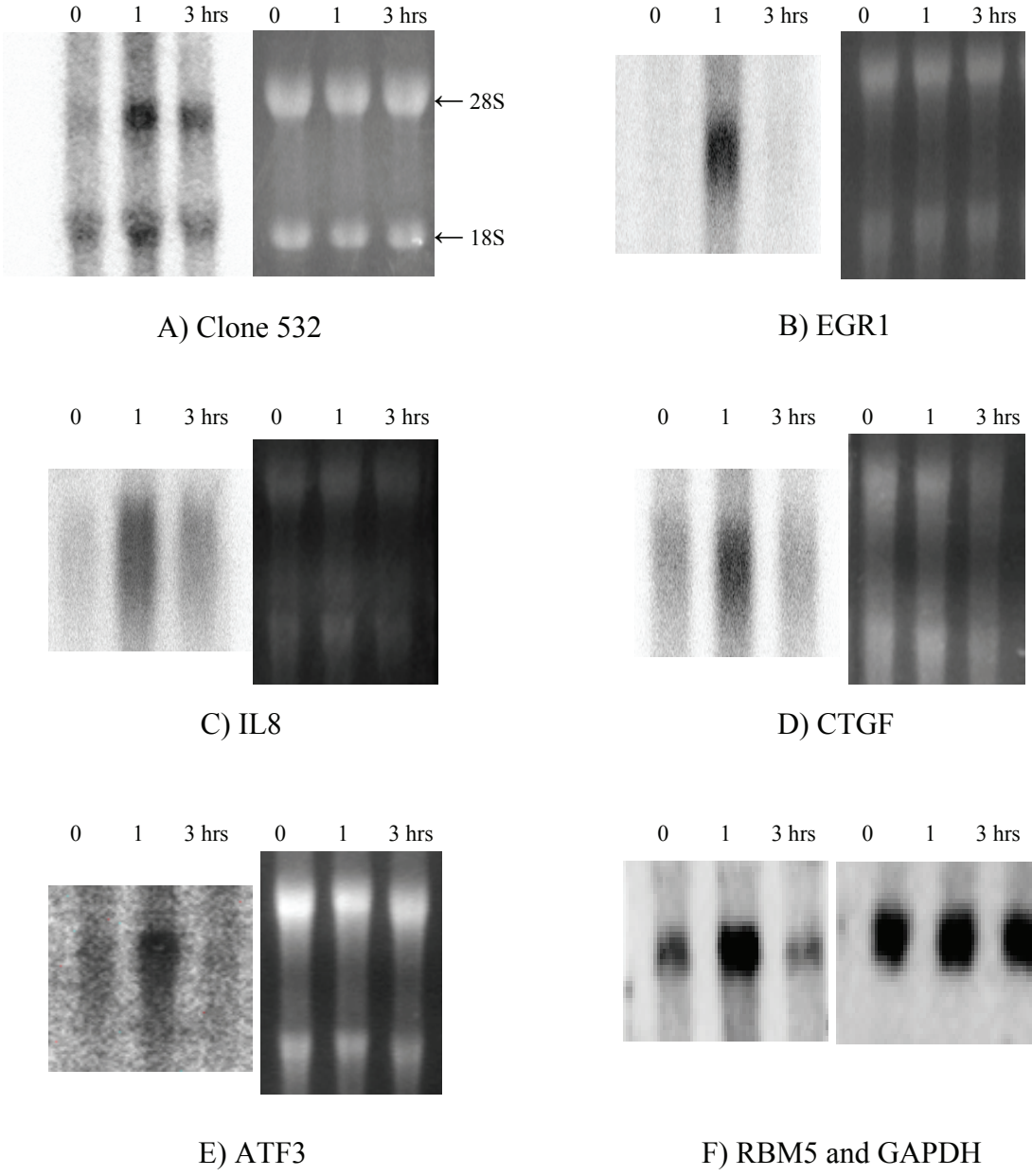

Figure 9: Representative Northern analysis blots (A-F) showing induction of some of the immediate early genes in endothelial cells stimulated with VEGF-A in absence of cycloheximide. Northern analysis was performed to rule out any false positives identified by the differential screening of cDNA library created by suppression subtractive hybridization. The identified IEGs are induced within 1 hour of VEGF-A stimulation and return to basal levels within 3 hours. Equal loading of total RNA was confirmed by gel analysis showing 28S and 18S rRNA bands (A-E) or by striping and re-probing the blots with a housekeeping gene GAPDH (F). Densitometry analysis showed approximately 2.5 fold up-regulation of RBM5 as compared to GAPDH.

Immediate early genes induced by VEGF in endothelial cells

While this project was at its beginning, a cDNA microarray (7267 genes) study to identify global expression as a result of VEGF-A stimulation in endothelial cells (HUVEC) was conducted by Abe and Sato in 2001. However, there was very little overlap in the genes identified as induced by VEGF-A in this study and the cDNA microarray study conducted by Abe and Sato. This discrepancy may be possible due to several reasons such as lack of specificity of cDNA microarray probes, different experimental settings or that some of the known and novel genes identified in this study were not represented by the 7267 clones in the microarray study (Kothapalli et al., 2002). The only overlapping genes identified as induced in both the studies were EGR2 and COX2. Although an in depth discussion of each IEG identified is beyond the scope of this chapter, a brief overview of each IEG class based on their function and their significance in angiogenesis is presented below.

Transcription factors - In this study, six transcription factors formed a major component of the 17 IEGs induced by VEGF-A in endothelial cells. So far only three transcription factors identified in this study, EGR2, FOS and FOSB have been cited in the literature as being induced by VEGF-A. Induction of the FOS gene is not very surprising since its induction has been shown to be most promiscuous in various studies and is known to be widely induced during stress responses, exposure of cells to mitogens and hormones (Greenberg and Ziff, 1984; Kruijer et al., 1984; Mitchell et al., 1985; Sassone-Corsi, 1994). Like FOS many of the VEGF-A inducible IEGs such as, EGR2, and CYR61 have the SRE (serum response element) in their promoters (Treisman, 1995). The FOS gene also has CRE (cAMP-response element)

in its promoter which governs its induction as a response to stimulators of adenylyl cyclase pathway and changes calcium concentration (Sassone-Corsi et al., 1988). Members of the FOS gene family (FOS, FOSB, FOSL1 and FOSL2) are all leucine zipper proteins capable of heterodimerizing with JUN family of proteins, forming the AP-1 transcription factor complexes which govern cell differentiation, proliferation and other biological processes (Angel and Karin, 1991). Induction of FOSB gene and its dominant negative alternatively spliced counterpart ΔFOSB by VEGF and PlGF (placental growth factor) a member of VEGF growth factor family, which selectively activates through the VEGFR1 or Flt-1 receptor has been recently confirmed by Holmes and Zachary in 2004.

Early growth response gene 2 (EGR2) containing three tandem C2H2 type zinc fingers was first discovered by Joseph et al. in 1988 by using a mouse EGR1 to probe a cDNA library coupled with low stringency washes. Microarray analysis by Matsushima-Nishiu et al. in 2001 revealed a 2.5 fold induction of EGR2 by PTEN a tumor suppressor gene encoding a phosphatase, which downregulates the phosphatidylinositol-3-kinase pathway. It is now known that EGR2 mediates PTEN induced apoptosis in various cancer cell lines by inducing pro-apoptotic BNIP3L and BAK (Unoki and Nakamura, 2003). Other than this study, induction of EGR2 (3.2 and 1.1 fold in 0.5 and 2 hours respectively) by VEGF was also reported by Abe and Sato. However, the relevance of EGR2 induction in angiogenesis is not known.

Immediate early response 2 (IER2/ETR101/pip92) was first discovered by Charles et al. in 1990 as an IEG induced by serum growth factors and TPA (12-O-tetradecanoyl-phorbol-13-acetate) in fibroblasts. Induction of IER2 has since been

demonstrated as a response to activation of muscarinic acetylcholine receptors and by human T-cell leukemia virus type I Tax oncoprotein (von der Kammer et al., 2001; Chen et al., 2003). Although, IER2 has also been implicated to control apoptosis in primary neurons, the physiological function of this IEG is still unknown (Schneider et al., 2004).

Activating transcription factor 3 (ATF3) homodimer is a transcriptional repressor rather than an activator of promoters containing ATF/CRE elements. ATF3 is a 22 kDa basic leucine zipper protein (bZip) and is classified under ATF/CREB (cAMP responsive element binding) family of transcription factors (Hai et al., 1999). All proteins classified under the ATF/CREB family are capable of forming heterodimers with each other and also with other bZip proteins of the AP-1 and C/EBP (CCAAT/enhancer-binding protein) family. Although, ATF3 homodimer acts as a transcriptional repressor, it is now known that ATF3 heterodimers with JUN-D (c-jun) acts as a transcriptional activator (Hai and Hartman, 2001). Other bZip proteins capable of forming heterodimers with ATF3 include JUN-B, ATF2 and DDIT3/GADD153, one of the IEGs identified in this study. ATF3 is induced by various stress signals such as hypoxia or by cytokines, cycloheximide, anisomycin or agents capable of inducing JNK/SAPK pathway in cultured cells (Hai et al., 1999; Cai et al., 2000; Hai and Hartman, 2001; Wek et al., 2006). However, northern analysis has confirmed that induction of ATF3 is due to stimulation by VEGF-A and not due to adverse action of cycloheximide used to construct the cDNA library (this study). Even though ATF3 was discovered in 1989 by Hai et al., its physiological role remained a mystery until recently. It is now thought that ATF3 interacts with

p53 thereby stabilizing it and promoting its tumor suppressor activity (Yan and Boyd, 2006).

Similar to ATF3, DDIT3/CHOP (c/EBP homologueous protein) a bZip nuclear protein which dimerizes with C/EBP transcription factors is induced as a result of cellular stress (specifically endoplasmic reticulum) response (Ron and Habner, 1992; Oyadomari and Mori, 2004). Overexpression of DDIT3 results in cell growth arrest and may also induce apoptosis by decreasing the level of Bcl-2 protein (Matsumoto et al., 1996; Oyadomari and Mori, 2004). The DDIT3 protein under normal conditions is expressed at low levels in the cytosol, but undergoes phosphorylation mediated by p38 MAP kinase and is transported into the nucleus during cellular stress (Oyadomari and Mori, 2004).

Growth factors – Connective tissue growth factor (CTGF) like VEGF, ATF3 and DDIT3 is up-regulated under ischemia or low oxygen induced stress. Up-regulation of CTGF as a result of VEGF stimulation of endothelial cells has been confirmed in this study and by Suzuma et al in 2000. CTGF (CCN2) is classified under the CCN family of cysteine-rich matricellular proteins which play an important role in mitosis, adhesion, extracellular matrix production, chondrogenesis, osteogenesis and angiogenesis (Brigstock, 2003; Leask and Abraham, 2003; Perbal, 2004). Both CTGF and CYR61 (CCN1) are significantly induced by VEGF and estrogen, and are considered as downstream targets of TGF-β (Abe and Sato, 2001; Brigstock, 2003; this study). Similar to VEGF, CCN proteins are found associated with the heparan sulfate proteoglycans at the cell surface or in the extracellular matrix (Brigstock, 2003). It has been shown recently that CTGF can act as an anti-

angiogenic factor by binding to VEGF. This binding is abrogated by the selective digestion of CTGF by MMP-1, -3, -7 and -13 (matrix metalloproteinase) to release VEGF and recover its angiogenic potential (Hashimoto et al., 2003). Thus, there are two controversial roles of CTGF suggested so far, both as an anti-angiogenic and a pro-angiogenic factor. Future research defining its precise role in both physiological and pathological angiogenesis will indeed be exciting.

Cytokines – IL8 was first discovered as a chemotactic factor for leukocytes. Pro-angiogenic activity of IL8/CXCL8 was first demonstrated by Koch et al. in 1992. They demonstrated that IL8 triggered chemotaxis and proliferation of HUVEC and also induced angiogenesis when injected in rat cornea (Koch et al., 1992). Like VEGF, IL8 is also potently induced under hypoxic conditions (Papetti and Herman, 2002; Mizukami et al., 2005). Production of IL8 by endothelial cells in cutaneous inflammation and also by various tumors such as melanomas, non small cell lung carcinomas, colon and bladder cancer is well documented (Huang et al., 2002; Rosenkilde and Schwartz, 2004). Treatment of melanoma cells *in vitro* by humanized ABX-IL8 antibodies suppressed metastasis of melanoma cells and also decreased the induction of MMP-2, a key enzyme involved in degradation of basement membranes (Huang et al., 2002; Papetti and Herman, 2002). However, the induction of IL8 directly by VEGF-A has not yet been documented. IL8 was induced within 1 hour in endothelial cells stimulated with VEGF-A (figure 9).

Enzymes – Two enzymes PTGS2/COX-2 (cyclooxygenase) and DUSP1/CL100 (dual specificity phosphatase) were among the 17 IEGs induced by VEGF in endothelial cells. COX-2 is rapidly induced by various cytokines,

endotoxins, mitogenic factors and is inhibited by glucocorticoid (Cheng et al., 2005; Wu et al., 2005). The enzyme cyclooxygenase also known as prostaglandin-endoperoxide synthase is localized in the inner surface of the endoplasmic reticulum and nuclear envelope and governs the two step process of converting arachidonic acid to hydroperoxy endoperoxide and then to hydroxy endoperoxide (PGH_2) (Ristimaki, 2004; Rouzer and Marnett, 2005; Wu et al., 2005). PGH_2 is further converted to active prostanoids PGI_2 and PGE_2. Increased levels of COX-2 (via increased prostaglandin production) in tumors can confer a pro-angiogenic effect by increasing VEGF production, immunosuppression and by inhibiting endothelial cell apoptosis via increased production of Bcl-2 and Akt signaling (Gately and Li, 2004; Patrignani et al., 2005; Surh and Kundu, 2005). The pro-angiogenic effects of COX-2 are reversed by COX-2 inhibitors and NSAIDS (non-steroidal anti-inflammatory drugs), thus making it a possible therapeutic target against cancer, chronic inflammatory diseases and retinopathies (Iniguez et al., 2003).

Activation of the MAP kinase pathway is an essential part of many signal transduction cascades, translating the extracellular signal of mitogens or stress to a cellular response (Roux and Blenis, 2004). Prolonged activation of MAP kinase results in transformation of fibroblast cells or may inhibit or activate apoptosis depending on the extracellular signal the kinase involved (Sánchez-Pérez, 2000). Thus, each MAP kinase is tightly regulated by phosphatases and dephosphorylation at even one amino acid (tyr/thr) results in the inactivation of kinase. DUSP1/MKP1 (dual specificity phosphatase-1/MAP kinase phosphatase-1) was discovered in 1992 by Keyse and Emslie as a nuclear phosphatase transcriptionally induced by growth

factors, oxidative and heat stress. Usually the same set of signals governing the activation of MAP kinases also induce the respective phosphatases, thus representing a negative feed back loop to regulate the MAPK activity (Sohaskey and Ferrell, 2002). DUSP1 binds and inactivates ERK1/2, JNK and p38α isoforms (Slack et al., 2001).

Secreted factors/proteins –Induction of EGFL7/ZNeu1 (EGF-like domain, multiple 7) transcript by VEGF was first discovered in this study by Dr. Brown. Sequence analysis shows the presence of two EGF-like domains which can bind calcium along with a cysteine rich cluster capable of forming disulfide bonds. However, function of this protein was not known until 2003, when Soncin et al. demonstrated that ZNeu1 is secreted by endothelial cells and can inhibit migration of smooth muscle cells. ZNeu1 has no effect on proliferation of smooth muscle cells, unlike TGF-β and PTEN which affect both migration and proliferation. Based on this function they named this protein VE-statin (vascular endothelial statin). Localization of VE-statin in endoplasmic reticulum has been confirmed in our lab by Dr. Brown and by Soncin et al. EGFL7 transcripts are expressed on day 7.5 of embryonic development, slightly behind the flk-1 transcripts, the earliest marker for endothelial cell differentiation in uncommitted embryonic mesoderm. EGFL7 expression parallels with the expression of tie-2 and VE-cadherin endothelial markers (Sato et al., 1993; Shalaby et al., 1995; Soncin et al., 2003). Loss of function analysis of Egfl7 in zebra fish implies its crucial role in formation of vascular tubes or tubulogenesis, a key step in which vascular cords form vessels with a central lumen (Parker et al., 2004). Despite the confirmation of an important role played by EGFL7

in embryonic development, both the downstream targets and its precise role in angiogenesis is unknown.

Secretory/Exocytosis pathway - Exocyst 4 (EXOC4/SEC8) was first discovered in *S. cerevisiae* by Novick and Schekman in 1979 as one of the 10 SEC proteins responsible for regulating vesicular traffic from the Golgi to the plasma membrane. Bowser et al. in 1992 cloned SEC8 and concluded it to be an essential gene along with SEC15 for exocytosis in yeast. Recent evidence shows that the mammalian sec6/8 complex is essential for docking vesicles to specific sites on plasma membrane (Hsu et al., 1999). Sec6/8 complex is found both on the trans-Golgi network and at the plasma membrane cell-cell contact sites where it is involved in polarization of epithelial cells (Yeaman et al., 2001; Yeaman et al., 2003). Unfortunately, induction of SEC8 by Northern analysis could not be confirmed in this study.

Regulator of G-protein signaling – RGS3 (Regulator of G-protein signaling 3) is one of the more than 20 proteins in the RGS gene family discovered so far. RGS proteins can modulate the function of both activated GPCRs (G protein receptors) (Riddle et al., 2005; Abramow-Newerly et al., 2006). These proteins were initially identified as GAPs (GTPase activating proteins) capable of increasing the intrinsic GTPase activity of Gα subunit of heterotrimeric G proteins. But recent findings suggest that their role is much more complicated than previously thought. RGS3 was first discovered in 1996 by Druey et al. as a human homologue of yeast SST2 protein, which downregulates the MAP kinase signaling pathway induced through a pheromone activated GPCR. Mouse PDZ-RGS3 interacts with ephrin B and inhibits

the GPCRs activated by chemoattractants SDF-1 (Lu et al., 2001). Bidirectional signaling by ephrin B and ephrin B receptors govern key physiological processes such as axon guidance and blood vessel formation (Chapter1, Part I). Given the important role played by RGS3 in modulation of Ca^{2+} dependent $G\alpha_{q/11}$ linked muscarinic M_3 and gonadotropin-releasing hormone receptor, ephrin B signaling and inhibition of Gαs-stimulated adenylyl cyclase activation, its role in VEGF mediated angiogenesis is unknown (Tovey and Willars, 2004; Jaen and Doupnik, 2005; Abramow-Newerly et al., 2006). Induction of RGS3 by VEGF-A was not confirmed by northern analysis in this study due to lack of a good probe.

Tumor Suppressor Genes – RNA binding motif protein 5 (RBM5) was the only tumor suppressor gene discovered in this study as inducible by VEGF-A. Induction of a tumor suppressor gene by VEGF-A has not been reported in any of the studies designed to discern global expression patterns induced by VEGF (Abe and Sato, 2001). Thus, this was a not only an intriguing but an exciting avenue of research that I decided to pursue as my dissertation topic. Moreover, the fact that the function of this multi-modular gene was as yet unknown presented an opportunity to design multiple projects to discern the structure and function relationships of RBM5. An in depth discussion of RBM5 is presented in the next section of this dissertation (Chapter 1, Part II).

Other immediate early genes – MIDN, clones 532 and 648 are discussed in this section since their function is not yet known. Midnolin (MIDN/midbrain nucleolar protein) gene was first cloned by Tsukahara et al. in 2000 from mouse embryonic stem cells and is expressed in mesencephalon from embryonic day 11.5 to

12.5. It is implicated that MIDN localized in the nucleolus plays a role in regulation of genes involved in neurogenesis (Tsukahara et al., 2000). The probable human ortholog of mouse MIDN is present on chromosome 19p13.3.

DKFZp686D0473, a 3.3 kilobase cDNA isolated from human endometrium cancer cell line corresponds to insert isolated from clone 532 (Altschul et al., 1997). Northern analysis using clone 532 insert demonstrates the induction of two transcripts with molecular weights of approximately 6.5 and 3.5 kilobases during both 1 and 3 hours time points of VEGF-A stimulation (figure 9). BLAST search analysis of sequence corresponding to clone 648 reveals that it may correspond to GENE 33 polypeptide located on chromosome 1p36.12 (Altschul et al., 1997). Although domain search carried out by InterProScan shows the presence of two transmembrane domains and a signal peptide, there is no known molecular function for this gene at present (Zdobnov and Apweiler, 2001).

CONCLUSION

As a step towards defining the mechanism of VEGF-A action on endothelial cells I focused on identifying the immediate early genes induced by VEGF-A, a hitherto uncharted research area. Using differential screening of a cDNA library created by suppression subtractive hybridization technique I identified 17 immediate early genes up-regulated by the mitogenic stimulation of VEGF-A in the normally quiescent endothelial cells. VEGF-A mediated induction of a majority of the IEGs

identified in this study was further confirmed by Northern analysis thus, proving the efficacy of this powerful technique. Transcription factors such as FOS, ATF3, DDIT3 and EGR2 constituted a major portion of the 17 different IEGs identified in this study. Surprisingly, immediate early genes with varying functions such as, secreted factors, growth factors, cytokines and novel genes were also rapidly induced by VEGF-A. Undoubtedly, identification of 17 IEGs in this unique VEGF-A response gene set opened up numerous exciting avenues for further research, each possibly leading to a more clear understanding of the pleiotropic effects manifested by VEGF-A in endothelial cells. Among these 17 IEGs, I decided to focus on RBM5 (RNA binding motif protein 5), the only VEGF-A inducible tumor suppressor gene identified so far, whose role in angiogenesis if any seemed paradoxical. The second part of my dissertation summarizes research done on RBM5 (Chapter 1, Part II) and also investigates some of its structure and function relationships (Chapter 2, Part II).

PART II

CHAPTER 1

RNA BINDING MOTIF PROTEIN 5 – RBM5

INTRODUCTION

As mentioned in Part I Chapter 2, RBM5 was identified as one of the 17 immediate early genes induced in endothelial cells stimulated by VEGF-A. RBM5 represents an exciting finding since it is the only putative tumor suppressor gene (TSG) identified in this unique immediate early gene set comprising of many transcription factors and growth factors among others. This chapter summarizes the findings on RBM5 including its discovery, role as a tumor suppressor gene and structure and function relationships. When I started working on this project, the role of RBM5 as a regulator of apoptosis had been discovered by Sutherland et al. in 2000 and since has also been reported by Oh et al. in 2006.

DISCOVERY OF RBM5

RBM5 along with RBM6 was one of the genes identified on chromosome 3p21.3 by Wei et al. in 1996. Cytogenic analysis showed that chromosome 3p14-23

region was frequently deleted in malignancies of head, neck, gastrointestinal, breast, in addition to vestibular schwannomas, renal cell and small cell lung carcinomas (SCLC) (Naylor et al., 1986; van der Berg et al., 1996; Kok et al., 1997; Timmer et al., 1999a). Allelotyping, LOH (loss of heterozygosity) and overlapping homozygous deletion analyses in three SCLC cell lines NIH-H1450, NIH-H740 and GLC20 pinpointed a 370 kilobase region corresponding to the chromosomal locus 3p21.3 as a region most likely to harbor TSGs (Wei et al., 1996). This region was first cloned and mapped as a 600 kilobase contig in 1996 by Wei et al. in an attempt to discover putative tumor suppressor genes present at this region. Drabkin et al. and Timmer et al. in 1999 simultaneously reported presence of LUCA15 (lung cancer 15) and RBM5, respectively corresponding to Gene 15 discovered by Wei et al. in 1996.

RBM5 HOMOLOGUES

Sequence comparison of RBM5 using HomoloGene (National Center for Biotechnology Institute website) shows that it is evolutionary conserved across the species with homologues found in rat (98.3%), mouse (89.9%), *Drosophila* (35.1%), *Arabidopsis* (33.1%) and zebrafish (99.6%). A cartoon representing taxonomic tree constructed using the SMART software demonstrates this in figure 10 (Shultz et al., 1998; Letunic et al., 2006). RBM5 shares a 51% homology with RBM10 (DXS8237E) located on Xp11.23 and a 30% homology with RBM6 present on the telomeric end of 3p21.3 next to RBM5 (Coleman et al., 1996; Timmer et al., 1999a).

Another gene UBE1L present on chromosome 3p21 is homologous to UBE1 on the X chromosome next to RBM10. The orientation between RBM10 and UBE1 on X chromosome and RBM6, RBM5 along with UBE1L on chromosome 3 is inverted (figure 11). RBM6 is closely related to RBM5 in terms of exon structure with over nine exons sharing more than 25% homology (Timmer et al., 1999a). Thus, these data suggests that there has been a rearrangement of chromosome Xp11 (3-23) in 3p 21.3 region at some point in evolution (Timmer et al., 1999b). The region Xp11.3-11.23 is known to be a hotspot for neurogenetic disorders (Thiselton et al., 2002).

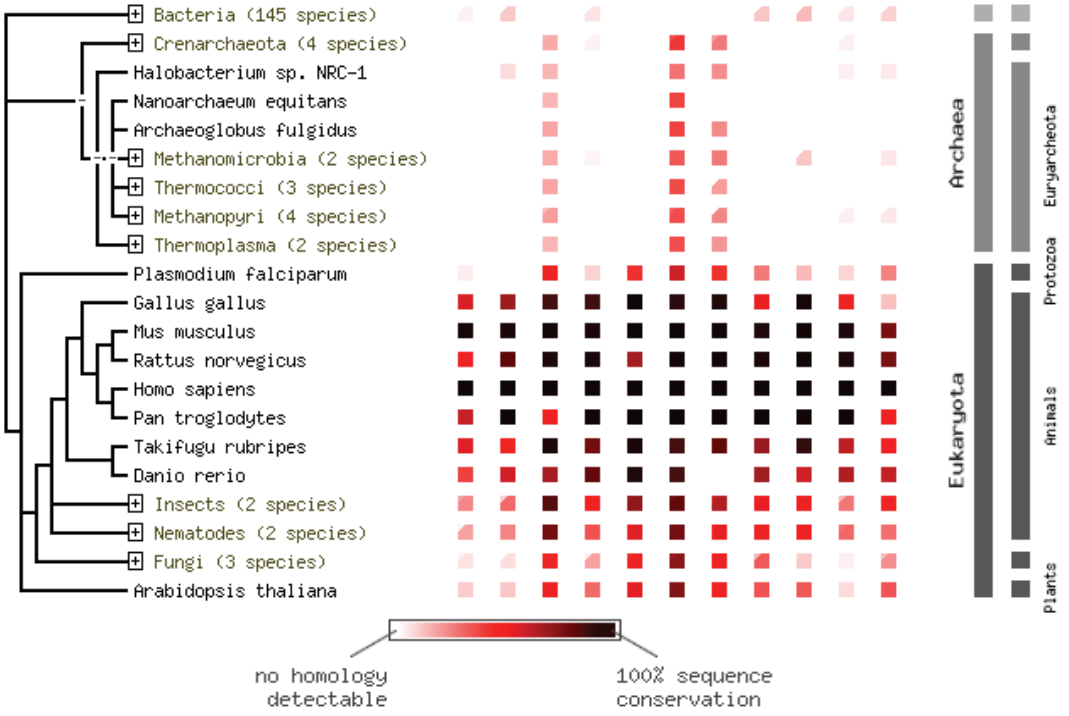

Figure 10: A model constructed using the SMART (Simple Modular Architecture Research Tool) software demonstrating the presence of proteins homologous to RBM5 across the species, in eukaryotes – rat, mouse, chicken and also in plants – *Arabidopsis*. Even though there is negligible presence of homologous proteins in Archae, proteins sharing almost 100% similarity with RBM5 exist throughout eukaryota suggesting its evolutionary significance. The SMART program is provided online by EMBL (European Molecular Biology Laboratory) through EBI.

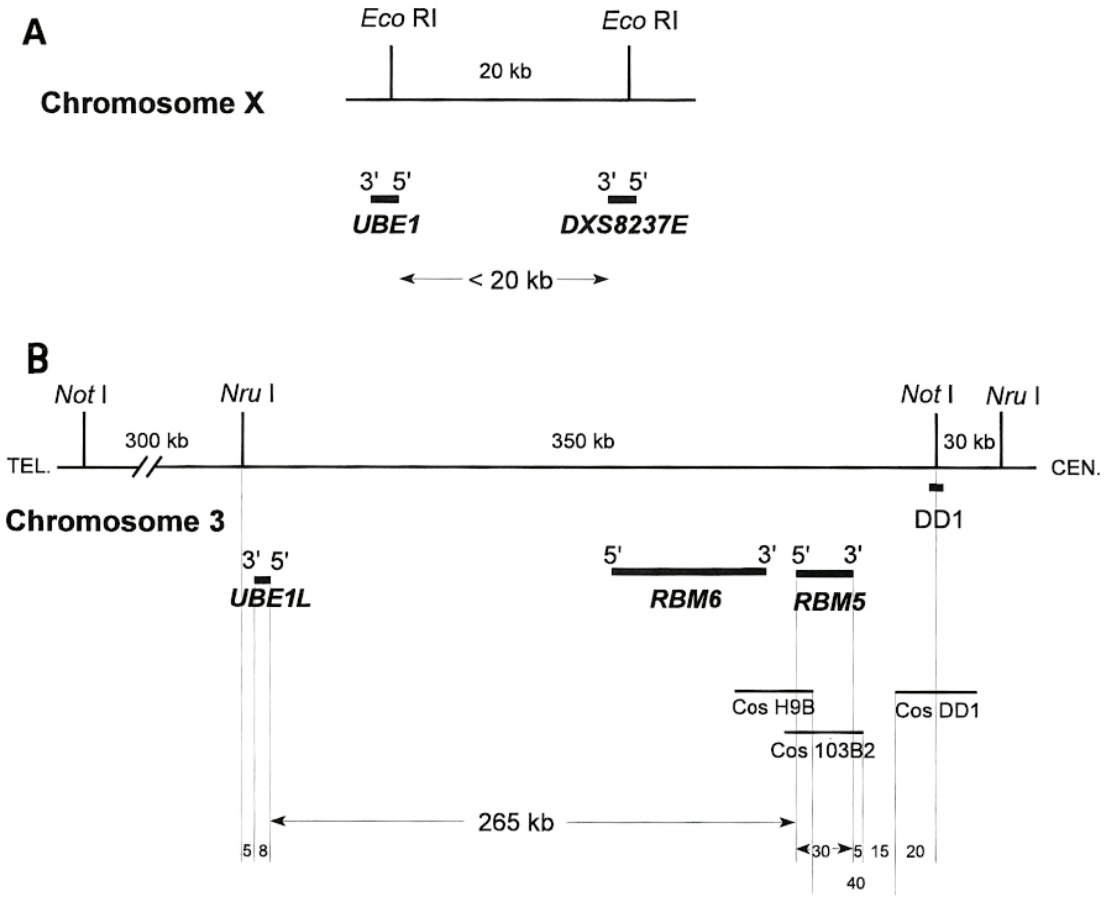

Figure 11: Chromosomal location of RBM5 with respect to RBM6 and UBE1L on chromosome 3p21.3. Part A shows the gene arrangement of an RBM5 homologue RBM10 (DXS8237E) with respect to UBE1 on chromosome Xp11.3-11.23. Comparison of chromosomal regions Xp11.3-11.23 (A) and 3p21.3 (B) suggests that there was an inverse genetic rearrangement of Xp11.3-11.23 region during evolution. RBM6 which is present on the telomeric end shares a greater similarity with RBM5 than with RBM10, indicating that RBM6 resulted from gene duplication of RBM5. The numbers below indicated the distance between the genes in kilobases. Both the regions 3p21.3 and Xp11.3-11.23 are known hotspots for various cancers and neurogenetic disorders, respectively. This figure was adapted from Timmer et al., 1999b.

RBM5 DOMAINS

The 2448 basepair RBM5 coding sequence is made up of 25 exons ranging from 61 basepairs (exon 8) to 627 basepairs (exon 25) and codes for a 815 amino acid protein with a molecular weight of 120 kDa (Timmer et al., 1999b; Sutherland et al., 2000; this study). The annotated sequence of 3135 basepairs RBM5 mRNA depicting exon boundaries and SNP as provided by Ensembl Transcript report available at EMBL (European Molecular Biology Library) is shown in figure 12. Sequence analysis using PROSITE, PSORT and SMART programs reveal multiple domains present in the full-length RBM5 protein (Bairoch, 1991; Schultz et al., 1998; Nakai and Horton, 1999). The various domains along with their amino acid positions are given below.

Domains	**Amino acid positions**	**Exon number**
BIPARTITE NLS [**RR**DSDYKRSSDD**RRGDR**]	34-50	3
RRM1/RNP1 (OCTAMER) [RGFAFVEF]	140-147	6
ZnF1 (ZnF type C4) [C(x2)C(x10)C(x2)C]	181-210	7-8
RRM2/RNP1 (OCTAMER) [RGFAFVQL]	274-281	10
GLUTAMINE RICH REGION	362-385	13-14
OCTAMER REPEAT/OCRE DOMAIN	452-511	17-18
KEKE MOTIF	523-535	19
AMPHIPATHIC HELIX	536-553	19
COILED COIL	614-648	21
ZnF2 (ZnF TYPE C2H2) [C(x2)C(x12)H(x6)H]	647-677	21
COILED COIL	672-711	21-23
BIPARTITE NLS [**RR**EKYGIPEPPE**PKRKK**]	708-724	23
GLYCINE RICH REGION (G PATCH DOMAIN)	743-789	25

Table 4: Various domains and their respective positions in the full-length 815 amino acid RBM5 protein along with contributing exons are highlighted (Timmer et al., 1999b).

RNA Binding Motif Protein 5

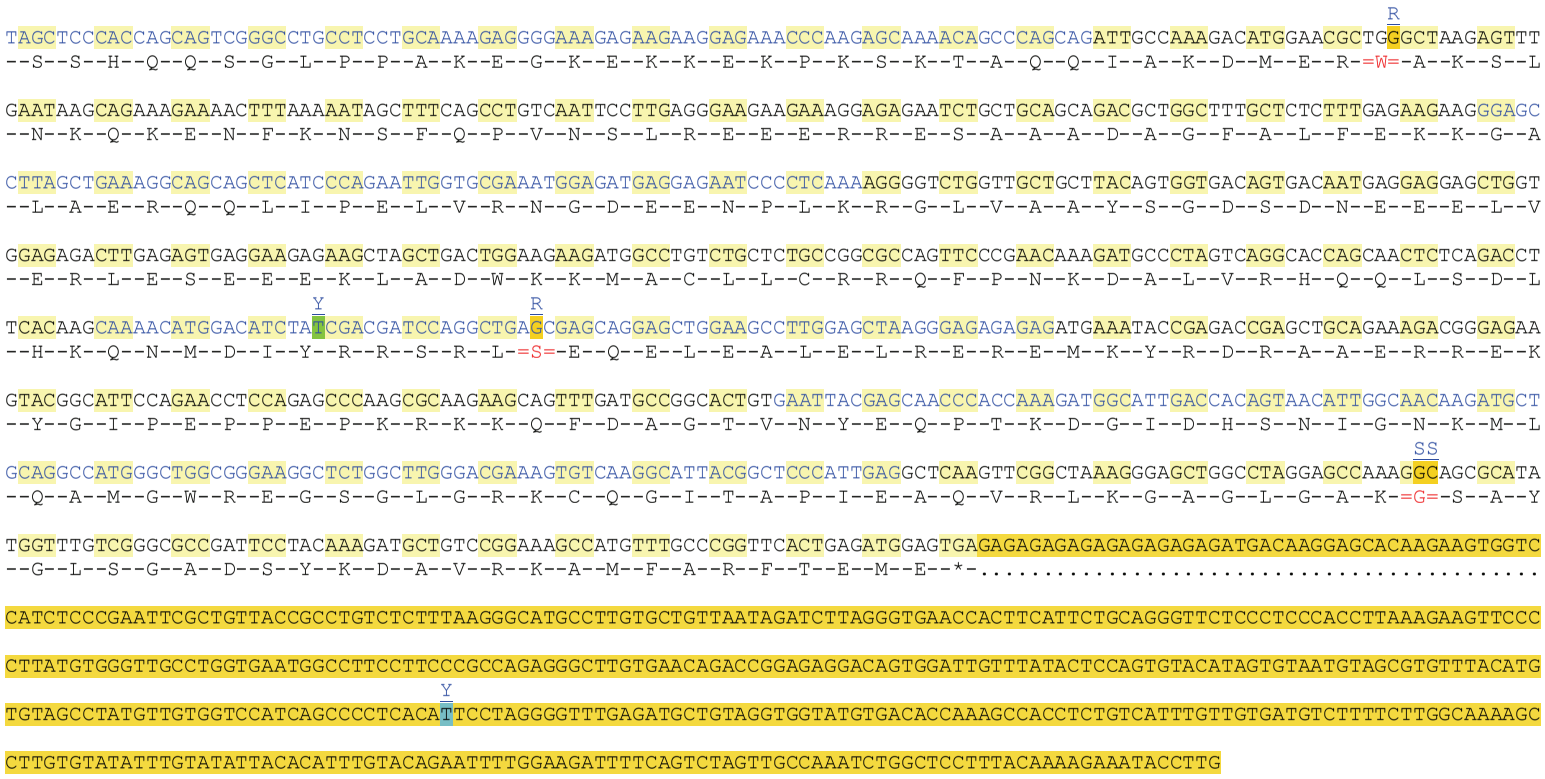

Figure 12: Ensembl Transcript report for RBM5. Full-length RBM5 mRNA is made up of 3135 bp containing 2447 bp coding sequence for 815 amino acid protein. The first methionine codon is located at 149 bp with an in frame stop codon at 2446 bp followed by a 3' UTR of 504 bp. There are six single nucleotide polymorphisms in the coding sequence most of which occur in the wobble base. Alternate exons are colored blue and black demarking exon-exon boundaries. The above figure was modified from Ensembl Transcript report for RBM5 (ENSG00000003756) available online through EMBL.

As the name suggests RBM5 has two RRM (RNA-recognition motif) domains RRM1 (98-178) and RRM2 (231-315). Each RRM domain comprises two conserved sequence motifs, an octapeptide (RNP1) and a hexapeptide (RNP2) embedded within a highly variable sequence of approximately 80-100 amino acids. The structure of RRM domain is βαββαβ, with the conserved octamer and hexamer sequences present in the β-sheets. Both RNP1 and RNP2 domains can function in RNA binding. However, the specificity of RNA bound is determined by the amino acid residues surrounding the RNP domains (Burd and Dreyfuss, 1994). The RNP2 domains (hexapeptide) of RBM5 are less conserved than the RNP1 (octapeptide) domains (Sutherland et al., 2005). The N-terminal and C-terminal portions of RBM5 produced in *E.coli* and HEK293 cells have been shown to preferentially bind poly (G) RNA homopolymer tracts *in vitro* (Drabkin et al., 1999; Edamatsu et al., 2000). This is surprising since the C-terminal portion contains only the G-patch domain and a zinc finger domain but none of the RRM domains. Along with two RRM domains RBM5 also contains two bipartite nuclear localization signals (NLS) and two types of zinc finger domains, C2H2 and RanBP2 type (C4). RanBP2 (Ran Binding Protein) zinc finger domains have been shown to bind RanGDP and exportin-1 proteins which regulate the nucleocytoplasmic transport within the cell (Singh et al., 1999). Zinc finger of the C2H2 type mediating nucleic acid binding were first found in *Xenopus* oocytes transcription factor TFIIIA (Miller et al., 1985). These domains are commonly found across the species in transcription factors such as EGR2 and also *Drosophila* proteins Hunchback and Escargot to mention a few (Rosenfeld and Margalit, 1993). Bipartite NLS are discussed in detail in Chapter 2 (Part II).

In addition to the above mentioned domains there are also a number of low complexity regions within the RBM5 protein. These regions are usually enriched in one or more amino acids. The N-terminal region is rich in arginine residues and the C-terminal contains the G-patch domain. The G-patch domain is about 40 amino acids long with seven highly conserved glycine residues and is thought to aid in RNA binding (Aravind and Koonin, 1999). OCRE (Octamer Repeat) domain consisting of imperfectly repeated octameric sequences forming a β-strand was recently described in RBM5 and VG5Q protein, an angiogenic factor implicated in a vascular disorder, the Klippel-Trenaunay syndrome (Callebaut and Mornon, 2005). Although, OCRE domains are common in a family of RNA binding motif proteins containing both RBM5 and RBM10, the function of this domain remains to be elucidated.

RBM5 SPLICE VARIANTS

Screening of multiple tissue northern blots have shown the presence of two RBM5 transcripts of 3.4 kb and 7.4 kb in length (Drabkin et al., 1999; Mourtada-Maarabouni et al., 2002; this study). The expression of RBM5 is highest in adult thymus, fetal kidney and is also expressed in various organs such as heart, brain, placenta and skeletal muscle (Drabkin et al., 1999; Lerman and Minna, 2000; Sutherland et al., 2000). Lerman and Minna have also reported presence of 1.5 kb and 2 kb RBM5 transcripts in some tissues, although these transcripts have not been detected either in this study or by Sutherland et al. (2000). A number of splice variants have been predicted by Sutherland

et al. (2000 and 2005) by conducting RT-PCR with RBM5 specific primers (figure 13). The first splice variant RBM5+5+6 retains introns 5 and 6 and was discovered as a partial 5' cDNA Clone 26 by Sutherland et al. (2000) and Clone 86 by Edamatsu et al. (2000). The full-length clone representing RBM5+5+6 has not yet been isolated. Clone 26 codes for a 21 kDa protein when overexpressed in Jurkat cells or translated *in vitro* by rabbit reticulocyte lysate. Depending on the molecular weight of the protein produced it seems that translation of the RBM5+5+6 mRNA terminates within intron 6 with the intron 5 spliced out (Mourtada-Maarabouni et al., 2003). The second splice variant RBM5+6 retains intron 6 with the open reading frame also terminating within intron 6. Although the predicted molecular weight of this splice variant is 17 kDa, this product has not been detected thus far. The absence of any protein product corresponding to RBM5+5+6 and RBM5+6 transcripts may be attributed to nonsense-mediated decay (NMD) (Mourtada-Maarabouni et al., 2003; Sutherland et al., 2005). Both RBM5+5+6 and RBM5+6 splice variants appear to be represented by the 7.4 kb transcript on the northern analysis (Drabkin et al., 1999; Sutherland et al., 2000; this study). The NMD hypothesis might be true since the amount of 7.4 kb transcript detected is always lower than the 3.4 kb transcript (this study).

A third splice variant RBM5Δ6 without exon 6 overexpressed in three T-leukaemic cell lines was cloned by Mourtada-Maarabouni et al. in 2003. As seen from table 4 the RNP1 domain of RRM1 is coded for by exon 6. RBM5Δ6 codes for a 17 kDa protein since deletion of exon 6 creates a frameshift mutation. Lastly, a 326 bp Je2 cDNA sequence antisense to intron 6 was isolated from bone marrow library. Overexpression of Je2 in CEM-C7 T cells reduces the amount of RBM5 protein and up-

regulates 17 kDa protein probably coded by RBM5Δ6. This finding cannot be explained by antisense effect of Je2 since neither full-length RBM5 not RBM5Δ6 contain intron 6 a region complimentary to Je2 (Sutherland et al., 2005).

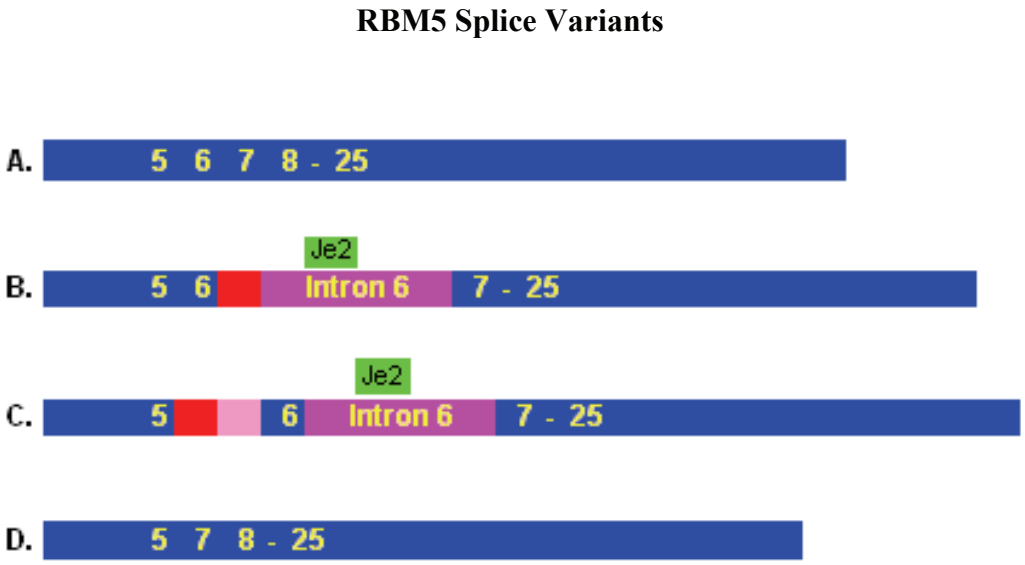

Figure 13: Structure of RBM5 and its splice variants. Full-length 3135 bp RBM5 (A) mRNA is made up of 25 exons coding for 815 amino acid protein with a molecular weight of 100-120 kDa. The predicted stop codon within introns 6 and 5 (pink boxes) for RBM5+6 (B) and RBM+5+6 (C), respectively are shown as red boxes. RBM5+6 and RBM+5+6 probably encode 7.4 kb transcript seen on northern blots. A 326 bp antisense Je2 (green boxes) cDNA maps to a region within intron 6 of RBM5+6 and RBM+5+6 splice variants. Although, overexpression of Je2 protects cells from apoptosis the mechanism for this effect is not yet known. The fourth splice variant RBM5Δ6 (D) encodes a 17 kDa protein since a frameshift mutation due to deletion of exon 6 leads to early termination of the transcript. The exon and intron lengths are not drawn to scale. This figure was adapted from Sutherland et al., 2005.

RBM5 - TUMOR SUPPRESSOR GENE AND APOPTOSIS REGULATOR

RBM5 was first described as Gene 15 by Wei et al. (1996), as a potential tumor suppressor gene (TSG) since it was frequently deleted in various cancers and 100% deleted in non small cell lung carcinomas. Scanlan et al. in 1999 using SEREX identified antibodies against Ren-9/RBM5 in patients suffering from renal cell carcinomas, thus identifying it as a potential tumor antigen. The level of RBM5 was down-regulated in vestibular schwannomas and in rat cells transformed with a mutated constitutively active Ras (G12V) protein (Edamatsu et al., 2000; Welling et al., 2002). However, the role of RBM5 as a TSG was disputed because of consistent expression and a lack of any sequence altering mutations within the RBM5 genomic region in several of the lung cancer cell lines studied (Lerman and Minna, 2000). Also, RBM5 mRNA is up-regulated in many aggressive breast cancers expressing Her-2/*neu* oncogene (Oh et al., 1999). Some of the evidence summarized below however may suggest tumor suppressor activity of RBM5.

Overexpression of full-length RBM5 in CEM-C7 T cells arrested the cell cycle in G1 phase and reduced the growth of MCF-7 $RBM5^{-/-}$ anchorage dependent and independent breast adenocarcinoma cells (Oh et al., 2002; Rintala-Maki et al., 2004b). Growth arrest was also observed in A9 mouse fibrosarcoma cells (anchorage independent) and A549 lung cancer cells (Oh et al., 2006). Ectopic expression of RBM5 along with subcutaneously injected A9 cells in nude mice resulted in tumor suppression (Oh et al., 2002). Recent findings by Oh et al. (2006) and Mourtada-Maarabouni et al. (2006) imply that tumor suppressor activities of RBM5 are mediated by both cell cycle

arrest and apoptosis. RBM5 sensitizes Jurkat T cells to apoptosis induced through Fas (CD95), TNF-α or TRAIL death receptor ligands (Rintala-Maki and Sutherland, 2004a). Downstream effects of RBM5 analyzed by microarray showed induction of Stat5b and BMP5 and down-regulation of Pim-1 (proto-oncogene), AIB1, BIRC3 (caspase antagonist) and CDK2 (Mourtada-Maarabouni et al., 2006). Decreased levels of cyclin A and phosphorylated RB and increased expression of pro-apoptotic Bax protein were also observed in A549 lung cancer cells stably transfected with RBM5 (Oh et al., 2006). Together these results suggest that RBM5 may act as a tumor suppressor gene also regulating apoptosis.

Given that full-length RBM5 is pro-apoptotic, splice variant RBM5Δ6 and antisense Je2 both act as anti-apoptotic. Overexpression of antisense Je2 in CEM-C7 cells rescues the cells from FasL, TNF-α and dexamethasone mediated apoptosis. Similar suppression of Fas mediated apoptosis by Je2 is also observed in Jurkat T cells (Mourtada-Maarabouni et al., 2002). Cell proliferation and anti-apoptotic effects of RBM5Δ6 are observed in CEM-C7 cells but not in Jurkat cells (Mourtada-Maarabouni et al., 2003).

OVERVIEW

RBM5/LUCA15 was first isolated in 1996 as a potential tumor suppressor gene frequently found deleted in the lung cancer hotspot 3p21.3. Based on recent evidence it is tempting to hypothesize that the tumor suppressor activity of RBM5 may be mediated

by apoptosis. However, the exact pathway by which RBM5 and its splice variants can differentially mediate apoptosis is still unclear. Up-regulation of RBM5 by Her-2/*neu* in breast cancer cells and as an immediate early gene by VEGF-A in endothelial cells seems anomalous with the current evidence and does not support the putative role of RBM5 as a TSG. However, it should be noted that the putative VEGF-A induced immediate early gene set also contains negative regulators other than RBM5 such as DUSP1, ATF3 and EGR2 (Chapter 1, Part I).

The following work in this dissertation is an attempt to understand and shed some light on RBM5. Based on the domains present in RBM5 it can be hypothesized that RBM5 might be a nuclear protein and functions in RNA metabolism. Chapter 2 in this section analyzes the localization of RBM5 in specific nuclear domains and also dissects the two bipartite NLS affecting its nuclear localization. Moreover, the two bipartite NLS are differentially distributed in RBM5 and its splice variants. Thus, determining the localization of RBM5 in specific nuclear domains might give a clue to the potential function of RBM5 and its splice variants. Additionally, discerning the identity of the RNA species bound by RBM5 may abet in dissecting the mechanism by which it plays a seemingly common role in different scenarios of apoptosis, angiogenesis and tumor suppression. Production of full-length RBM5 protein in vitro is a step closer towards the goal of identifying the family of RNA bound by RBM5 by conducting SNAAP analysis (Appendix A). Finally, I have also attempted to analyze the signal transduction cascade emerging from VEGF-A leading to the induction of RBM5 by using inhibitors and quantitative real time RT-PCR analyses (Appendix B).

CHAPTER 2

SITE-DIRECTED MUTAGENESIS OF BIPARTITE NUCLEAR LOCALIZATION SIGNALS OF RBM5

INTRODUCTION

As discussed in chapter 1, RBM5 (RNA binding motif protein 5) a putative tumor suppressor gene and regulator of apoptosis is evolutionary conserved across a variety of organisms and taxa. The RBM5 protein contains two RRM domains, two zinc finger motifs and two bipartite nuclear localization signals along with a G-patch domain. The correct subcellular localization of a protein is essential to ensure its correct function/activity. There are two bipartite nuclear localization signals (NLS) located near the N-terminal and C-terminals ends of RBM5 protein making it very likely that RBM5 is a nuclear protein.

Ions and molecules smaller than 50-60 kDa can passively transit in and out of the double membrane bound nucleus gated by nuclear pore complexes (NPC). However, larger molecules such as RNA and the 100-120 kDa RBM5 protein are actively transported through the NPC via a multi-step process by a superfamily of nuclear transport receptors known as importins or karyopherins. Importin-α, containing an NLS-binding site made of armadillo repeats, recognizes and binds to the cargo proteins to be transported via NLS signal (Pemberton and Paschal, 2005; Poon and Jans, 2005).

Importin-β binds to this complex via the IBB (importin-β binding) domain on importin-α and docks it on the cytosolic face of NPC which then passes through to the nuclear side. In some cases importin-β can directly bind to the cargo protein, bypassing the adaptor protein importin-α (Pemberton and Paschal, 2005; Poon and Jans, 2005). Binding of karyopherins to their cargo is mediated by small GTP binding proteins known as Ran (Ras-related nuclear protein). Activity of Ran is in turn regulated by proteins controlling its GTPase activity (RanGEF and RanGAP) and its import back into the nucleus by NTF2 (Moore, 1998; Pemberton and Paschal, 2005). The entire process of nuclear import is thus dependent on the differential concentration of RanGTP in the nucleus as compared to that in the cytosol (figure 14). In contrast to nuclear import, nuclear export depends on NES (nuclear export signal) and is mediated by exportins (CAS, Crm1). No known NES domains have been predicted in RBM5 so far.

A majority of the domains constituting the nuclear localization signals are made up of karyophilic clusters of the positively charged amino acid residues arginine and lysine (Boulikas, 1993). Classical NLS are classified either as monopartite or bipartite. The first monopartite NLS (PKKKRKV) was discovered in SV40 large T antigen by Kalderon et al. in 1984. Bipartite NLS with split clusters of karyophilic amino acids reconstituted by protein folding was first discovered in *Xenopus* nucleoplasmin protein by Robbins et al. in 1991. The consensus for bipartite NLS is a cluster of positively charged amino acids (Arg/Lys) separated by 10-12 mutation tolerant spacer region followed by another cluster with at least three out of five amino acids being either arginine or lysine residues (table 5).

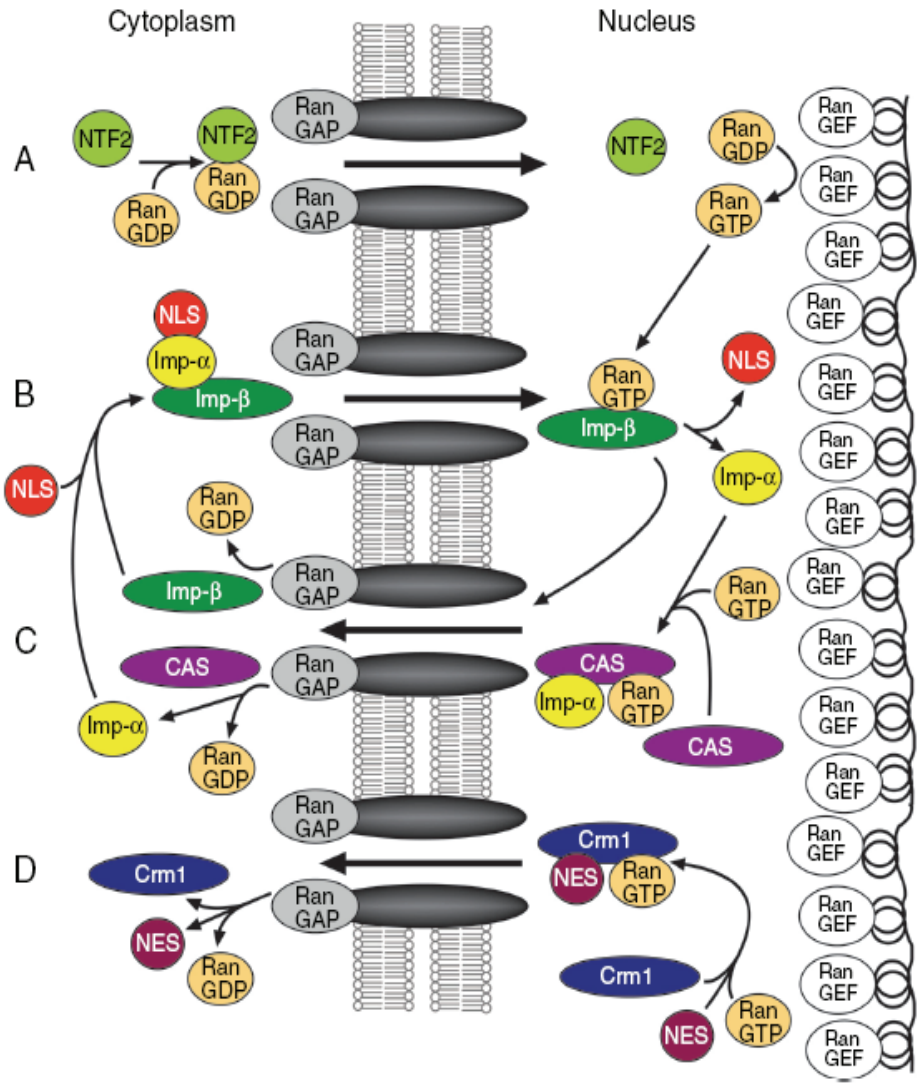

Figure 14: Key players of the nuclear import and export pathway. Differential concentrations of small GTPase protein-Ran a key mediator of both the nuclear export and import pathway in nucleus and cytosol is regulated by NTF2, RanGAP and RanGEF (A). Protein displaying NLS are transported inside the nucleus by forming a complex with importin-β alone or along with an adaptor protein importin-α (B). Once the complex reaches the nucleus, RanGTP selectively binds to importin-β thereby, releasing the cargo. Importin-α is recycled back into the cytosol by exportin 2 or CAS (C). The nuclear export also controlled by differential concentration of Ran operates in an opposite fashion as compared to nuclear import. Nuclear export is dependent on NES domains and action of exportin 1 or Crm1 (D). This picture was adapted from Pemberton and Paschal, 2005.

Many nuclear proteins have atypical NLS instead of the classical monopartite or bipartite type. The best known examples NLS domains deviating from the classical NLS are that found in c-Myc (PAAKRVKLD), KNS sequence of hnRNP K and the 38 amino acid M9 signal of hnRNP A1 (Dang and Lee, 1988; Pollard et al, 1996; Michael et al., 1997).

It is not uncommon to see nuclear proteins containing one or more functional NLS domains. However, some cytosolic proteins also contain sequence motifs similar to bipartite NLS. Thus, not all putative NLS are functional (Dingwall and Laskey, 1991; Zacksenhaus et al., 1993). On the other hand, some cytosolic proteins such as hormone receptors (androgen receptor), transcription factors (p53, NFκB) or kinases (PKC, MAPK) when activated rapidly translocate to nucleus as a result of hidden or cryptic NLS exposed either by phosphorylation or dephosphorylation or dissociation of an inhibitory subunit (Shaulsky et al., 1990; Boulikas, 1993 and 1996; Kau and Silver, 2003; Pemberton and Paschal, 2005).

Although nuclear localization of RBM5 was confirmed by Edamatsu et al. in 2000 using RBM5 and c-myc epitope fusion construct, the subnuclear localization of RBM5 was not defined. Using deletion mutagenesis on c-myc constructs they also suggested that the C-terminal NLS may be responsible for the nuclear localization of RBM5. However, numerous studies have shown that the nucleus is organized in various subnuclear domains such as Cajal bodies, nucleoli, PML bodies, OPT domain nuclear speckles and paraspeckles (Spector, 2001). Identifying the subnuclear localization of RBM5 may also help in predicting its probable function. Therefore, I aimed to resolve the subnuclear localization of RBM5 by using enhanced GFP (green fluorescent protein) fusion constructs.

Protein	NLS	Reference
	Monopartite NLS	
SV40 large T antigen	PKKKRKV	Kalderon et al., 1984
v-Jun	KSRKRKL	Chida and Vogt, 1992
Choline acetyltransferase	ELPAPRRLRWK	Gill et al., 2003
	Bipartite NLS	
Xenopus nucleoplasmin	KRPAATKKAGQAKKKKLDK	Robbins et al., 1991
Human RB protein	KRSAEGSNPPKPLKKLR	Zacksenhaus et al., 1993
S. cerevisiae SW15	KKYENVVIKRSPRKRGRPRK	Moll et al., 1991
Human IL 5	KKYIDGQKKKCGEERRRVNQ	Jans et al., 1997
Human p53	KRALPNNTSSSPQPKKKP	Shaulsky et al., 1990
Parafibromin (TSG)	KRAADEVLAEAKKPR	Hahn and Marsh, 2005
Ste20-like protein kinase	KKTSYLTELIDRYKRWK	Lee et al., 2004
Rbm5 NLS1 (putative)	RRRDSDYKRSSDDRRGDRY	Edamatsu et al., 2000 and this study
Rbm5 NLS2 (putative)	ERREKYGIPEPPEPKRKKQ	
Consensus	K/R K/R-10-12 aa-K/R K/R K/R	
	Atypical NLS	
RanBP3	PPVKRERTS	Welch et al., 1999
c-myc	PAAKRVKLD	Dang and Lee, 1988

Table 5: Examples of various types of nuclear localization signals (NLS) identified so far. The consensus for monopartite NLS is a contiguous cluster of four to five karyophilic amino acids as compared to the bipartite NLS where the cluster is divided by a mutation resistant spacer region of 10-12 amino acids. This table was partially adapted from Romanelli and Morandi, 2002.

One of the major advantages of using EGFP to study localization is that recombinant fluorescent proteins can be discerned directly in live cells diminishing any fixation and staining artifacts introduced by processing cells for detection of epitope tags by indirect immunofluorescence. Moreover, EGFP fusion constructs have been reliably used to discern the localization and dynamics of nuclear proteins in many studies (Phair and Misteli, 2000; Bubulya and Spector, 2004). I further used this recombinant EGFPRBM5 construct and engineered point mutations in individual RBM5 NLS to discern the functionality of the two bipartite NLS. Dissecting the functional bipartite NLS of RBM5 by site-directed mutagenesis instead of deletion mutants considerably improves the chances of conserving the protein confirmation of RBM5 thus, eliminating any false positive results obtained due to exposure of hidden NLS. Results from this study indicate that RBM5 is localized in the nuclear speckles and its nuclear targeting is governed by only one bipartite NLS.

MATERIALS AND METHODS

Plasmid constructs

Construction of pEGFPRBM5 - RBM5 coding sequence isolated from HUVEC cDNA by Dr. Brown in our lab was inserted into pEGFP-N2 vector MCS (Clontech) between the Sac I and EcoR I restriction sites. The RBM5 open reading frame was extended into EGFP by changing the RBM5 stop codon (TGA) to glutamic acid (GAA) constituting a part of the EcoR I restriction site (GAATTC).

Construction of pEGFPRBM5NLS1M – The entire N-terminal bipartite NLS (NLS1) between Sac I and BsiHKA I (New England Biolabs) sites was mutated by PCR amplification in two overlapping pieces, NLS1MA and NLS1MB. The two pieces were constructed using four oligonucleotides, with all the mutations engineered into two overlapping oligonucleotides spanning the first bipartite NLS. The sequences (5'-3') of the four oligonucleotides depicting restriction sites (underlined), mutated nucleotides (bold) and overlapping section between the two oligonucleotides (italics) are as below:

Sac I
1) NLS1.1 (GCGCGC<u>GAGCTC</u>ATCGAAGGTCGCATGGGTTCAGAAAAA CGAGTG)

2) NLS1.2 (*ATCATCACTAGAA**A**CT**G**TTG**G**A*ATCTGAGTC**G**CT**C**CCCTGCT)

3) NLS1.3 (*T**C**CAA**C**AG**T**TCTAGTGATGAT*G**G**AG**C**GGTGATAG**T**TATGAT)

EcoR I BsiHKA I
4) NLS1.4 (GCGCGC<u>GAATTCGTGCTC</u>ACCATAGTCACCATCTGAATG)

RBM5 coding sequence spliced out from pEGFPRBM5 (Sac I-EcoR I) and gel purified using DEAE membrane (see Chapter 2, Part 1) was used as a template in a 50 µl PCR reaction to make two pieces (A and B) of NLS1M as follows:

10X Advantage 2 PCR buffer (Clontech)	5 µl
50X dNTP	1 µl
10 µM NLS1.1 (A)/NLS1.3 (B)	2 µl
10 µM NLS1.2 (A)/NLS1.4 (B)	2 µl
Sac I - EcoR I (pEGFP)RBM5	1 µl (25 ng)
50X polymerase	1 µl

The PCR cycle parameters used were: 1X 95ºC/1 minute; 9X 95ºC/30 seconds, 60ºC/30 seconds, 68ºC/1 minute and 14X 95ºC/30 seconds, 68ºC/1 minute. The NLS1M pieces

made by PCR were gel purified using DEAE membrane, redissolved in 25 µl of dH_20 and used to reconstruct the entire NLS1M by PCR as follows:

NLS1MA	1 µl
NLS1MB	1 µl
10 µM NLS1.1	2 µl
10 µM NLS1.4	2 µl
10X Advantage 2 PCR buffer (Clontech)	5 µl
50X dNTP	1 µl
50X polymerase	1 µl

The PCR cycle parameters used were: 1X 95ºC/1 minute; 9X 95ºC/30 seconds, 37ºC/30 seconds, 68ºC/1 minute and 14X 95ºC/30 seconds, 68ºC/1 minute. The amplified NLS1M was gel purified and digested with Sac I and EcoR I (Promega) enzymes and ligated into CIP dephosphorylated pGEM®3Z(f+) vector digested with the same enzymes. Competent JM109 cells (Promega) were transformed with this ligation mixture and plated on LB agar plates containing 100 µg/ml ampicillin. After overnight incubation at 37°C the recombinant colonies were picked up and processed further for plasmid isolation as described before in Chapter 2, Part 1. Presence of NLS1M insert was confirmed by dye terminator sequencing method at our campus facility. The NLS1M insert was spliced out from pGEM®3Z(f+)NLS1M using Sac I and BsiHKA I, gel purified and used to construct pEGFPRBM5NLS1M by performing a three fragment ligation as follows:

(Sac I - EcoR I) CIP dephosphorylated pEGFP-N2 vector	1µl (100 ng)
(Sac I - BsiHKA I) NLS1M	1µl (20 ng)

(BsiHKA I - EcoR I) RBM5	1 µl (50 ng)
10X T4 DNA ligase buffer (Promega)	1 µl
T4 DNA ligase	1 µl
dH_2O	5 µl

Ligation reaction was incubated overnight at 16ºC. Competent JM109 cells were transformed with the above ligation reaction and plated on LB agar plates containing 30 µg/ml of kanamycin. After, overnight incubation recombinant colonies were processed for plasmid isolation and sequenced to confirm the orientation of ligations as described before.

Construction of pEGFPRBM5NLS2M – The second bipartite NLS flanked by the Nhe I and EcoR I sites was mutated by assembling two pieces NLS2MA and NLS2MB using the same PCR amplification strategy used to construct NLS1M. The sequences (5'-3') of the four oligonucleotides depicting restriction sites (underlined), mutated nucleotides (bold) and overlapping section between the two oligonucleotides (italics) are as below:

BamH I Nhe I
1) NLS2.1 (GCGCGC<u>GGATCCGCTAGC</u>TGACTGGAAGAAGATG)

2) NLS2.2 (*TGGAGGTTCTGGAATGCCG**G**A**G**TTC*TCCC**CA**CTTTCTGC)

3) NLS2.3 (GAGAA**C**T**C**CGGCATTCCAGAACCTCCAGAGCCCAA**C**G**G**CAA**C**AA **C**CAGTTT)

EcoR I
4) NLS2.4 (GCGCGC<u>GAATTC</u>CTCCATCTCAGTGAACCGGGCAAAC)

The pEGFPNLS2M construct was assembled by performing three fragment ligation of Sac I - EcoR I (CIP) pEGFP-N2 vector, Sac I - Nhe I RBM5 and Nhe I - EcoR I digested PCR amplified NLS2M as detailed in the above section for pEGFPNLS1M.

Recombinant clones obtained by subsequent transformation of competent JM109 were scaled up and sequenced to confirm the site-directed mutagenesis of NLS2M.

Construction of pEGFPRBM5NLS1MNLS2M – Constructs with both the bipartite NLS mutated were constructed in parallel to pEGFPRBM5NLS2M by substituting Sac I-Nhe I RBM5NLS1M instead of Sac I-Nhe I RBM5 in the above three fragment ligation reaction. All procedures subsequent to ligation were carried out similar to that for construction of pEGFPRBM5NLS2M. Mutations were confirmed by sequencing.

Cell culture

HT-6 cells (SV40 large T-antigen transformed immortalized HUVEC cells) produced in our lab by Dr. Brown and pooled HUVEC cells were grown in EGM medium supplemented with 1 ng/ml of bFGF as mentioned in Chapter 2 (Part I). NIH3T3 cells and HepG2 cells were grown in Dulbecco's modified Eagle's medium supplemented with 10% fetal calf serum, 50 units/ml penicillin, 50 μg/ml streptomycin (Invitrogen) and 200 ng/ml amphotericin B (Sigma Aldrich) at 37ºC in a 5% CO_2 humidified incubator. Before transfection cells were harvested using ice cold 1 mM EDTA in PBS and grown on 22 X 22 mm Corning® number 1½ cover glasses or in Lab-Tek™ four well chambered cover glasses (Nalge Nunc International).

Transient transfections

Each plasmid construct (1-3 μg per cover glass of cells) was diluted in 99 μl of Opti-MEM I reduced serum medium (Invitrogen). Simultaneously, 6 μl of Lipofectin® (Invitrogen) was diluted in 94 μl of Opti-MEM I and incubated at room temperature for

30 minutes. The plasmid and the Lipofectin® dilutions were then combined and further incubated for 15 more minutes, following which 0.8 ml of Opti-MEM I was added. This mixture was used to transiently transfect cells pre-washed with 2 ml of Opti-MEM I. After 3 hours of incubation at 37°C/5% CO_2 the cells were allowed to recover in respective cell culture media for 18-20 hours. For transcription inhibition studies cells were treated with 10 μg/ml actinomycin D (3 hours) or 50 μg/ml α-amanitin (5 hours) at 37°C/5% CO_2.

Fluorescence microscopy

Organelle staining - Cellular organelles were stained with either 500 nM MitoTracker Red CMXRos (mitochondria/45 minutes) or 75 nM LysoTracker Red DND-99 (lysosomes/1 hour). Cells on each cover glass were fixed with 3.7% formaldehyde in cell culture medium for 15 minutes at room temperature and subsequently washed five times in 1 ml of PBS each. Cells were then permeabilized using 1 ml of 0.2% Triton X-100 in PBS for 5 minutes at room temperature and then washed twice in PBS. Alternatively, cells were fixed and permeabilized in 100% acetone at -20ºC for 1 minute and then rinsed several times in PBS to remove any traces of acetone. Subsequently, cells were either stained for five minutes with 300 nM DAPI (nuclear DNA) or further processed for indirect immunofluorescence as given below. Live cells were stained as above and visualized in respective cell culture media after extensive washings to remove unincorporated dyes. Excitation and emission spectra of all the fluorescent dyes used in this study are demonstrated in figure 15.

Indirect immunofluorescence – Non-snRNP splicing factor SC35 was detected by incubating fixed and permeabilized cells in 1 ml of 1:1,000 diluted anti SC35 monoclonal IgG1 antibody (Sigma Aldrich, USA) per cover glass for 1 hour at 4ºC. Unbound primary antibody was washed off by rinsing the cells in PBS for 5 minutes each. Bound primary antibody was detected by using 10 µg/ml Alexa Fluor® 633 (figure 15) goat anti-mouse IgG (H+L) (Invitrogen) per cover glass for 1 hour at 4ºC. For microscopy, cover glasses were washed four times in PBS and mounted on slides in a drop of SlowFade® antifade reagent (Invitrogen).

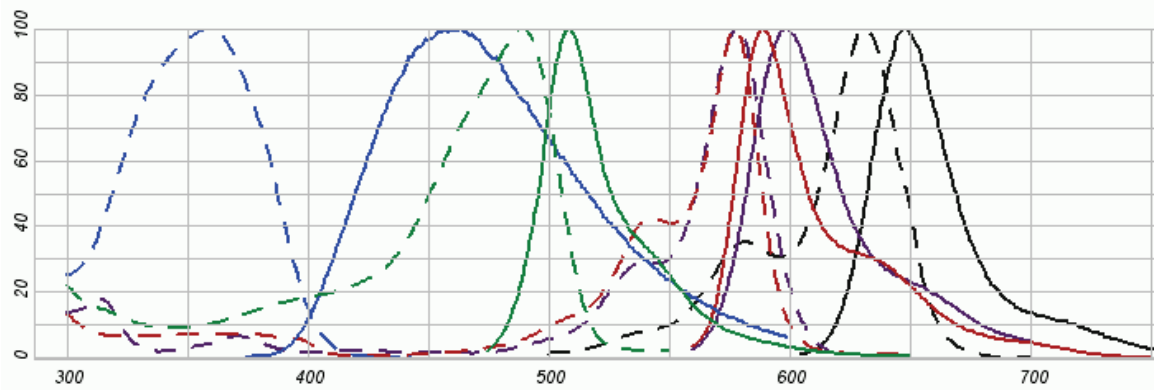

Legend:

- 4', 6-diamidino-2-phenylindole, dihydrochloride (DAPI)
- Enhanced green fluorescent protein (EGFP)
- LysoTracker Red DND-99
- MitoTracker Red CMXRos
- Alexa Fluor®633 goat anti-mouse antibody

Figure 15: Excitation (dotted lines) and emission (bold lines) spectra of various fluorescent molecules used in this study are illustrated. Wavelength of the light in nanometers is displayed on X-axis and the percent fluorescence is displayed on the Y-axis. This figure was configured and adapted from the Fluorescence Spectraviewer available at www.invitrogen.com.

Microscopy - Live and fixed cells were observed using 63X water and 100X oil immersion lenses, respectively on either Zeiss LSM 510 confocal or Deltavision deconvolution microscopes at our campus facility. Channel colors green (EGFP), pink (Alexa Fluor® 633) and red (MitoTracker Red CMXRos or LysoTracker Red DND-99) are digitally assigned after scanning the sample.

Colocalization parameters – The following quantitative parameters available in the Zeiss colocalization software were used for determining the colocalization between two colored pixels, green (Ch1) and red/pink (Ch2).

1. Colocalization coefficients:

$$c_1 = \frac{pixels_{Ch1,coloc}}{pixels_{Ch1,total}} \qquad c_2 = \frac{pixels_{Ch2,coloc}}{pixels_{Ch2,total}}$$

2. Weighted colocalization coefficients:

$$M_1 = \frac{\sum_i Ch1_{i,coloc}}{\sum_i Ch1_{i,total}} \qquad M_2 = \frac{\sum_i Ch2_{i,coloc}}{\sum_i Ch2_{i,total}}$$

3. Overlap coefficient or Manders coefficient (Manders et al., 1993):

$$r = \frac{\sum_i Ch1_i * Ch2_i}{\sqrt{\sum_i (Ch1_i)^2 * \sum_i (Ch2_i)^2}}$$

4. Pearson's correlation coefficient:

$$R_p = \frac{\sum_i (Ch1_i - Ch1_{aver}) * (Ch2_i - Ch2_{aver})}{\sqrt{\sum_i (Ch1_i - Ch1_{aver})^2 * \sum_i (Ch2_i - Ch2_{aver})^2}}$$

Values of the first three quantitative colocalization parameters range between 0 (no colocalization) and 1 (all pixels colocalize). Pearson's correlation coefficient values lie between -1 and 1, with 1 representing complete colocalization.

RESULTS

Colocalization of RBM5 in nuclear speckles

Based on the fact that RBM5 has two bipartite NLS, it is reasonable to suspect that RBM5 may localize to nucleus. Transient transfection of HUVEC cells with pEGFPRBM5 indeed shows a diffuse nuclear localization pattern with majority of the fluorescence concentrated in 25-50 distinct speckles, with no fluorescence detected in nucleoli or cytosol. This pattern of localization is similar to that of IGCs (interchromatin granule clusters) or nuclear speckles which are enriched in pre-mRNA splicing factors. Localization of RBM5 in nuclear speckles was replicated for both live and fixed cells in various cell lines (HUVEC, HT-6, NIH3T3 and HepG2) ruling out any discrepancy caused due to fixation artifacts (figure 16A).

Previous studies have demonstrated that nuclear speckles contain little or no chromatin. Most of the speckles are observed at the periphery of the active transcription sites (Misteli, 2000; Lamond and Spector, 2003). Predictably, staining for nuclear DNA with DAPI shows no discernable presence of chromatin within the RBM5 nuclear speckles (figure 16B). Despite the fact that nuclear speckles contain many pre-mRNA splicing factors they do not participate directly in pre-mRNA splicing or transcription

but, are rather thought to be storehouses from which these factors are recruited to sites of transcription. This dynamic of nature of nuclear speckles can be disrupted by inhibiting transcription using heat shock (45ºC/15 minutes) or transcriptional inhibitors such as actinomycin D (10 μg/ml/3 hours) or α-amanitin (50 μg/ml/5 hours) (Carmo-Fonseca et al., 1992; Lamond and Spector, 2003; Shav-Tal et al., 2005). Protocols for disruption of transcription in cell culture are well established in the literature. It should be noted that, the time and concentrations of transcriptional inhibitors (actinomycin D and α-amanitin) used throughout this study potently inhibit RNA polymerase II. As expected, inhibition of transcription by actinomycin D or α-amanitin dramatically changed the nuclear speckle organization of RBM5 with all the fluorescence concentrated in 3-4 rounded clusters measuring 2-3 μm across (figure 16C and 16D). Thus, the absence of DNA and clustering in presence of transcriptional inhibitors are key characteristics displayed by nuclear speckle proteins. Although RBM5 demonstrated both of these distinguishing characteristics, the presence of RBM5 in nuclear speckles was further confirmed by colocalization with another well characterized nuclear speckle protein SC35.

Colocalization of transiently transfected pEGFPRBM5 (green) with SC35 (pink) labeled with indirect immunofluorescence was quantified for various colocalization parameters using LSM510 Image Examiner software available from Zeiss. As seen from figure 17A RBM5 (green) shows a great degree of colocalization with SC35 (pink). Colocalization and weighted colocalization coefficients are the most commonly used parameters for defining colocalization between two colored pixels (green and pink/red).

Localization of EGFPRBM5 in nuclear speckles

A)

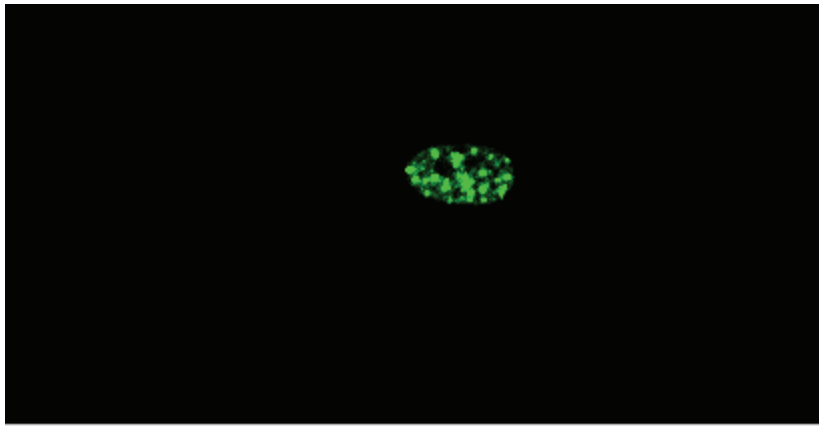

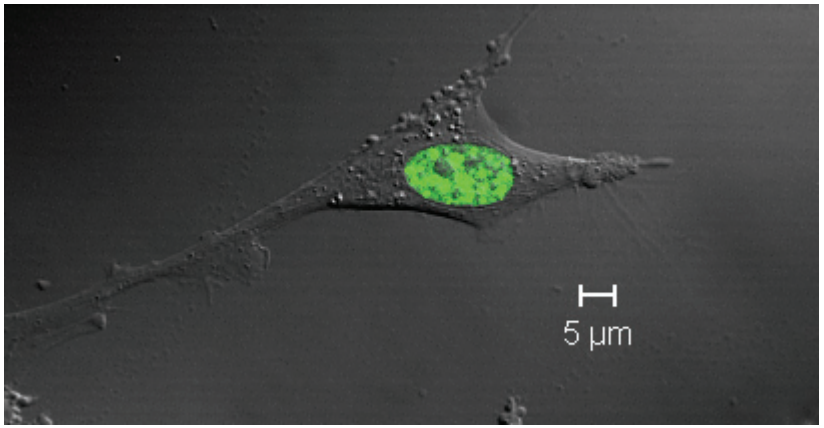

B)

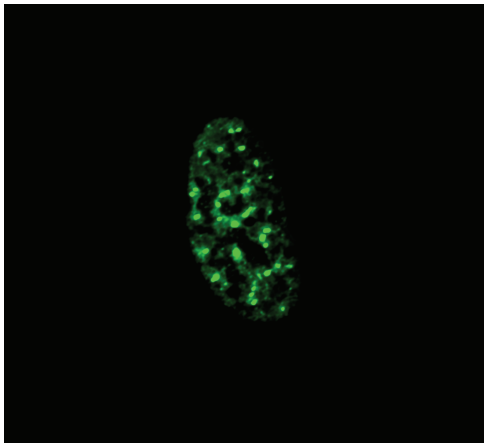

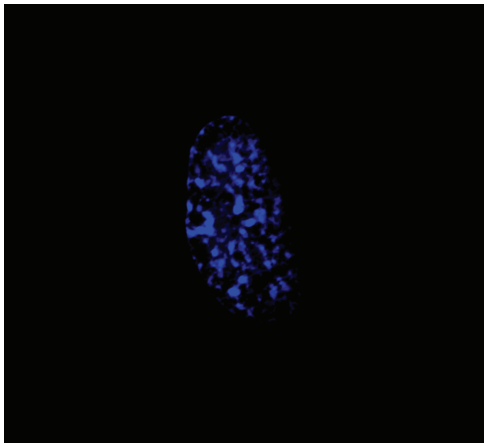

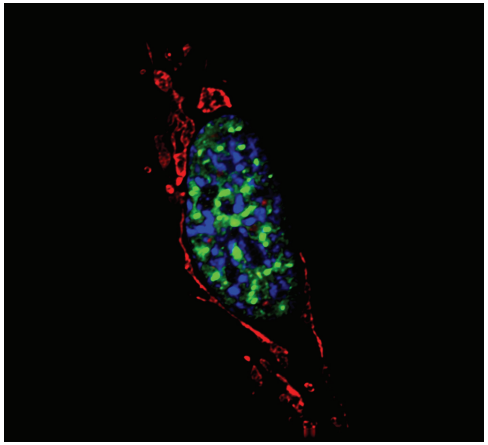

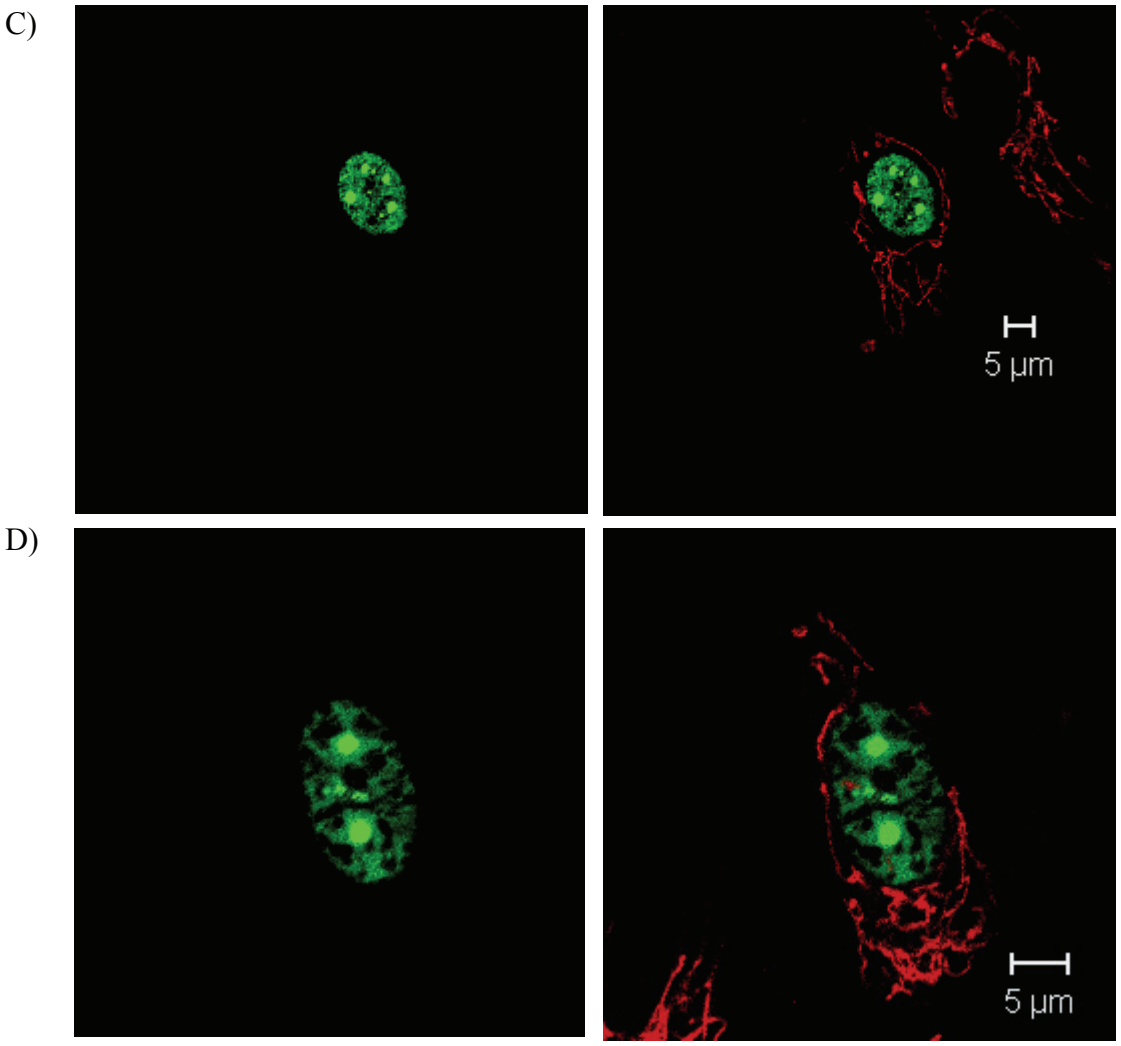

Figure 16: Localization of EGFPRBM5 in nuclear speckles. Localization of RBM5 as determined by expression of pEGFPRBM5 transiently transfected in HUVEC cells by Lipofectin. RBM5 shows a characteristic nuclear speckle localization in both live (A) and fixed cells (B). For live cell microscopy, cells grown and transiently transfected on chambered cover glasses were processed further for fluorescence microscopy using 63X water immersion lens and Zeiss LSM 510 confocal microscope. Nuclear boundary was determined by Nomarski (DIC) image shown here as an overlay of two images. RBM5 associated fluorescence (green) is excluded from chromatin stained blue with DAPI (B). Treatment of cells with transcriptional inhibitors actinomycin D (10 µg/ml/3 hrs) (C) and α-amanitin (50 µg/ml/5 hrs) (D) results in clustering of EGFPRBM5, a feature shared by proteins localized in nuclear speckles. Overall cellular architecture is highlighted by staining the cells with MitoTracker Red CMXRos (B, C and D). Staining and fixation techniques are as detailed in Materials and Methods. Images in part B were taken using a 100X oil immersion lens and Deltavision deconvolution microscope and is a representative of image stacks obtained after running deconvolution algorithms. Images in parts C and D were captured using confocal microscope and 100X oil immersion lens.

Colocalization coefficients measure the relative number of colocalizing pixels in two channels green (EGFPRBM5) and pink (SC35). The values indicate that 97% of pink pixels colocalize with 95% green pixels (figure 17C). Weighted colocalization coefficients show a higher degree (100%) of colocalization since more weight is given to brighter pixels in both the channels. Overlap coefficient (Manders coefficient) is a convenient but relatively insensitive parameter to compare the degree of overlap between the two channels, which in this case is 0.9 or 90% overlap (Manders et al., 1993). A much more sensitive parameter to measure colocalization is the Pearson's correlation coefficient (R) which in this case shows a lower value of 0.83 or 83% colocalization. This lower value can be partly explained by the fact that there are many more green pixels due to overexpression of RBM5 as compared to pink pixels attributed to native SC35. All computations were performed by taking into account the background pixels which are defined by randomly assigning an ROI (region of interest) removed from the area marked for determination of colocalization. Similar calculations were repeated for at least 15 different nuclei from various cell lines in more than three independent experiments. Pearson's correlation coefficient values ranging from 0.6-0.8 were routinely obtained. All images were obtained by scanning the cells sequentially with each laser (488 nm and 633 nm) to avoid any observed colocalization due to bleed through between the two channels. Absence of any channel crosstalk was also confirmed when same colocalization results were obtained by switching the order of laser scanning.

Colocalization of EGFPRBM5 with SC35

A)

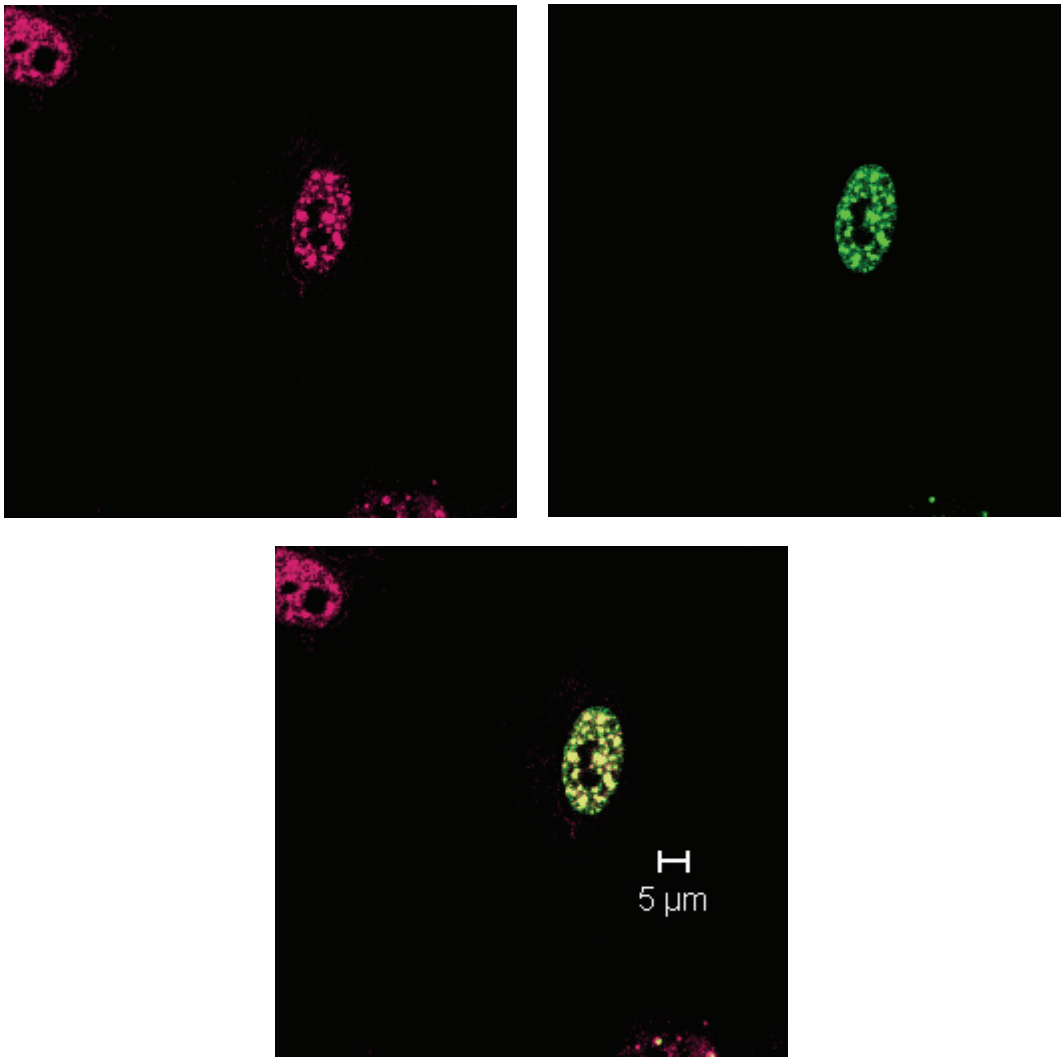

B)

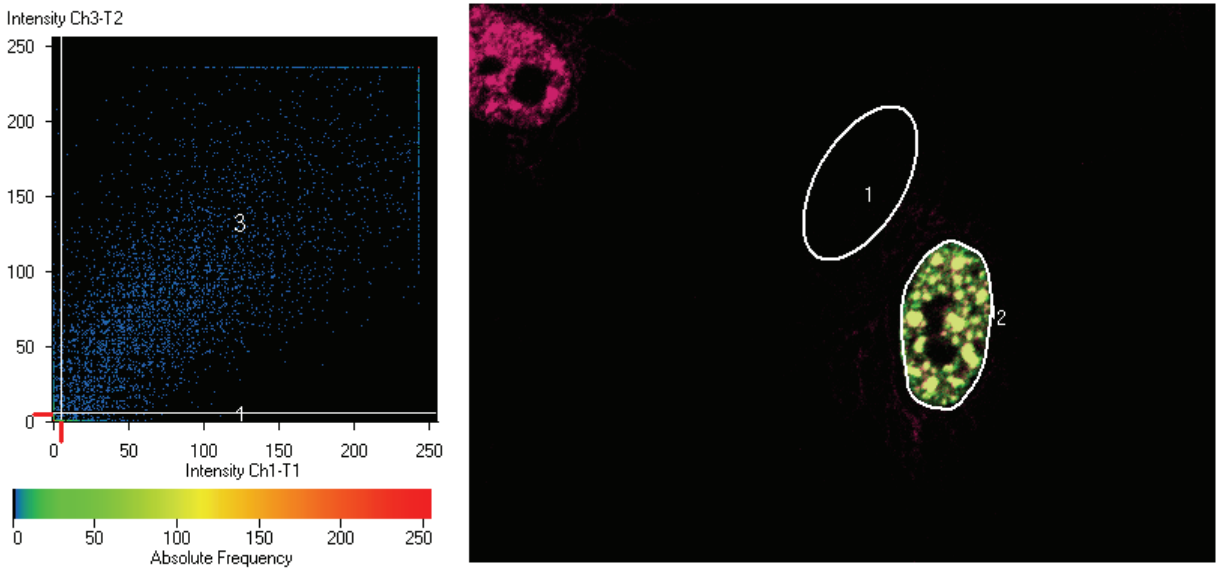

C)

Image Region	Number Pixels	Area µm X µm	Relative Area [%]	Mean Intensity		Standard Deviation		Colocalization Coefficient		Weighted Coloc. Coefficient		Overlap Coefficient	Correlation R	Correlation R x R
				Ch1-T1	Ch3-T2	Ch1-T1	Ch3-T2	Ch1-T1	Ch3-T2	Ch1-T1	Ch3-T2			
1-1	56	1.81	0	10	0	5	0							
1-1	0	0	0	0	0	0	0							
1-1	0	0	0	0	0	0	0	0.000	0.000	0.000	0.000	0.00	0.00	0.00
2-1	144	4.66	0.1	21	1	15	1							
2-2	255	8.26	0.1	1	33	1	29							
2-3	4553	147.4	1.7	116	118	78	71	0.969	0.947	1.000	1.000	0.9	0.83	0.68

Figure 17: Colocalization of EGFPRBM5 with SC35. Colocalization of RBM5 (green) with SC35 (pink) in HUVEC cells (A) was calculated using the Zeiss colocalization software. Background fluorescence was adjusted by randomly defining an area (region 1) outside the cellular boundaries. For estimating colocalization, nuclear area including SC35 and RBM5 fluorescence was defined by region 2 also represented as a scattergram on the left side (B). The third quadrant of scattergram represents colocalizing pixels from green and pink channels. Various parameters for EGFPRBM5 (Ch3-T2) and SC35 (Ch1-T1) fluorescence are highlighted under green and pink channels respectively (C). As seen from the colocalization coefficient, 97% of the pink (SC35) pixels colocalize with 95% of the green (EGFPRBM5) pixels. Weighted colocalization coefficient calculates a 100% colocalization since more weight is given to brighter pixels than duller ones. This high degree of overlap between the SC35 and EGFPRBM5 is also reflected by overlap coefficient value of 0.9. A much more sensitive parameter, Pearson's correlation coefficient (R) is slightly lower with a value of 0.83. This colocalization is representative of similar estimations done for at least 15 different cells from more than three independent experiments done in various cell lines.

Colocalization of RBM5 and SC35 in transcriptionally inhibited cells

As mentioned before, transcriptional inhibition results in nuclear speckle proteins including RBM5 to concentrate in 3-4 clusters. Colocalization for RBM5 and SC35 in presence of actinomycin D and α-amanitin was determined based on the hypothesis that if indeed both the proteins are localized in the nuclear speckles then they must be equally affected by transcriptional inhibitors. The redistribution of a non-snRNP spliceosome component and nuclear speckle protein, SC35 due to transcription inhibition is well documented and was first demonstrated by Spector et al. in 1991. Indeed both RBM5 and SC35 display the same loss of speckled localization and share a common pattern of clustering when treated with either actinomycin D or α-amanitin, transcriptional inhibitors with different modes of action (figure 18A and 19A). Although, the pattern of localization for both the proteins is similar, there is very little colocalization as determined from low Pearson's correlation coefficient of 0.43 and 0.3 for α-amanitin and actinomycin D, respectively (figure 18C and 19C). Clusters of both RBM5 and SC35 appear to lie adjacent to each other with a small band of colocalization between them. This pattern of localization for RBM5 and SC35 in transcriptionally inhibited cells was seen consistently in a series of repeated experiments in more than 20 nuclei from various cells types.

Colocalization of EGFPRBM5 with SC35 in presence of α-amanitin

A)

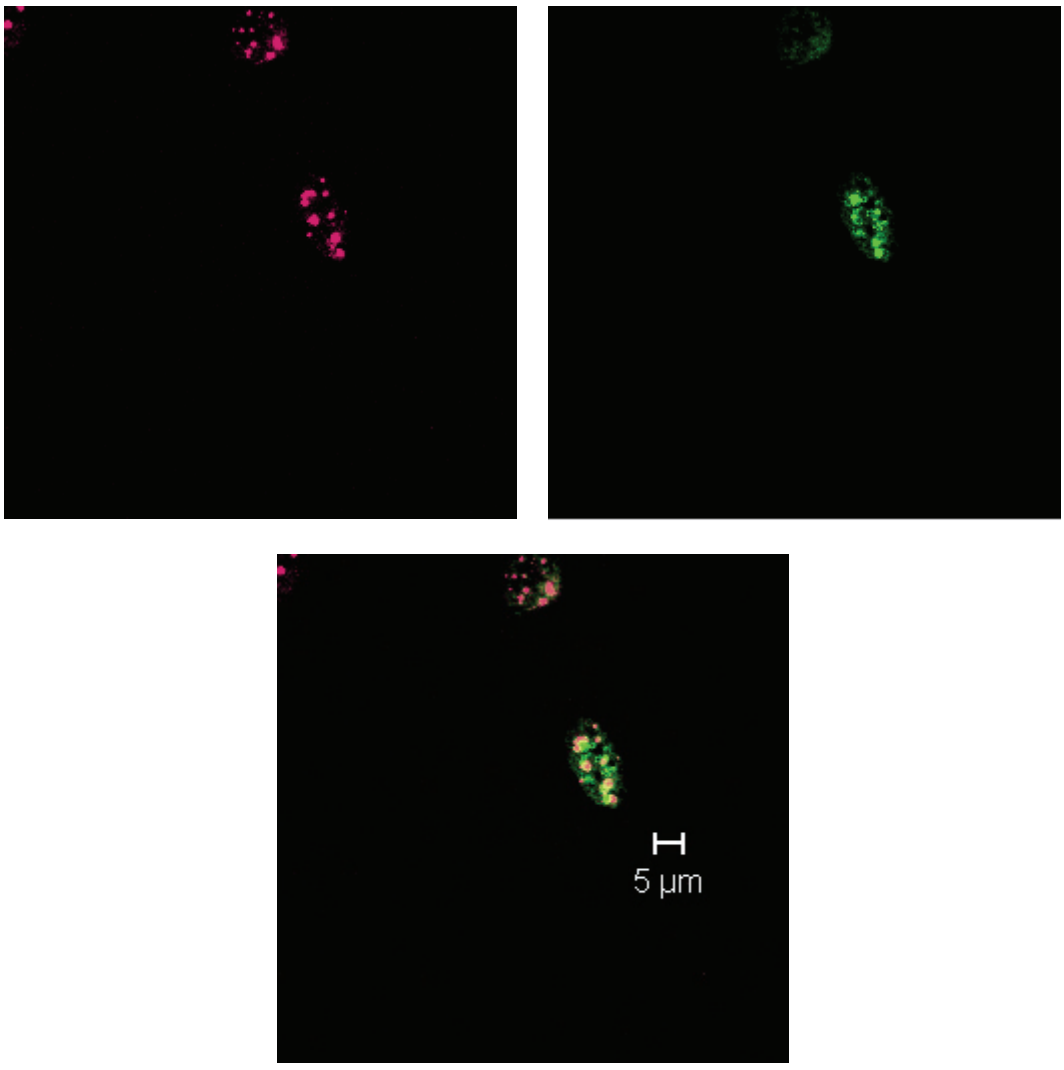

B)

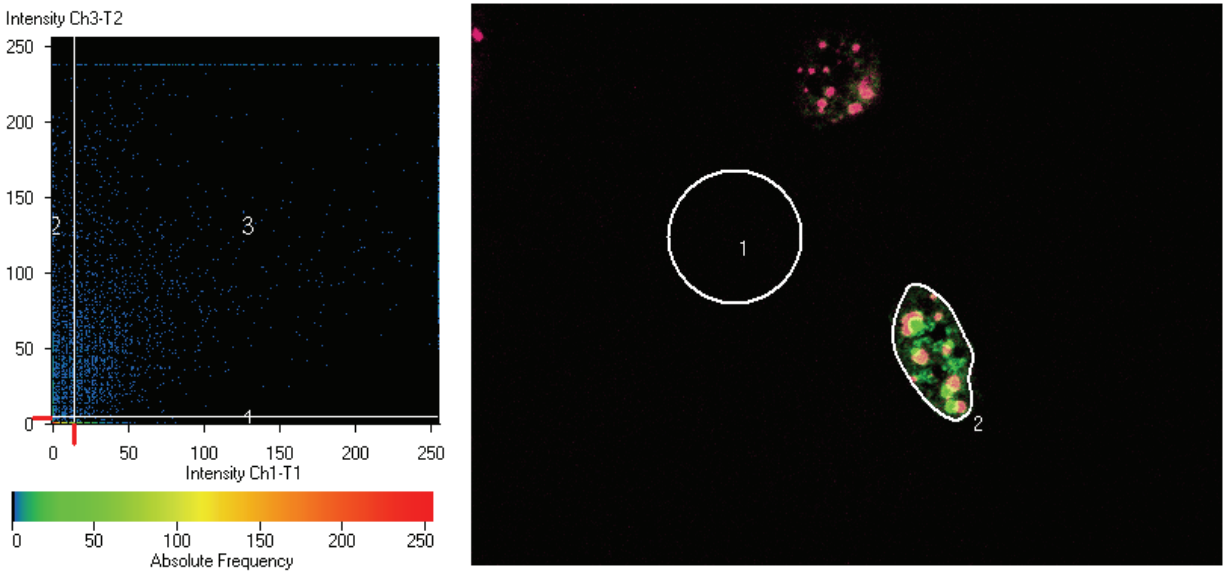

C)

Image Region	Number Pixels	Area µm X µm	Relative Area [%]	Mean Intensity		Standard Deviation		Colocalization Coefficient		Weighted Coloc. Coefficient		Overlap Coefficient	Correlation R	Correlation R x R
				Ch1-T1	Ch3-T2	Ch1-T1	Ch3-T2	Ch1-T1	Ch3-T2	Ch1-T1	Ch3-T2			
1-1	228	7.38	0.1	21	0	7	0							
1-1	0	0	0	0	0	0	0							
1-1	0	0	0	0	0	0	0	0.000	0.000	0.000	0.000	0.00	0.00	0.00
2-1	74	2.4	0	27	0	15	1							
2-2	856	27.72	0.3	5	56	5	48							
2-3	1654	53.56	0.6	58	95	50	70	0.957	0.659	1.000	0.961	0.8	0.43	0.18

Figure 18: Colocalization of EGFPRBM5 with SC35 in presence of α-amanitin. Cells transiently transfected with pEGFPRBM5 (green) were pretreated with 50 μg/ml (5 hours) α-amanitin for transcriptional inhibition before fixing and staining for non snRNP protein SC35 (pink). Both RBM5 and nuclear speckle protein SC35 behave in a similar fashion and form rounded clusters when transcription is shut down (A). However, both RBM5 and SC35 proteins do not colocalize as seen before in absence of any transcriptional inhibitors but, are instead side by side with a small band between them displaying colocalization. The Pearson's correlation coefficient is correspondingly lower at 0.43 (region 2) (B and C). This experiment is representative of more than three independent experiments and more than 12 different nuclei. Pearson's correlation coefficient value between 0.3-0.4 was routinely obtained. Background fluorescence was adjusted as explained before.

Colocalization of EGFPRBM5 with SC35 in presence of actinomycin D

A)

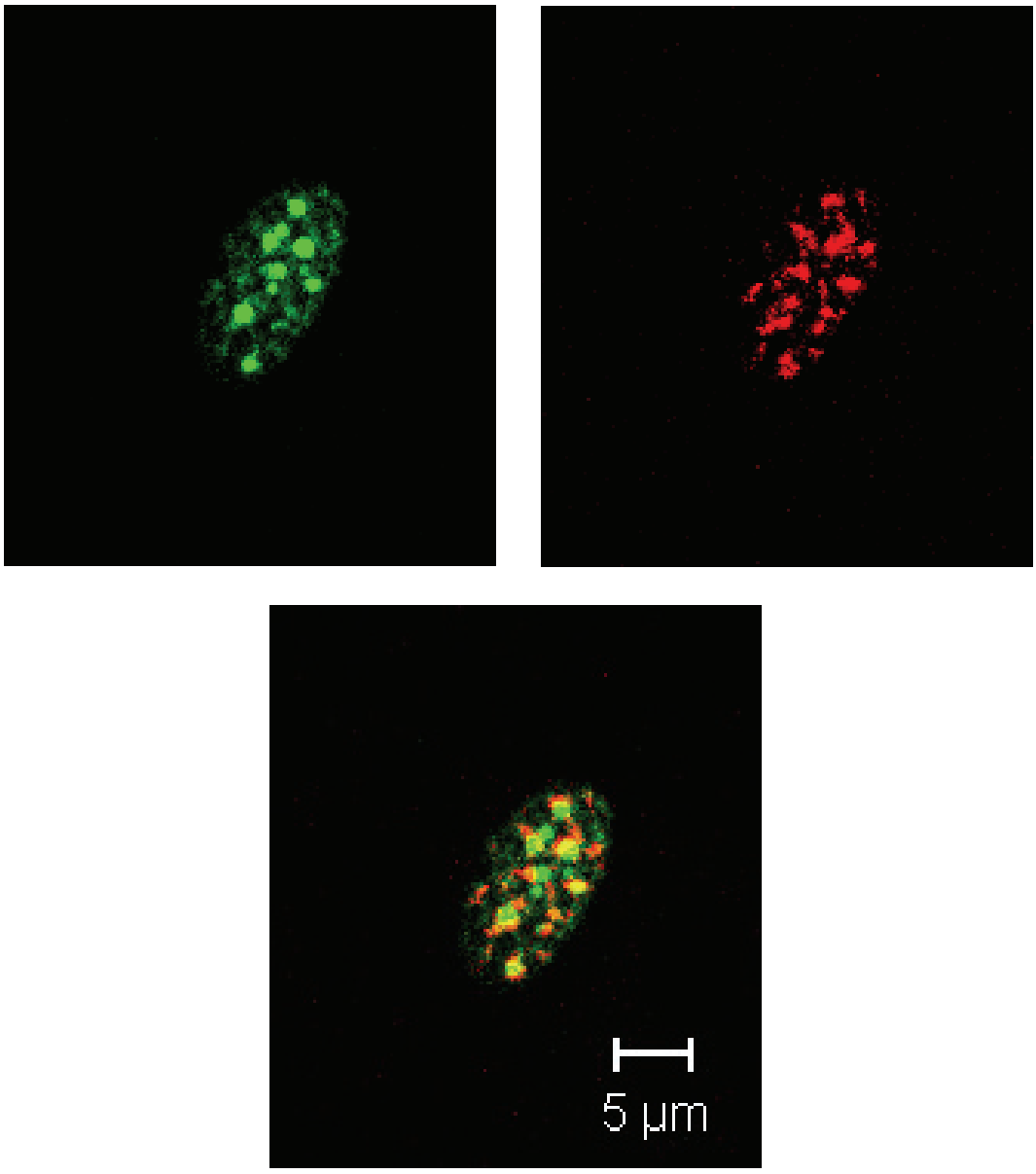

B)

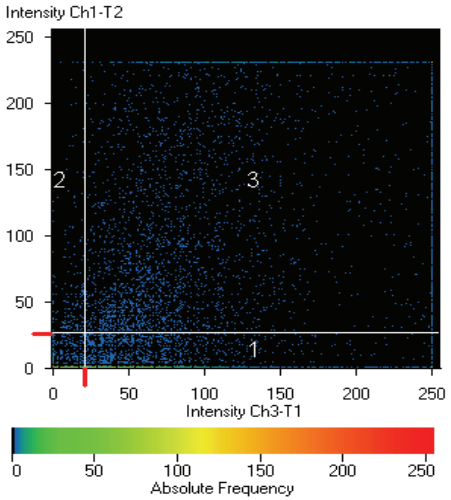

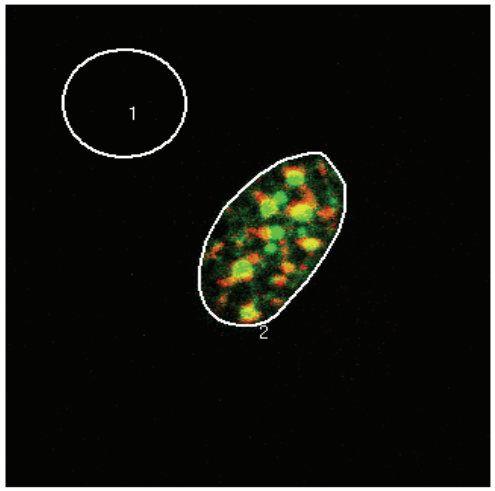

C)

Image Region	Number Pixels	Area µm X µm	Relative Area [%]	Mean Intensity		Standard Deviation		Colocalization Coefficient		Weighted Coloc. Coefficient		Overlap Coefficient	Correlation R	Correlation R x R
				Ch3-T1	Ch1-T2	Ch3-T1	Ch1-T2	Ch3-T1	Ch1-T2	Ch3-T1	Ch1-T2			
1-1	1	0.01	0	27	0	5	0							
1-1	5	0.05	0	0	57	0	34							
1-1	0	0	0	0	0	0	0	0.000	0.000	0.000	0.000	0.00	0.00	0.00
2-1	3453	36.17	3	65	3	51	7							
2-2	175	1.83	0.2	12	70	6	52							
2-3	3369	35.29	2.9	117	127	72	71	0.494	0.951	0.973	0.995	0.8	0.35	0.12

Figure 19: Colocalization of EGFPRBM5 with SC35 in presence of actinomycin D. Cells transiently transfected with pEGFPRBM5 construct were transcriptionally inhibited by treating with 10 μg/ml actinomycin D for 3 hours. Both RBM5 and SC35 round up when treated with actinomycin D, in a similar pattern also observed above in cells treated with α-amanitin. RBM5 (green) and SC35 (red) clusters are localized adjacently with only a small band showing colocalization between the two proteins, reflected by a correspondingly lower Pearson's correlation value of 0.3. Series of similar estimations for more than ten different nuclei from more than three independent experiments consistently gave an overlap coefficient of 0.8 and a Pearson's correlation coefficient value between 0.3-0.4.

Accuracy of colocalization measurements

Having determined the colocalization of RBM5 with SC35 in nuclear speckles, question remained if the values calculated were indeed accurate and sensitive enough to predict colocalization between two channels. To test this, experiments analogous to those for determining the RBM5 and SC35 colocalization were set up. An empty pEGFP-N2 vector instead of EGFPRBM5 was used to transfect the cells transiently and determine the colocalization with SC35 (figure 20A). The 27 kDa native EGFP can passively diffuse inside the nuclei and does not need any nuclear localization signals. As seen from figure 20A an excess of EGFP completely overlaps the SC35 present in the nucleus. All colocalization estimations were done after eliminating any fluorescence contributed by background pixels. Colocalization and weighted colocalization coefficient values indicate that SC35 (pink) completely colocalizes with most of the EGFP (green) with an 80% overlap between the two channels (figure 20C). However, the Pearson's correlation value of zero indicates that there is no correlation between two channels. Similar low Pearson's correlation coefficients were obtained in three repetitions. Thus, the degree of colocalization between two proteins is best determined by taking into account all the parameters weighing in both their limitation and relative sensitivities.

Colocalization of EGFP (control) with SC35

A)

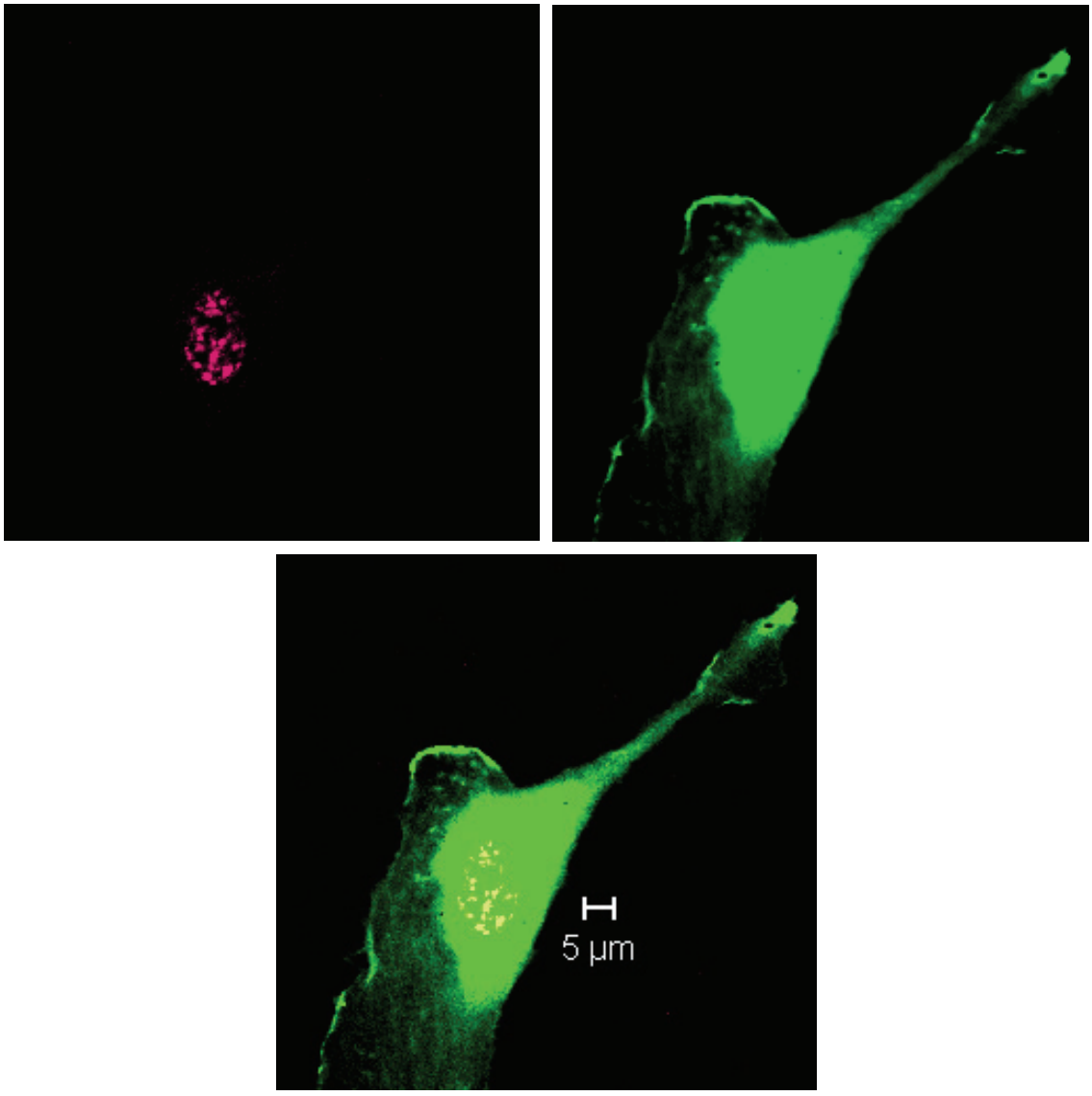

B)

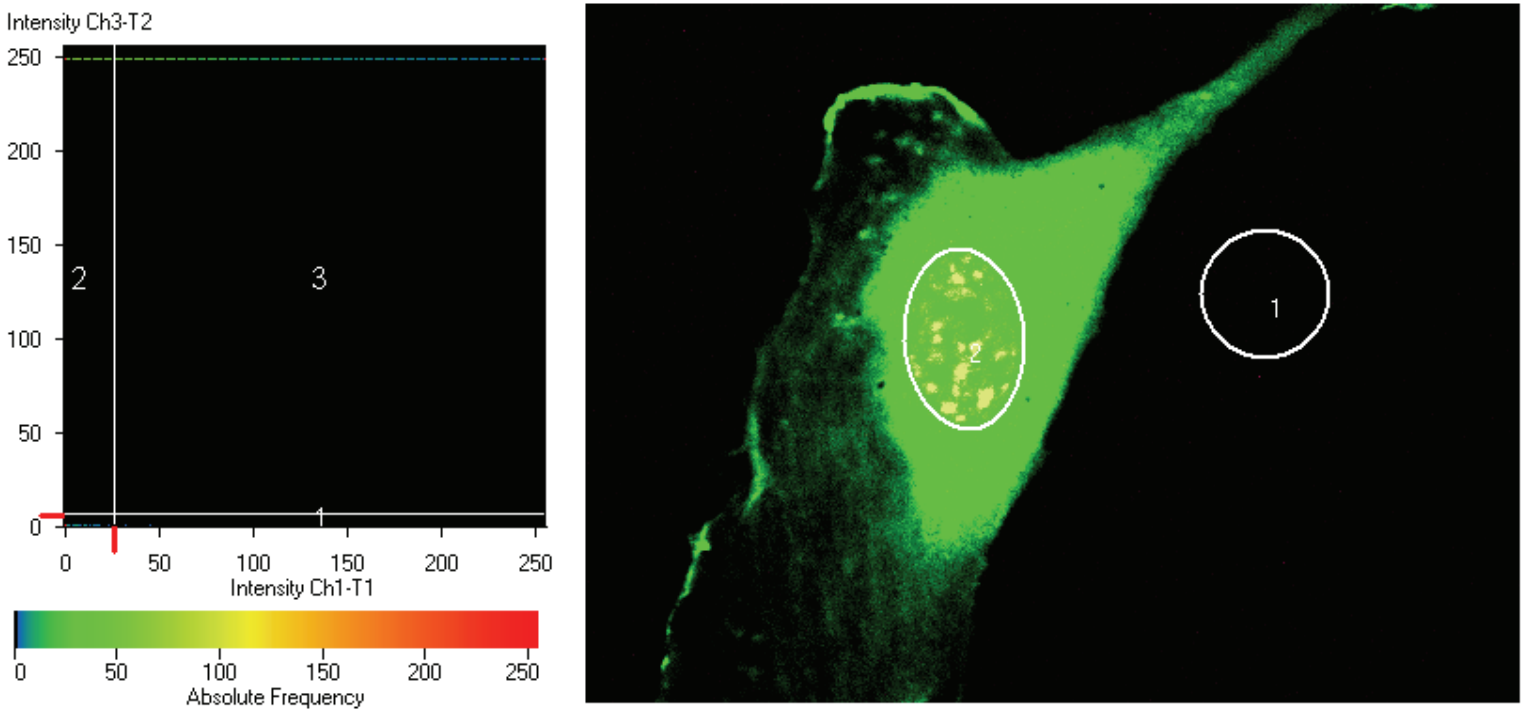

C)

Image Region	Number Pixels	Area µm X µm	Relative Area [%]	Mean Intensity		Standard Deviation		Colocalization Coefficient		Weighted Coloc. Coefficient		Overlap Coefficient	Correlation R	Correlation R x R
				Ch1-T1	Ch3-T2	Ch1-T1	Ch3-T2	Ch1-T1	Ch3-T2	Ch1-T1	Ch3-T2			
1-1	2	0.06	0	39	0	9	0							
1-1	0	0	0	0	0	0	0							
1-1	0	0	0	0	0	0	0	0.000	0.000	0.000	0.000	0.00	0.00	0.00
2-1	0	0	0	0	0	0	0							
2-2	2292	74.22	0.9	4	248	7	0							
2-3	2050	66.39	0.8	89	248	57	0	1.000	0.472	1.000	0.949	0.8	0.00	0.00

Figure 20: Colocalization of EGFP (control) with SC35. The software efficacy in determining the colocalization was tested by transfecting the cells with pEGFP-N2 vector alone and subsequently localizing SC35 (Alexa Fluor® 633) by indirect immunofluorescence as done for experiments with pEGFPRBM5. As expected, the 27 kDa EGFP protein shows a diffuse cytosolic and nuclear distribution (A). After adjusting the background fluorescence highlighted as region 1, nuclear colocalization was determined for region 2 containing EGFP and SC35 (B). Although, the overlap coefficient is 0.8 and colocalization coefficient for pink pixels is the highest (1.0), there is no colocalization of EGFP and SC35 as determined by the zero value of Pearson's correlation coefficient (C). Channels for EGFP and SC35 are highlighted by their respective colors green and pink. This experiment is representative of three separate colocalization determinations done in a similar way. Pearson's correlation coefficient value ranging from 0.0 to 0.1 were obtained in these repetitions.

Site-directed mutagenesis of N-terminal bipartite NLS (NLS1)

As detailed in the Materials and Methods section, the strategy of introducing point mutations instead of deletion mutagenesis was used to change the overall structure of the bipartite NLS (figure 21A and 21B). As compared to deletion mutagenesis, this technique conserves the overall structure of the protein to a large extent thereby increasing the chances of mimicking the true protein architecture *in vivo* and also considerably reducing the chances of false positive results due to exposure of cryptic NLS. The N-terminal NLS is well conserved among the RBM5 proteins across species (figure 21C). All the karyophilic amino acids making up the bipartite NLS were replaced by uncharged amino acids glycine or serine by changing a single base in each codon representing the same. Transient transfection of pEGFPRBM5NLS1M and subsequent colocalization studies with SC35 demonstrate that the mutant NLS1M not only retains nuclear targeting and but is also localized in speckles, similar to the non-mutated form of RBM5 (figure 22 and 23A). These results were consistently observed in both live and fixed cells from different human and mouse cell lines. A representative example of colocalization calculations for RBM5NLS1M and SC35 shows a similar range of values for quantitative parameters as demonstrated for the parent molecule - RBM5 (figure 23C). Colocalization and weighted colocalization coefficients both reveal complete (100%) colocalization of SC35 (pink) with RBM5NLS1M. This result is confirmed by a high overlap coefficient value of 0.9 or 90%. As seen before for RBM5 there are more green pixels (RBM5NLS1M) than for native SC35 which might be responsible for 90% overlap coefficient and a slightly lower Pearson's correlation coefficient value of 0.61. Since Pearson's correlation coefficient accounts for thousands of individual pixels and is

easily affected if one protein is overexpressed, even a lower value is statistically significant (Manders et al., 1993; Kreft et al., 2004).

A)

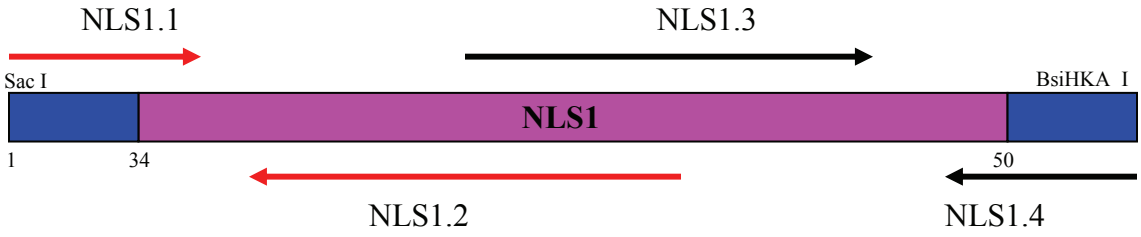

B)

```
  R  R  R  D  S  D  Y  K  R  S  S  D  D  R  R  G  D  R  Y
AGGCGGAGGGACTCAGATTACAAAAGATCTAGTGATGATCGGAGGGGTGATAGATAT
|||  ||||  ||||||||||  |||  ||  ||||||||||||  ||||  ||||||||  |||
AGGGGGAGCGACTCAGATTCCAACAGTTCTAGTGATGATGGGAGCGGTGATAGTTAT
  R  G  S  D  S  D  S  N  S  S  S  D  D  G  S  G  D  S  Y
```

C)

```
NP_005769.1:     Homo sapiens (RBM5)          34  RRDSDYKRSSDDRRGDR  50
XP_517024.1:     Pan troglodytes (RBM5)       34  .................  50
AAH31899.1:      Mus musculus (RBM5)          34  .................  50
XP_885474.1:     Bos Taurus (RBM5)            34  .................  50
XP_861224.1:     Canis familiaris (RBM5)      34  .................  50
XP_217263.3:     Rattus norvegicus (RBM5)     34  .................  50
NP_001012798.1:  Gallus gallus (RBM5)         33  ..RD......EE.....  49
RBM5NLS1M:       Homo sapiens (RBM5)          34  GSDSDSNSSSDDGSGDS  50
```

Figure 21: Strategy for site-directed mutagenesis of RBM5NLS1M. The first bipartite NLS (pink box) of RBM5 (blue box) was mutated by constructing two pairs of oligonucleotides amplifying overlapping regions of NLS1 as shown in part A and detailed in Materials and Methods. All the point mutations for site-directed mutagenesis of NLS1 (B) were engineered in the two overlapping oligonucleotides NLS1.2 and NLS1.3. The first bipartite NLS is well conserved across the species except in chickens where there is a discrepancy in four amino acid residues outside the bipartite NLS shaded in green. Homology search was done by running the BLASP algorithm available through NCBI. Figures are not drawn to scale.

Localization of EGFPRBM5NLS1M in nuclear speckles

A)

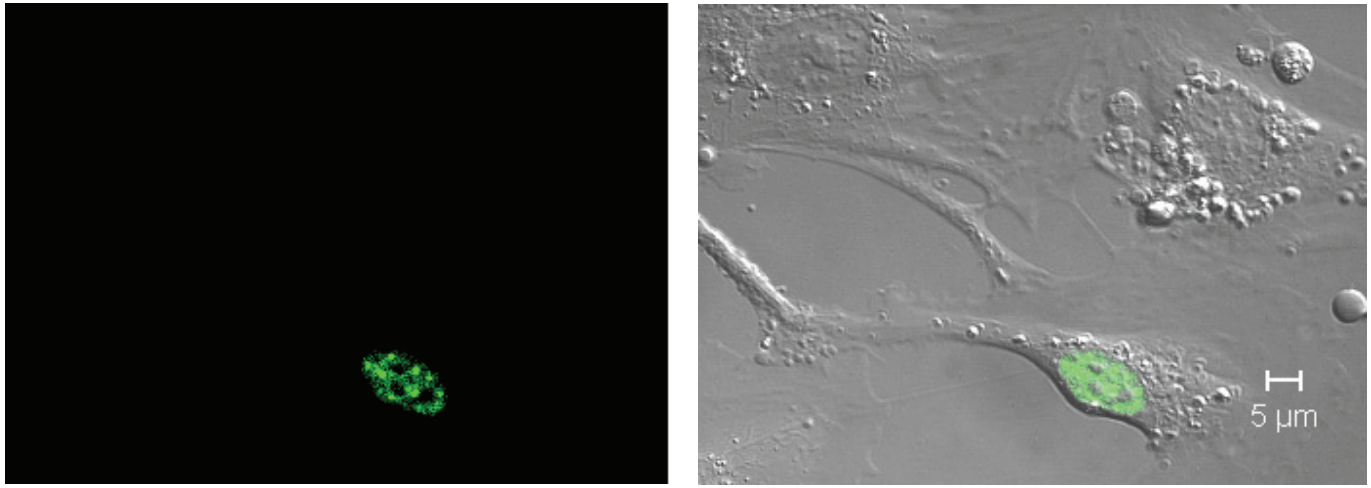

B)

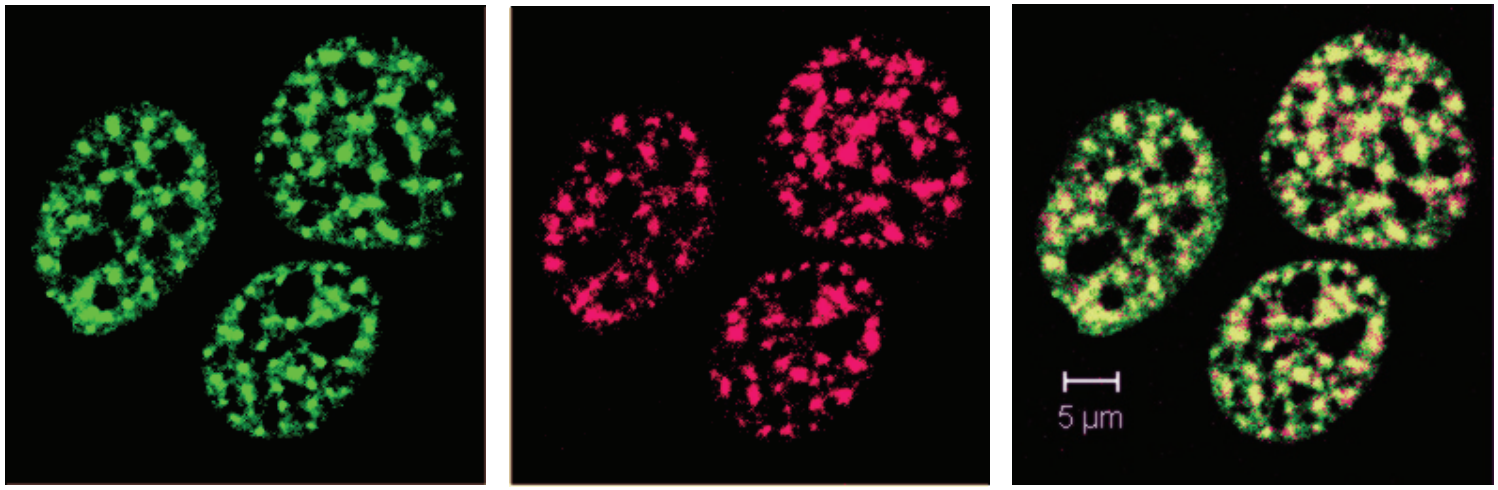

Figure 22: Localization of EGFPRBM5NLS1M in nuclear speckles as seen in live HUVEC cells (A) and in HT-6 cells (B). SC35 in HT-6 cells was visualized by indirect immunofluorescence using monoclonal anti-SC35 and goat anti-mouse Alexa Fluor 633 as detailed in Material and Methods. Images were captured using 63X water immersion lens (A) and 100X oil immersion lens on Zeiss LSM 510 confocal microscope. Image B was zoomed in to reveal details of stained nuclear speckles.

Colocalization of RBM5NLS1M with SC35

A)

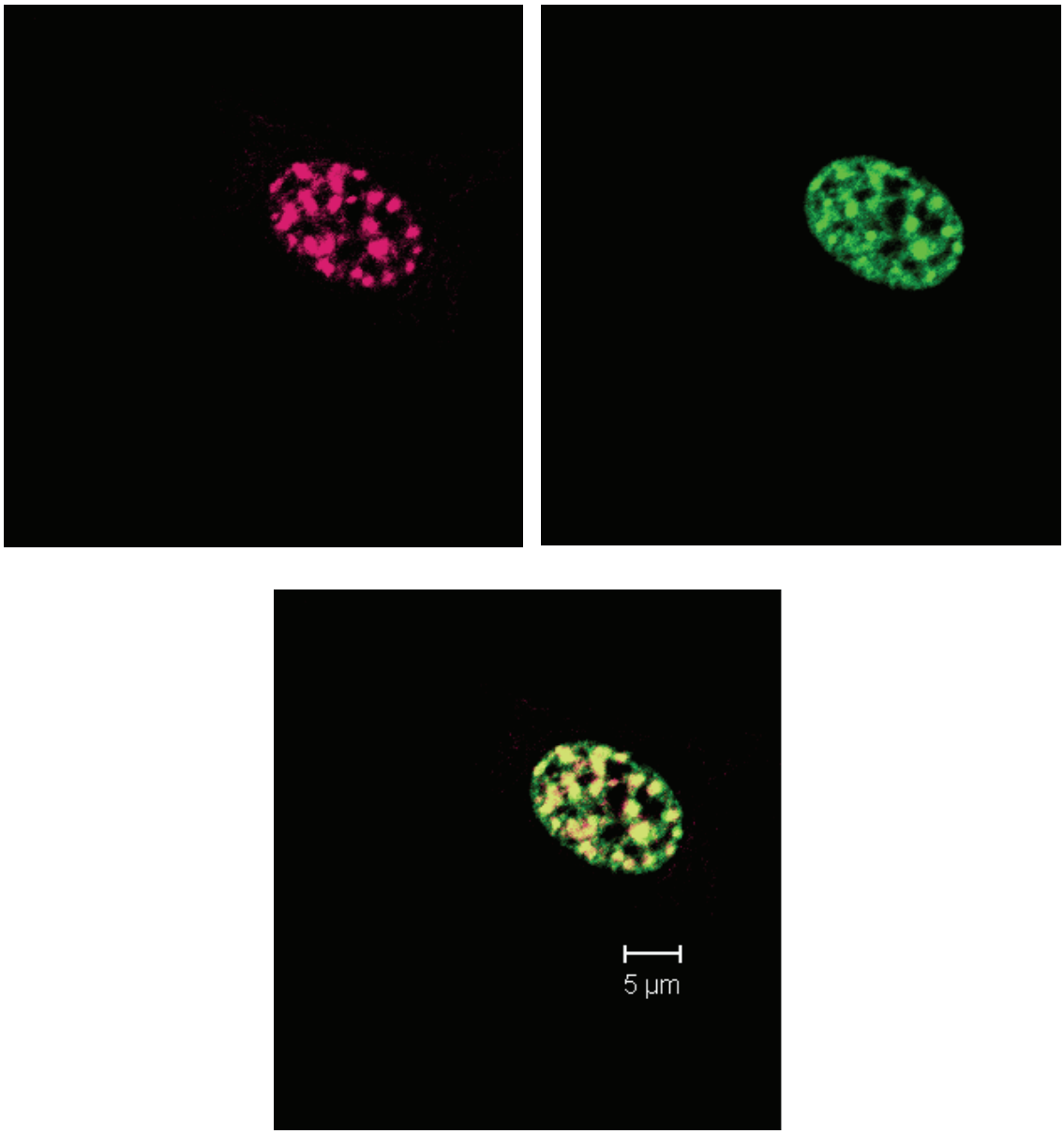

B)

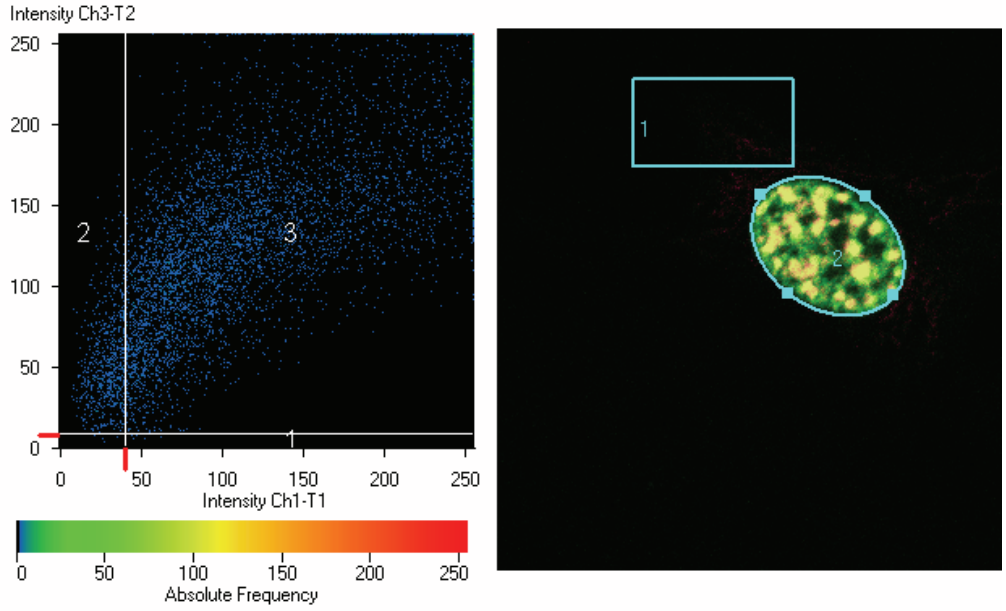

C)

Image Region	Number Pixels	Area µm X µm	Relative Area [%]	Mean Intensity		Standard Deviation		Colocalization Coefficient		Weighted Coloc. Coefficient		Overlap Coefficient	Correlation R	Correlation R x R
				Ch1-T1	Ch3-T2	Ch1-T1	Ch3-T2	Ch1-T1	Ch3-T2	Ch1-T1	Ch3-T2			
1-1	464	10.51	0.4	54	5	13	1							
1-1	591	12.93	0.6	16	9	10	1							
1-1	109	2.38	0.1	53	9	12	1	0.190	0.156	0.295	0.383	1.0	0.08	0.01
2-2	1	0.02	0.0	62	6	0	0							
2-2	557	12.19	0.5	29	58	8	28							
2-3	4381	95.84	4.2	114	126	55	47	1.000	0.887	1.000	0.969	0.9	0.61	0.38

Figure 23: Colocalization of RBM5NLS1M with SC35. Transient transfection and colocalization studies of pEGFPRBM5NLS1M (green) with SC35 (pink) reveal the same results as those obtained for pEGFPRBM5. Resident of nuclear speckles, SC35 is completely colocalized with an excess of RBM5NLS1M as seen from the colocalization coefficient and overlap coefficient values. A slightly lower Pearson's correlation value of 0.61 also reflects the excess of green pixels as compared to the pink pixels. These set of calculation represent similar experiment done in various human and mouse cell lines for more than three times.

Site-directed mutagenesis of C-terminal bipartite NLS (NLS2M)

An approach similar to mutation of N-terminal bipartite NLS (NLS1) was used to mutate the second bipartite NLS (NLS2) located at the C-terminal end of the RBM5 protein, preceding the EGFP coding sequence in the fusion construct (figure 24A). An overview of the mutations introduced to completely change characteristic arrangement of charged residues in the bipartite NLS is outlined in figure 24B. Protein BLAST (BLASTP) analysis reveals that NLS2 is not only conserved in RBM5 proteins across species but is also remarkably well conserved in RBM10 with minor replacements of one karyophilic amino acid with another (figure 24C). Transient transfection studies reveal that unlike NLS1M, NLS2M completely disrupts the nuclear translocation of the mutated RBM5 protein. The observed EGFPRBM5NLS2M fluorescence was in many cases faint and indistinguishable from the background due to a decreased signal to noise ratio. Since it was difficult to locate many transfected cells after the normal fixation and SC35 staining techniques, I decided to observe live transfected cells and switch to new, quicker acetone fixation techniques as detailed in Material and Methods. Adoption of these new techniques not only dramatically changed the results obtained for EGFPRBM5NLS2M, but also increased the number of transfected cells visualized. This acetone fixation however did not alter the localization of either EGFPRBM5 or EGFPRBM5NLS1M in nuclear speckles as validated by additional SC35 colocalization studies done as before. Instead of diffuse cytosolic staining obtained by traditional formaldehyde/Triton X-100 fixation and permeabilization techniques (figure 25A), EGFPRBM5NLS2M fluorescence was observed as discrete spots outside the nucleus reminiscent of lysosomal localization pattern (figure 25B and 25C). Indeed, dual staining with LysoTracker Red DND-99 a

dye which specifically stains acidic organelles shows complete colocalization with pEGFPRBM5NLS2M (figure 25D). Absence of autofluorescence and channel crosstalk was ascertained by detecting EGFP or LysoTracker Red alone in both the channels scanned by single track scans and also by switching the order of channels scanned in cells dually labeled.

Thus, it is clear that the C-terminal bipartite NLS (NLS2M) is the functional NLS responsible for targeting full-length RBM5 protein into the nucleus and its subsequent localization in splicing factor enriched nuclear speckles. Disruption of both the N- and C-terminal bipartite NLS (pEGFPRBMNLS1MNLS2M) also gave identical results of disrupted nuclear targeting and colocalization with lysosomes as obtained for the mutated NLS2M. This again confirms that the C-terminal NLS (NLS2) mediates nuclear targeting of RBM5 either because it is exposed or is the only functional NLS present. In retrospect, the difficulty in observing the mislocalized proteins by EGFP fluorescence can be explained by the fact that the EGFP is quenched by almost 50% at acidic pH – a hallmark of lysosomal organelles with pH ranging from 4.5 to 5.

A)

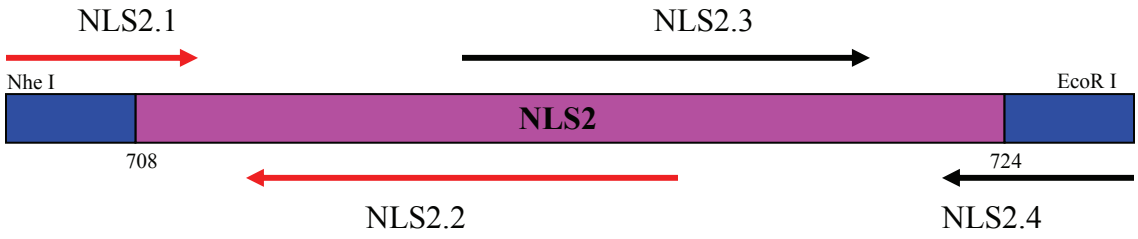

B)

```
 E  R  R  E  K  Y  G  I  P  E  P  P  E  P  K  R  K  K  Q
GAAAGACGGGAGAAGTACGGCATTCCAGAACCTCCAGAGCCCAAGCGCAAGAAGCAG
|||||  |||||||  |  ||||||||||||||||||||||||  ||||  ||  |||
GAAAGTGGGGAGAACTCCGGCATTCCAGAACCTCCAGAGCCCAACGGCAACAACCAG
 E  S  G  E  N  S  G  I  P  E  P  P  E  P  N  G  N  N  Q
```

C)

```
NP_005769.1:    Homo sapiens (RBM5)              708  RREKYGIPEPPEPKRKK  724
AAH31899.1:     Mus musculus (RBM5)              708  ................  724
XP_885474.1:    Bos taurus (RBM5)                649  ................  665
XP_861224.1:    Canis familiaris (RBM5)          634  ................  650
CAJ81574.1:     Xenopus tropicalis (RBM5)        725  ...............R  741
AAH77408.1:     Xenopus laevis (RBM5)            643  ...............R  659
XP_694937.1:    Danio rerio (RBM5-prov)          605  ..........V..KR.  621
NP_005667.2:    Homo sapiens (RBM10)             821  ..............R.  837
XP_521033.1:    Pan troglodytes (RBM10)          111  ..............R.  127
XP_582084.2:    Bos taurus (RBM10)               658  ..............R.  674
XP_538013.2:    Canis familiaris (RBM10)         895  ..............R.  911
XP_913742.1:    Mus musculus (RBM10)             743  ..............R.  759
NP_690600.1:    Rattus norvegicus (RBM10)        743  ..............R.  759
RBM5NLS2M:      Homo sapiens (RBM5)              708  SGENSGIPEPPEPTGGG  724
```

Figure 24: Strategy for site-directed mutagenesis of RBM5NLS2M. The second bipartite NLS (pink box) located near the C-terminal end of RBM5 (blue box) was mutated by constructing four oligonucleotides (A) containing the point mutations as done for constructing NLS1M. Part B shows all the point mutations engineered for site-directed mutagenesis of NLS2M. BLASTP analysis reveals that the second bipartite NLS is conserved across the species not only in RBM5 but also in RBM10 which is present on chromosome Xp11.3-11.23 in humans and also shares a 51% homology to RBM5. Figures are not drawn to scale. BLASTP search algorithm is available online from NCBI (www.ncbi.nlm.nih.gov).

Localization of EGFPRBM5NLS2M

A)

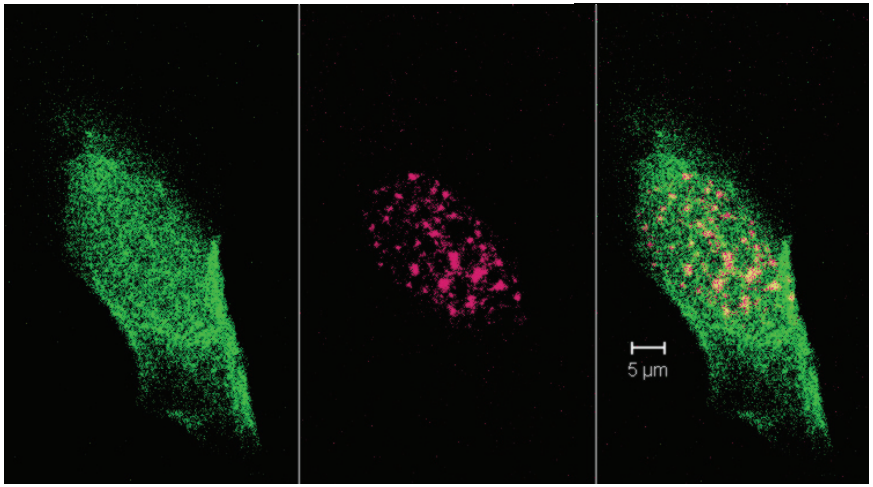

B)

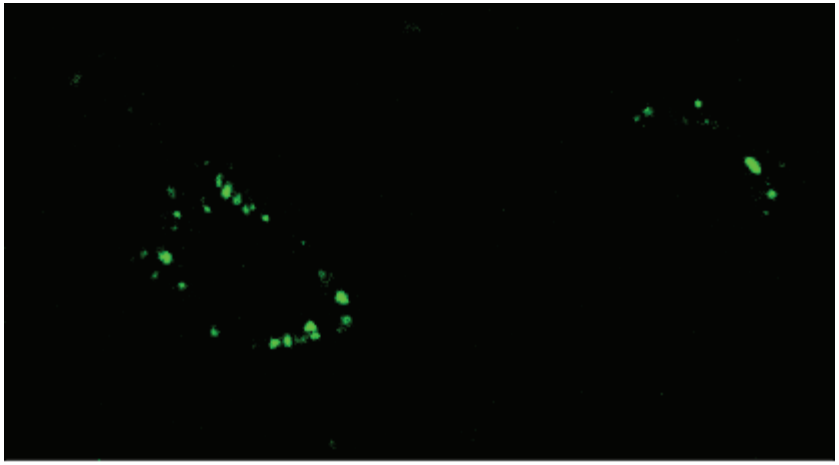

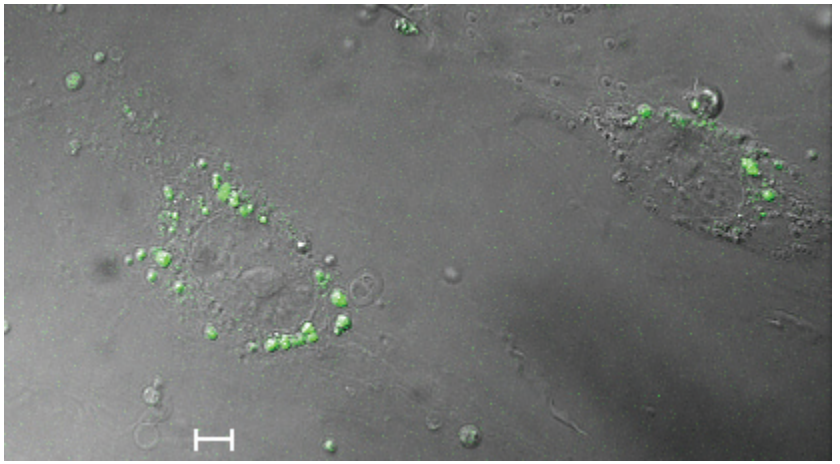

C)

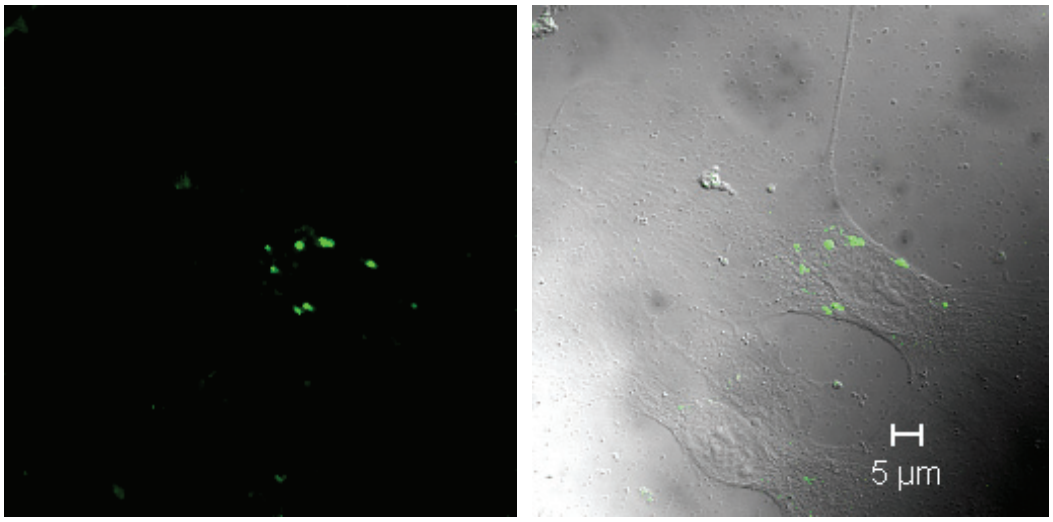

D)

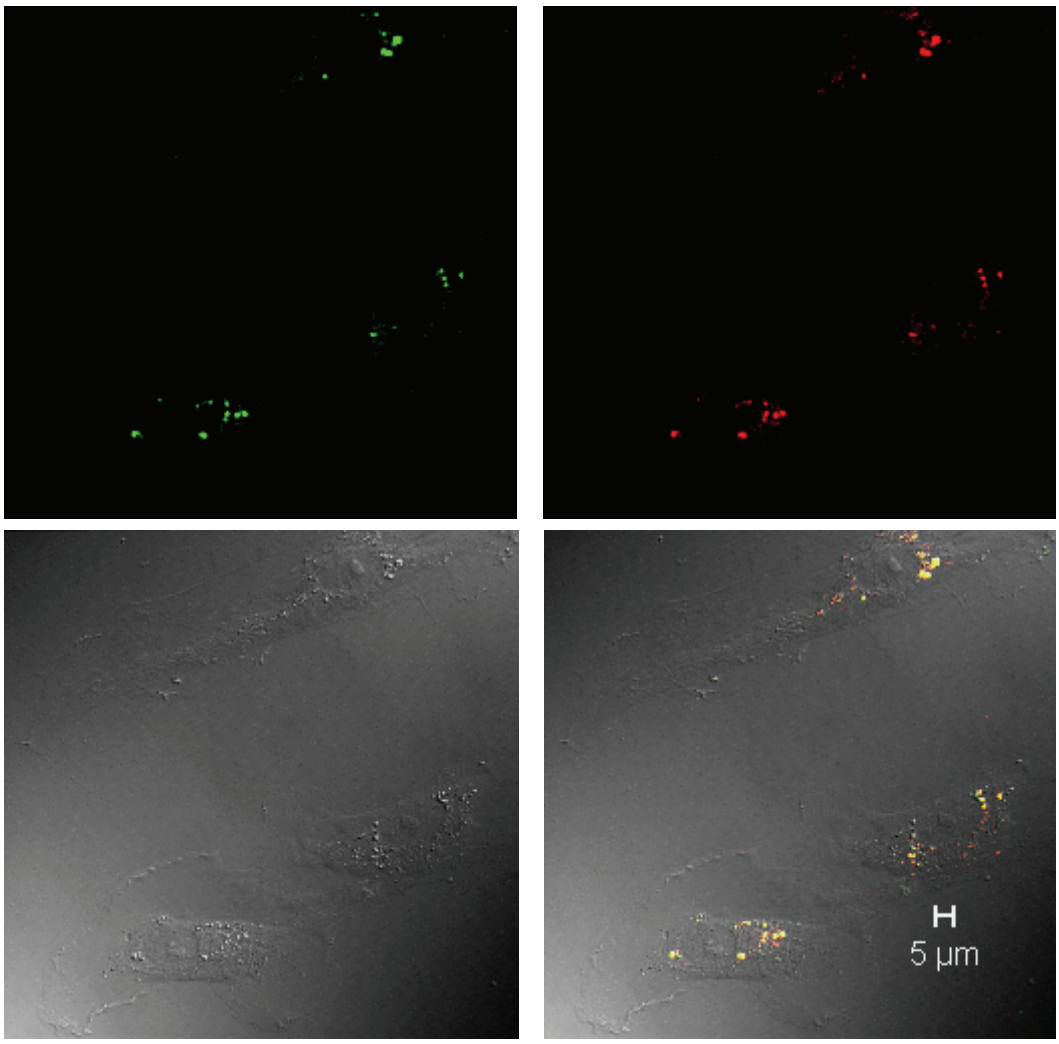

Figure 25: Localization of EGFPRBM5NLS2M. Site-directed mutagenesis of the C-terminal bipartite NLS (NLS2) in full-length RBM5 tagged with EGFP disrupts its nuclear localization. Cells processed for SC35 labeling by formaldehyde fixation and Triton X-100 permeabilization (A) demonstrate an appreciably different localization pattern of RBM5NLS2M as compared to live cells (B). Cell fixation with -20ºC acetone for one minute replicates the data obtained in live cells (C). Live HUVEC cells dually stained with LysoTracker Red DND-99 reveals that pEGFPRBM5NLS2M is targeted to acidic organelles or lysosomes (D). Green fluorescence (EGFP) completely colocalizes with a fraction of the red fluorescence contributed by LysoTracker Red DND-99. Although, all the above images represent HUVEC cells, similar experiments repeated in NIH3T3 and HT-6 cells with either pEGFPRBM5NLS2M or pEGFPNLS1MNLS2M lead to same results. There was no channel crosstalk between LysoTracker Red DND-99 and EGFP. Bars, 5μm.

DISCUSSION

Localization of 815 amino acid full-length RBM5 in nuclear speckles or interchromatin granule clusters (IGCs) was confirmed in this study by creating fusion constructs with enhanced green fluorescent protein. Although a previous study by Edamatsu et al. (2000) confirmed the nuclear targeting of RBM5 by c-myc fusion constructs and indirect immunofluorescence, its subnuclear localization was not clear. Previous studies have demonstrated that the cell nuclei are organized in many specific domains apart from the most clearly visualized cell nucleoli involved in synthesis and processing of ribosomal RNA and assembly of ribosomal subunits (Spector 2001). Correct compartmentalization of any protein is not only essential for its individual activity but can also provide essential clues about the structure and functional relationship of an unknown protein. Some of the nuclear domains discovered so far are Cajal/Coiled bodies (snRNP biogenesis, snRNP and snoRNP trafficking), Gems (snRNP assembly), cleavage bodies (cleavage and polyadenylation steps of pre-mRNA processing), PML bodies (transcriptional regulation), nuclear speckles (pre-mRNA splicing factors) and paraspeckles (Spector, 2001, 2003).

Colocalization studies of EGFP tagged RBM5 with another frequently used non-snRNP nuclear speckle protein SC35 demonstrated that RBM5 localizes to nuclear speckles. This hypothesis was further confirmed by the fact that there is a drastic change in the unique nuclear speckle compartmentalization of RBM5 in the presence of transcriptional inhibitors, mimicking a characteristic displayed by proteins resident in speckles. Absence of RBM5 in chromatin stained with DAPI,

another key feature attributed to nuclear speckle proteins was also confirmed in this study. A high overlap coefficient value ranging from 80% to 90% combined with a Pearson's correlation coefficient value ranging from 0.6-0.8 indicates that the two proteins are not perfectly colocalized. Although, it must be noted that for colocalization computations done in this study, EGFPRBM5 was relatively overexpressed as compared to the native SC35 protein stained by indirect immunofluorescence. Thus, a variation in the observed Pearson's correlation values can be attributed to experimental variation in SC35 staining technique, un-localized excess EGFPRBM5 or indeed that the two proteins do not colocalize completely. Colocaliztion studies of RBM5 and SC35 in the presence of transcription inhibitors although displays a same rearrangement pattern, the degree of overlap is less than that seen in untreated cells. This difference suggests that either overexpressed RBM5 causes SC35 displacement or else the two proteins are not perfectly colocalized and this result may have been amplified in the presence of transcription inhibitors which cause clustering of proteins in fewer speckles. However, it is now a well known fact that various subdomains known as subspeckles exist within the nuclear speckle domains. This subspeckle architecture was demonstrated by staining various RNA processing factors using high antibody titers (Mintz and Spector, 2000). It is possible that both RBM5 and SC35 are present in nuclear speckles but in separate subspeckles. However, these questions can only be effectively addressed if the relative expression of the two proteins is comparable and the same techniques are used to identify both proteins. These questions can be resolved by the availability of RBM5 specific

antibody capable of labeling nuclear speckles. In the future FRET analysis could be used to assess interactions between RBM5 and other nuclear speckle proteins.

Based on the localization of RBM5 in nuclear speckles and the presence of RNA binding motifs, it is possible that full-length RBM5 is involved in pre-mRNA processing. Biochemical isolation of nuclear speckles coupled with proteomic analyses by Saitoh et al. in 2004 revealed more than 146 different proteins including RBM5 present in the speckles. Identification of RBM5 in the nuclear speckle proteomic and this study reinforces the idea that RBM5 is indeed a speckle protein. Also, a majority fraction (81%) of the 146 proteins identified by IGC proteomic analysis were previously associated with RNA metabolism including 51% involved in pre-mRNA splicing (Saitoh et al., 2004). Studies in live cells have shown that nuclear speckle proteins are dynamic and not stationary as suggested by the images of fixed cells. However, there is still a great deal of controversy regarding the role of nuclear speckles in transcription. One school of thought suggests that nuclear speckles are merely store houses of splicing factors from which they are recruited to active sites of transcription, the perichromatin fibrils (Lamond and Spector, 2003). Contrary to this viewpoint, several groups have reported colocalization of pre-mRNA transcripts of highly transcribed genes with nuclear speckles. However, this phenomenon appears to be gene specific and is not seen for all highly transcribed genes (Smith et al., 1999; Shopland et al., 2002). Undoubtedly, resolving the issue of the presence or absence of nascent transcripts within the nuclear speckles will in part define the role of nuclear speckle domains.

As discussed before, RBM5 proteins are well conserved across the species and also shares considerable homology with another RNA binding protein-RBM10. In addition to the two bipartite nuclear localization domains (NLS), the multi-modular structure of RBM5 contains a G-patch domain along with two RNA binding (RRM) and two zinc finger domains, which might function in defining its subnuclear localization in speckles. This study also aimed at discerning the role of the two bipartite NLS at the N- and the C-terminal ends of full-length RBM5 protein. Site-directed mutagenesis and subsequent transient transfection studies of the two bipartite nuclear localization signals, NLS1 (N-terminal) and NLS2 (C-terminal) demonstrated that RBM5 relies on only one NLS for its nuclear targeting. Mutations in NLS1M had no effect on either the nuclear targeting or localization of RBM5 within the speckles. Subsequent SC35 colocalization and transcriptional inhibition studies gave results comparable to those obtained for unmutated RBM5. On the other hand, disruption of the C-terminal NLS (NLS2M) completely abolished nuclear localization of RBM5. Recombinant proteins with both the NLS mutated also displayed similar mislocalizations as expected. Surprisingly, the mislocalized proteins were targeted to lysosomes instead of proteasomes as expected. Localization of mislocalized proteins (EGFPRBM5NLS2M and EGFPRBM5NLS1MNLS2M) to lysosomes was confirmed by staining the acidic organelles with LysoTracker Red DND-99. The mislocalized proteins colocalize with only a part of the stained acidic organelles, confirming that the observed colocalization was not due to channel cross-talk. Autofluorescence and absence of channel crosstalk was also confirmed by performing various controls.

A literature survey reveals that overexpressed or mislocalized proteins are dislocated from the endoplasmic reticulum to the cytosol where they are usually degraded by proteasomes in a ubiquitin dependent or independent manner. Massive loads of the mislocalized or aggregated proteins which cannot be rapidly degraded by ubiquitin-proteasome pathway are aggregated into inclusion bodies known as aggresomes which then might integrate with lysosomes for degradation (Kopito, 2000). Macromolecular or protein degradation by lysosomes can take place through multiple pathways such as macroautophagy (organelles), crinoautophagy (secretory proteins), heterophagy (endocytosis of plasma membrane proteins), microautophagy or chaperone-mediated autophagy (Knecht and Salvador, 2005). In chaperone-mediated autophagy cytosolic proteins are directly transported inside the lysosomes for degradation via the action of chaperone hsc73 and lamp2a receptor. A variety of signal sequences specific for lysosomal targeting such as KFERQ in cytosolic proteins and NPXY, YXXØ, [DE]XXXL[LI] or DXXLL (X is any amino acid and Ø is an amino acid with a bulky hydrophobic side chain) in transmembrane proteins have been discovered so far (Bonifacino and Traub, 2003; Knecht and Salvador, 2005). However, the exact mechanism by which mutated RBM5 with non-functional NLS is targeted to lysosomes is not clear. A recent study has shown that ubiquitinated Jun is primarily targeted to lysosomes and can be cosedimented with a lysosomal hexosaminidase activity. In this case the PPVY signal sequence mediates the ubiquitination of Jun by E3 ligase or Itch (Fang and Kerppola, 2004).

Thus, from the site-directed mutagenesis experiments it is clear that the C-terminal NLS of RBM5 is the primary NLS mediating its nuclear targeting. This

result concurs with a previous observation by Edamatsu et al. that the N-terminal half of RBM5 protein fails to localize to nucleus. Two scenarios for the N-terminal NLS (NLS1M) can be speculated – either the NLS1 even though well conserved is non-functional or alternatively it is cryptic or unexposed. If indeed, the N-terminal NLS is non-functional it is extremely tempting to speculate that all of the RBM5 splice variants, none of which possess the C-terminal NLS, will fail to colocalize in nuclear speckles. The fact that protein products for some of the splice variants have not been observed so far suggests that their role is deviant from the common function of translation to a protein product. As mentioned before, VEGF treatment of endothelial cells induced the expression of full-length RBM5 transcripts, but had no effect on the 7.4 kb transcript encoding the splice variants. Clearly, future studies to determine the role and cellular localization of these RBM5 splice variants will prove to be exciting.

PART III

CONCLUSIONS AND FUTURE STUDIES

The growth of blood vessels or vasculature plays a central role in many physiological and pathological conditions. Understanding the mechanisms fine-tuning angiogenesis through the study endothelial cells, a key component of blood vessels, has been a focus of intense research. Vascular endothelial growth factor (specifically VEGF-A) is a pro-angiogenic growth factor that performs a vital role in angiogenesis. Unraveling the signaling cascades emerging from VEGF-A stimulation of endothelial cells has provided valuable insights into the downstream effectors of angiogenesis. At the onset of this project there was clearly one key research area neglected - the role of immediate early genes induced by VEGF-A. Through this study I identified a unique set of 17 immediate early genes induced by VEGF-A, including several transcription factors, growth factors and also a putative tumor suppressor gene RBM5 (Chapter 2, Part I).

RBM5 (RNA binding motif protein 5) was initially discovered as a part of chromosomal region 3p21.3 frequently deleted in various cancers. Subsequent studies by Sutherland et al. (2000) and Oh et al. (2006) also implicated RBM5 and its splice variants as a regulator of apoptosis (Chapter 1, Part II). The role of RBM5 as an immediate early gene induced by VEGF-A opened an entire new avenue of possibilities. The domain rich full-length coding sequence of RBM5 provided an

exciting opportunity to design an array of projects aimed at understanding the structure and function relationship of RBM5. The gene RBM5 is well conserved across the species and also shares 51% homology with another RNA binding protein, RBM10. The localization of RBM5 in SC35 stained nuclear speckles was confirmed in this study. Nuclear localizations of RBM5 were completely abrogated by the disruption of the C-terminal NLS (NLS2) only. The N-terminal NLS of RBM5 is probably non-functional or unexposed. Non-functionality of the N-terminal RBM5 concurs with the results obtained by Edamatsu et al. (2000) using deletion mutants fused to c-myc epitope. Thus, now only the functional C-terminal NLS can be used to deduce the family of importins responsible for transporting RBM5 into the nucleus. Additionally, I suspect that RBM5 splice variants will fail to localize in the nucleus. This in turn raises intriguing questions regarding the physiological role and localization of these RBM5 splice variants. Moreover, full-length RBM5 with mutated NLS2 unexpectedly mislocalized to lysosomes instead of proteasomes as revealed by dual fluorescent staining with LysoTracker Red. Degradation of mono-ubiquitinated transcription factors including Jun in lysosomes is well known. However, further experimentation to determine ubiquitination of RBM5 was hampered by the non-availability of RBM5 specific antibodies.

Even though in this study RBM5 displayed absolute nuclear speckle localization, many RNA binding proteins are known to shuttle between the nucleus and cytosol. The pEGFPRBM5 construct used in this study can be applied to design heterokaryon assays to detect any nucleo-cytoplasmic shuttling of RBM5. Additionally, dynamics of RBM5 protein in nuclear speckles can be visualized using

the same construct coupled with live cell microscopy. Moreover, mutational analysis coupled with a reporter such as EGFP used in this study can aid in determining the domains responsible for localization of RBM5 specifically in nuclear speckles as opposed any other subnuclear site.

ANGIOGENESIS/APOPTOSIS/TUMOR SUPPRESSOR GENE?

Function of RBM5 in RNA metabolism can be speculated based on its localization in nuclear speckles and the presence of various domains such as RRM and G-patch domains. Apart from being an IEG induced by a pro-angiogenic factor VEGF-A, RBM5 is also implicated to function as a tumor suppressor gene and an apoptotic regulator. Identifying the family of RNA molecules it binds along with the development of knockout mice might help in deducing the function of RBM5 in these diverse roles. Although, previous studies demonstrated that RBM5 selectively binds to poly (G) RNA homopolymer, further RNA binding studies are hampered by difficulties in production of full-length RBM5 protein *in vitro* and the commercial unavailability of RBM5 specific antibody. Most of the popular methods designed to discern the RNA binding properties of proteins such as SELEX or SNAAP either require milligram quantities of the same protein or a specific antibody for immunoprecipitation studies. Unfortunately, in the case of RBM5 none of these products were readily available. Production of recombinant RBM5 with a GST (glutathione S-transferase) tag detailed in Appendix A is a huge step for future studies aimed at discerning the RNA substrate of RBM5.

Site-directed mutagenesis of the various RBM5 RNA binding domains can be subsequently used to deduce the amino acids influencing the binding affinity of its RNA substrates. Moreover, mutational analysis coupled with a reporter such as EGFP used in this study can aid in determining the domains responsible for localization of RBM5 specifically in nuclear speckles as opposed any other nuclear site.

VEGF AND INDUCTION OF RBM5

The induction of RBM5 by VEGF-A in endothelial cells raises another intriguing question regarding the signaling cascade involved. I attempted to answer this question by using various signal transduction inhibitors coupled with quantitative real time RT-PCR to discern any changes in RBM5 gene expression (Appendix B). However, these studies were greatly hindered by not only the slow growth rate of HUVEC, but also by the low copy number of native RBM5 transcript and difficulty in finding a good control gene not affected by VEGF-A. Despite these limitations a few conclusions affecting future studies to dissect the VEGF-A signal transduction pathway leading to RBM5 induction by various methods such as use of adenoviral constructs of constitutively active signal transducers or siRNA can be drawn from these experiments. Clearly, novel methods for equalizing gene expression experiments instead of relying on the standard housekeeping genes which are equally affected by VEGF-A in real time PCR are needed.

OTHER IMMEDIATE EARLY GENES

Although, this study focused mainly on RBM5, understanding the role of the remaining 16 immediate early genes will undoubtedly play a vital role in piecing together the big picture of angiogenesis. During the course of this study only a few of the immediate early genes such as COX-2, EGR2, ETR101 and ATF3 have been reported to be induced by VEGF-A. However, the overall role of the various immediate genes including many transcription factors identified and their downstream effectors is yet to be discovered. Understanding the mechanisms of VEGF-A induced angiogenesis and its downstream modulators may help in fine-tuning the derailed proliferation of blood vessels in various pathological conditions and may perhaps also lead to the design of new families of anti-angiogenic drugs.

APPENDICES

APPENDIX A

PRODUCTION OF FULL-LENGTH RBM5 AND DEVELOPMENT OF REAGENTS FOR SNAAP ANALYSIS

INTRODUCTION

As discussed before, RBM5 an immediate early gene induced by VEGF-A is also implicated to play a role in apoptosis and may also function as a tumor suppressor gene. In addition to the two bipartite NLS, RBM5 also contains two RRM domains, a G-patch domain and two zinc finger domains. Based on the presence of these domains and the fact that RBM5 localizes in nuclear speckles enriched in splicing factors, it may be deduced that RBM5 functions in RNA metabolism. Moreover, identifying the family of RNA substrates bound by RBM5 may provide an invaluable insight on the function of RBM5 as a TSG, in apoptosis and angiogenesis.

Loss of function of RNA binding proteins DAZ (deleted in azoospermia) and FMRP (fragile X mental retardation protein) have been shown to be important in genetic disorders azoospermia and fragile X mental retardation, respectively. Myotonic dystrophy on the other hand is caused due to the unusually tight binding and sequestering of CUGBP1 (CUG binding protein 1) to the CUG repeats present in

the 3' UTR of mutant myotonin protein kinase (DMPK) transcript, leading to aberrant processing of other CUGBP1-RNA substrates and manifestation of myotonic dystrophy (Rodgers et al., 2002; Sung et al., 2000). Thus, even though RNA binding proteins play a very important role in processing and turnover of RNA, relatively little is known about their function (Trifillis et al., 1999). A major hurdle faced in studying the function of an RNA binding protein is to resolve the RNA substrates that bind to it. Traditional methods such as SELEX (systemic evolution of ligands by exponential enrichment) and its variations can be used to resolve this problem. SELEX involves multiple rounds of PCR amplification and subsequent selection of the strongest binding RNA substrate. Although very powerful and utilized successfully in many cases, this method has two major drawbacks. The RNA substrates used are short artificially synthesized RNA molecules. Thus, the RNA substrates positively identified may not exist in vivo. Another drawback is that only molecules which are bound directly by the RNA binding protein are recognized (Trifillis et al., 1999).

To circumvent these problems, an alternative approach known as the SNAAP (specific nucleic acids associated with proteins) developed by Kiledjian et al. was chosen (Rodgers et al., 2002; Trifillis et al., 1999; Carr-Schmid, 2006). This method utilizes the intact endogenous cellular mRNA associated with its mRNP, maintaining the RNA-protein interaction occurring in vivo, followed by microarray or differential display analysis to identify the RNA substrate. Thus, both direct and indirect binding of RNA substrates to RBM5 can be discerned (Trifillis et al., 1999). False positive results obtained due to promiscuous binding by RNA binding proteins (RBP) are

eliminated by carrying out the analysis in parallel for protein of interest and another unrelated RBP. Thus, RNA molecules bound by both RBPs are probably false positives and are eliminated. Whereas, RNA molecules bound by one RBP only, most likely reflect its true RNA binding properties.

Efficacy of SNAAP was tested by the authors on existing RNA-protein interaction of mDAZL (murine autosomal deleted in azoospermia-like protein) with Tpx-1 and Cdc25A mRNAs and α complex protein 1 (αCP1) stabilizing human α-globin mRNA. In case of αCP1, the method not only identified the existing RNA protein interactions but also identified two new interactions with TAPA-1 and cox-2 mRNAs. All the results were further confirmed by studying direct interaction between the αCP1 and TAPA-1/coxII mRNAs using EMSA (electro-mobility shift assays) (Trifillis et al., 1999; Carr-Schmid, 2006).

However, in this study production of full-length RBM5 protein tagged to biotin (pPinpoint vector) in *E.coli* cells resulted in approximately 20 pre-maturely truncated products with very little full-length RBM5. It was hypothesized that presence of two to three consecutive arginine residues (an amino acid with rare tRNA in *E.coli* cells) throughout the sequence might have led to the pre-mature termination. Unfortunately, the problem of production of truncated products did not improve even in the presence of a helper plasmid pSJS1240 encoding rare *E.coli* tRNAs – a kind gift from Dr. Cameron, Pennsylvania State University (Kim et al., 1998). Therefore, I decided to attempt production of full-length RBM5 protein in *Sf9* insect cells which mirror eukaryotic systems more closely than prokaryotes. A GST (glutathione S-transferase) tag instead of charged histidine tag was used to produce RBM5 since

charged His residues may interfere with the RNA binding (Trifillis et al., 1999). The GST-RBM5 fusion protein expression is controlled by a strong AcNPV (*Autographa californica*) polyhedrin promoter. Indeed, it was possible to produce full-length RBM5 protein in these cells, a big step forward in an attempt to discern the RNA binding properties of RBM5. Since RBM5 is a nuclear speckle protein nuclear extracts from HT-6 cells were produced as a source of RNA substrates for SNAAP assay.

Unfortunately, due to technical difficulties and the length of time needed to conduct SNAAP analysis beginning from full-length protein production, a project worth another dissertation in itself, it was not possible to uncover the identity of RNA species bound by RBM5.

MATERIALS AND METHODS:

Cell Culture

The *Sf9* (ATCC) insect cell line established from ovarian tissues of *Spodoptera frugiperda* larvae (ATCC) was grown in either Grace's Insect cell or TNM-FH media (Invitrogen or Sigma Aldrich) supplemented with 5% fetal bovine serum at 28°C. The cells were passaged as soon as they reached 80% confluence either on 150 mm tissue culture dishes or in suspension in 250 ml suspension culture flask (Corning).

Recombinant plasmid production and Sf*9* transfection

Construction of pACG3XRBM5 vector – A baculovirus transfer vector encoding GST expression-pAcG3X (PharMingen, BD Biosciences) was modified to include Sac I (GAGCTC) restriction site. The adaptor carrying the Sac I restriction site was designed by annealing two oligonucleotides:

1) G3XSACD (5' GATCCCCTCAGAGCTCGGG 3')

2) G3XSACU (5' AATTCCCGAGCTCTGAGGG 3).

The annealing reaction (10 µl) was carried out as follows:

G3XSACD (476 µM)	2 µl
G3XSACU (430 µM)	2 µl
10X Advantage 2 PCR buffer (Clontech)	1 µl

The reaction was heated to 94ºC and allowed to cool gradually at room temperature. The annealing reaction was further diluted (1:100) and used to generate pAcG3X-Sac I vector by performing a ligation reaction as below:

(BamH I - EcoR I) CIP dephosphorylated pAcGX vector	1µl (100 ng)
Annealed product (1:100)	1 µl
10X T4 DNA ligase buffer (Promega)	1 µl
T4 DNA ligase	1 µl
dH_2O	6 µl

Ligation reaction was incubated overnight at 16ºC. Competent JM109 (Promega) cells were transformed with the above ligation reaction and plated on LB agar plates containing 100 µg/ml ampicillin. After, overnight incubation recombinant colonies were processed for plasmid isolation and sequenced to confirm the orientation of

ligations as described before (Chapter 2, Part II). The RBM5 coding sequence spliced out from pEGFPRBM5 (Sac I - EcoR I) and gel purified using DEAE membrane (Chapter 2, Part 1) was used as a template for the ligation reaction set up as below to generate pAcG3XRBM5:

(Sac I - EcoR I) CIP dephosphorylated pAcGX vector	1µl (60 ng)
(Sac I - EcoR I) RBM5	1µl (40 ng)
10X T4 DNA ligase buffer (Promega)	1 µl
T4 DNA ligase	1 µl
dH_2O	6 µl

Ligation reaction was carried out as mentioned before. Competent JM109 cells were transformed with the above ligation reaction and plated on LB agar plates containing 100 µg/ml of ampicillin. After, overnight incubation recombinant colonies were processed for plasmid isolation and sequenced to confirm the orientation of ligations as described before. Two recombinant pAcG3XRBM5 clones (#5 and #13) were selected and grown overnight in 100 ml of Terrific broth containing 100 µg/ml ampicillin at 37°C/200 rpm. Plasmid midipreps were carried out by alkaline lysis method (Sambrook et al., 1989). Purity of the isolated DNA was confirmed by measuring 260/280 absorbance ratio and agarose gel electrophoresis. The plasmid minipreps were further purified twice using cesium chloride density gradient (containing ethidium bromide) centrifugation as mentioned in Sambrook et al., 1989. Isolated plasmid bands were extracted five times with water saturated 1-butanol and subsequently precipitated by ethanol twice. The plasmid pellets were then dissolved in 200 µl of sterile TE buffer and used for subsequent transformation of insect cells as

detailed in the next section. All subsequent procedures were carried out for pAcG3X empty vector and both the pAcG3XRBM5#5 and pAcG3XRBM5#13 clones, in parallel.

Transfection of Sf9 cells - For construction of recombinant virus co-transfection experiments in *Sf9* (*S. frugiperda*) insect cells with purified plasmids (pAcG3XRBM5#5, pAcG3XRBM5#13 and pAcG3X) and linearized baculovirus DNA (BacPAK6 DNA Bsu36 I digest, Clontech) was carried out. All procedures for transfections including control were carried out as detailed in the Clontech manual PT1260-1. Briefly, 5 µl of each plasmid (100 ng/µl) and linearized baculovirus DNA were suspended in 86 µl of water and 4 µl of Bacfectin (Clontech) and incubated for 15 minutes at room temperature. The reaction was subsequently layered onto *Sf9* cells and further incubated for five hours at room temperature. After five hours of incubation additional media was added and plates were incubated further at 28ºC until the positive control plate developed a blue color. Media from all the plates containing recombinant viruses was transferred after five days and stored in 15 ml Falcon tubes at 4ºC.

Plaque Assay to purify recombinant viruses

Plaque Assay - All plaque assays were carried out in six well tissue culture plates. Briefly, each well was seeded with *Sf9* cells (95% viability) until 50% confluent in 2 ml of TNM-FH medium without any additives. Subsequently, each well was infected with 100 µl of individual dilution for each plasmid (10^{-4}, 10^{-5}, 10^{-6}, 10^{-7}, 10^{-8}) or TNM-FH medium as negative control and incubated for two hours at

28ºC. The media was then replaced with 2 ml of 1% low melting Sea-Plaque agarose dissolved in Grace's Insect cell medium. The plates were further incubated for eight days at 28ºC. Plaque clearings were observed by staining the plates with 0.03% neutral red solution for 2-3 hours at 28ºC. The stain was then removed and the plates were further incubated overnight for plaques to clear.

Virus Propagation – Individual plaques were picked up using sterile Pasteur pipettes and re-suspended in individual sterile microcentrifuge 1 ml TNM-FH medium containing 5% FCS. The tubes were rotated overnight at 4ºC to elute virus from agarose plugs. In total, 30 plaques (10 each for pAcG3XRBM5#5, pAcG3XRBM5#13 and pAcG3X) were picked. Viruses in each plaque elute (100 µl) were further amplified by infecting fresh *Sf9* cells seeded in TNM-FH medium with 5% FCS in six-well plates. All plates were incubated at 28ºC until cells displayed cytopathic effects. Cells were harvested and cell pellets were further processed for western analyses (see below) to determine protein production. These secondary amplification supernatants were stored at 4ºC and used for protein production as detailed in the next section. Titers of secondary amplifications were determined using rapid titer assay (Clontech). Subsequent, high titer viral stocks for protein production were made by infecting *Sf9* cells with secondary amplification stocks at an MOI of less than one.

Protein production

Sf9 cells grown as suspension cultures with more than 95% viability were used to seed 175 cm^2 T-flasks (Nalge Nunc International). Old media was replaced

with 30 ml of fresh TNM-FH. The cells were then infected at an MOI of 5 and incubated at 28ºC for three days for protein production. Cells were harvested and centrifuged at 10,000g for 5 minutes. The supernatant was subsequently discarded and cell pellets containing the recombinant protein were stored at -20ºC. Protein production for RBM5 and RBM5GST was done in *Sf9* cells. *E.coli* cells were used to produce αCP1GST protein – a kind gift from Dr. Kiledjian (Trifillis et al., 1999; Kiledjian et al., 1999). Protein extracts in lysis buffer (Appendix B) were prepared by nitrogen cavitation in presence of cocktail of EDTA free protease inhibitors (Roche Applied Science).

Western analysis

Approximately, 30-50 µg of cell pellet dissolved in 1X Laemmli buffer were boiled for five minutes and subsequently separated on 7.5% SDS-PAGE gels (Laemmli, 1970). Amount of recombinant protein was quantified by running 100 ng GST (Santa Cruz Biotechnology) on the same gel along with molecular weight markers (Sigma Aldrich). The gel was transferred onto a nitrocellulose membrane for 4 hours/220 mAmps/4ºC as detailed in Sambrook et al. 1989. The membrane was then air dried overnight and subsequently blocked for 1 hour in 10 ml of BlottoA (5% w/v non-fat dry milk in TBST). Primary monoclonal anti-GST antibody (50 µl in 10 ml BlottoA) (sc-138, Santa Cruz Biotechnology) was added to the membrane and further incubated for another hour. The membrane was then washed thrice in 10 ml of TBST (Appendix B) and incubated for one hour in 10 ml of BlottoA containing 10 µl of goat anti-mouse IgG-HRP (sc-2005, Santa Cruz Biotechnology). Blots were

then washed thrice in 10 ml of TBST and TBS each for five minutes and developed by Pierce ECL western blotting substrate for one minute (Pierce Biotechnology) for chemiluminescent detection. Membranes were blotted dry and exposed to BioMax X-ray films (Kodak) for one and five minutes.

Preparation of nuclear extracts

HT-6 (SV40 large T antigen transformed HUVEC) cells were grown in EGM medium as previously described for HUVEC cells (Chapter 2, Part I). Preparation of nuclear extracts from HT-6 cells was done as described in CelLytic™ NuCLEAR™ extract kit manual, a method adapted from Dignam et al. published in 1983 (Farrell, 1998).

RESULTS AND DISCUSSION

Production of recombinant proteins

Detection of RNA binding protein substrates is a major step in defining its function. Unfortunately, in case of RBM5 this process was hampered by the unavailability of pure isolated protein. As mentioned before RBM5 protein production in prokaryotic system resulted in 20-25 bands representing early truncation products with minimal amount of full-length product. Binding assay techniques such as SELEX and SNAAP designed to select RNA species bound by the RBP require pure protein. On the other hand, immunoprecipitation coupled with

cross-linking methodologies require a protein specific antibody, which was also commercially unavailable for RBM5.

Switching the host system from prokaryotic to insect cell cultures resulted in the production of full-length RBM5 protein. However, as seen from the western analysis (figure 26) two distinct clones, one producing full-length RBM5 and other resulting in truncated products (lanes 3 and 9) were observed. Large-scale production of full-length RBM5GST protein was also done successfully for two (#13PP1T1 and #5PP4T1) of the twenty plaque picks selected. The expected molecular weight of full-length RBM5 and RBM5GST proteins is 92 kDa and 118 kDa respectively. However, since the molecular weight of RBM5GST is higher (figure 26) than predicted, it is very likely that the RBM5 undergoes post-translational modifications. Western analysis of RBM5 by Sutherland et al. also showed similar results. Additionally, it is unlikely that the GST tag in RBM5GST undergoes any modifications since the predicted and the observed molecular weight of GST produced in insect cells on western blots is the same (figure 27A).

Elimination of false positive RNA binding in SNAAP analysis is done by running the experiments in parallel for two other controls, GST and αCP1GST. Polycytidylate-binding protein αCP1 was chosen in this study for two reasons. Firstly, αCP1 contains KH domains a different RNA binding domain as compared to the RRM domains present in RBM5. Secondly, as the name suggests αCP1 preferentially binds to poly (rC) instead of poly (rG) as displayed by RBM5. Thus, any RNA substrates bound by both proteins with different characteristics are probably false positives and must be discarded. Selection of GST as a third control is

necessary to eliminate any RNA molecules bound by the two RBP fusion constructs. Both GST and αCP1 were successfully produced in *Sf9* cells and *E.coli*, respectively (figure 27).

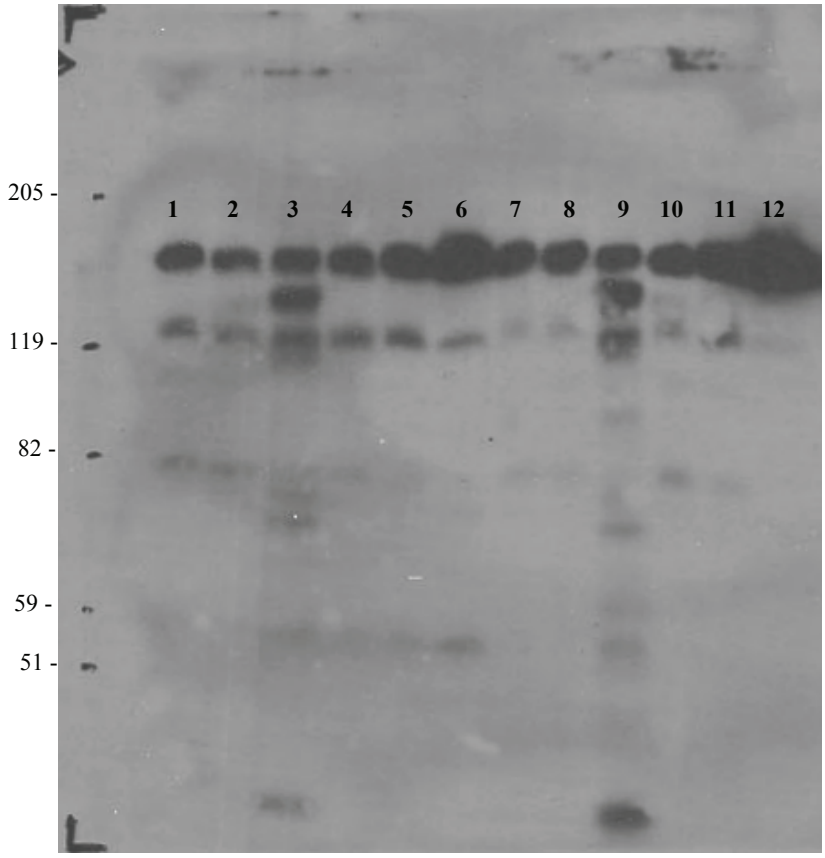

Figure 26: Western blot probed with anti-GST antibody. Cell pellets obtained during secondary amplification of four different RBM5GST plaque picks on day two and three of incubation are displayed in lanes 1-4 and lanes 7-10, respectively. Production of recombinant RBM5GST protein from high titer stocks after day two and three of incubation are shown in lanes 5-6 and lanes11-12, respectively. High titer stocks were produced for two different clones, #13PP1T1 (lanes 5 and 11) and #5PP4T1 (lanes 6 and 12). Molecular weights of pre-stained protein ladder are displayed on the left.

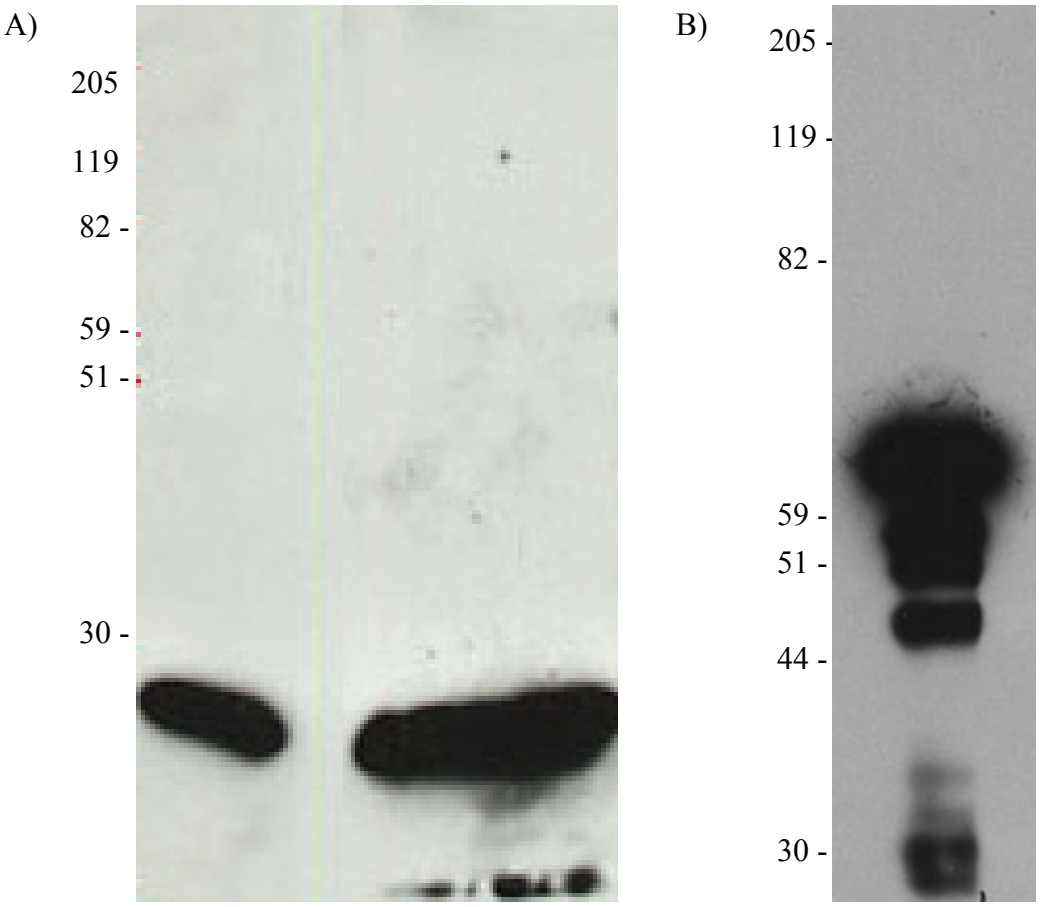

Figure 27: Production of two control proteins glutathione S-transferase (pAcG3X) in *Sf9* insect cells and αCP1GST protein in *E.coli* cells is shown in two western blots probed with anti-GST antibody. The molecular weight of the 26 kDa GST produced in insect cells (right side of blot A) concurs with the commercially available control GST (100 ng, left side of blot A). Protein production for 62 kDa αCP1GST protein was carried out in *E.coli* cells as detailed by Trifillis et al., 1999. Molecular weights of pre-stained protein ladder are displayed on the left.

SUMMARY

Determination of RNA substrates bound by any of RNA binding protein is vital for determining its probable function. Popular techniques require either milligram quantities of proteins (SELEX, SNAAP) or require antibodies with high binding affinities against the protein of choice, both of which were unavailable for RBM5. RNA binding studies for RBM5 were further hampered by the difficulty in producing full-length RBM5 protein in the commonly used prokaryotic systems. This experiment establishes a protocol for successful production of full-length RBM5 protein in insect cells using baculoviral vectors. Two other control proteins GST and αCP1GST necessary to rule out false positives in SNAAP analysis were also successfully produced. Production of full-length RBM5 defines the first key step necessary to experimentally deduce its RNA substrates. The same system can also be further used to introduce mutations in the two RRM domains to discern the amino acid residues vital for maintaining the RNA binding characteristics of RBM5.

APPENDIX B

DISSECTION OF VEGF-A/VEGFR SIGNAL TRANSDUCTION CASCADE IN HUVEC CELLS UPSTREAM OF RBM5

INTRODUCTION

Stimulation of normally quiescent endothelial cells by pro-angiogenic cytokine VEGF-A is a key step in both physiological and pathological angiogenesis. Induction of immediate early gene RBM5 within an hour in endothelial cells stimulated by VEGF-A was confirmed by northern analysis (Chapter 2, Part I). As discussed in Chapter 1 (Part I) the signal transduction cascade emerging from the stimulation of endothelial cells by VEGF-A has been delineated. Various pathways such as PI3K, MAPK and p38 MAPK are implicated in apoptotic survival, proliferation and migration of endothelial cells, respectively (Karkkainen et al., 2002; Chapter 1, Part I). Despite the fact that the VEGF-A/VEGFR signaling pathways have been defined, the downstream effectors and the manner in which VEGF regulates these functions in endothelial cells is unclear. Thus, defining the signaling cascade leading to the induction of the putative tumor suppressor gene and an apoptotic regulator RBM5 would represent an exciting avenue to categorize the function of RBM5 in the big picture of angiogenesis.

The use of pharmacological inhibitors is one of the quickest ways to get the initial raw data on the possible upstream signal transduction cascades regulating the gene in

question. Typically, serum starved cells (HUVEC) are pre-treated with inhibitors, usually four to five times the IC_{50} or K_i value followed by stimulation with growth factor (VEGF-A) (Liu et al., 2003; Calbiochem Inhibitor SourceBook™). Down- or up-regulation of RBM5 gene expression in presence or absence of inhibitors and VEGF can then be quantified by real time PCR with respect to the quantity of a stable house-keeping gene (Bustin et al., 2005). Although, initially this approach seemed reasonably simple, this project was greatly hampered by two main factors. Firstly, most of the house-keeping genes commonly used for normalization of RNA quantity were also up-regulated by VEGF thus, negating any discernment of RBM5 induction in HUVEC. Secondly, the slow growth of HUVEC cells in vitro also limited the number of repetitions that could performed for each inhibitor condition in a limited time frame thereby, making it impossible to conduct any further non-parametric statistical analyses (Tichopad et al., 2006). Despite these limitations the initial data obtained in this study can be vital to design further experiments using various other techniques such as, RNAi or constitutively active or inactive adenoviral vectors to discern the upstream signaling regulators.

METHODS AND MATRIALS

Cell culture and inhibitor treatments

HUVEC cell culture and VEGF-A induction studies were carried out as detailed in methods and material section of Chapter 2 (Part I). For inhibitor studies, HUVEC cells were pre-treated with respective concentrations of pharmacological inhibitors for 30 minutes and subsequently stimulated with 10 ng/ml of VEGF-A for 60 minutes in the

presence of inhibitors. Controls consisted of cells treated with an equivalent concentration of carrier (dimethyl sulfoxide/DMSO) used to make up inhibitor stock solutions and inactive analogs of inhibitors when available. List of inhibitors and the concentrations used as determined by literature survey and IC_{50} or K_i values is given in the table below.

	Inhibitors used	K_i/ IC_{50}	Conc. used	Dissolved in	Signaling response targeted
1.	LY294002	1.4 μM	5-30 μM	DMSO	PI3K activation
2.	LY303511	≥100 μM	5-30 μM	DMSO	Inactive analog of LY294002
3.	Wortmannin	5 nM	0.1-1 μM	DMSO	PI3K activation
4.	PD98059	2-7 μM	10-20 μM	DMSO	MEK1/2 activation
5.	U0126	10 μM	40-100 μM	DMSO	MEK1/2 activation
6.	U0124	-	40-100 μM	DMSO	Inactive analog of U0126
7.	SB220025	60 nM	1-10 μM	DMSO	p38 MAPK (α and δ isoforms)
8.	SB202190	100 nM	5-10 μM	DMSO	p38 MAPK (α and β isoforms)
9.	Gö6983	7-60 nM	1-3 μM	DMSO	PKC activation except PKC_{μ}
10.	Bisindolylmaleimide I HCl	10 nM	0.2-3 μM	DMSO	PKC activation
11.	BAPTA/AM	N/A	10-50 μM	DMSO	Ca^{+2} mobilization
12.	SU5416	1 μM	10-20 μM	DMSO	VEGFR2
13.	L-NIO.2HCl	500 nM	10-50 μM	EBM 0.5	eNOS
14.	L-NAME	500 nM	5-100 μM	EBM 0.5	eNOS

Table 6: Concentrations of the inhibitors used in this study and the points of signal transduction cascades targeted are listed. All inhibitor stock solutions were made up in DMSO (dimethyl sulfoxide) except for water soluble eNOS inhibitors which were dissolved in EBM 0.5. All inhibitors were purchased from Calbiochem excluding SU5416 which was obtained from Sigma Aldrich. IC_{50} values were obtained from the Calbiochem Inhibitor SourceBook™.

RNA isolation and cDNA production

Media from the tissue culture plates was aspirated after respective VEGF-A or VEGF-A and inhibitor treatment. Cells were immediately lysed using 3 ml of RNA Bee (Tel-Test) per 150 mm tissue culture dish (Corning). Protocols for RNA isolation were carried out according to manufacturer's directions and as detailed in Chapter 2 (Part I). Integrity of RNA was assessed by electrophoretic gel analysis of 28S and 18S rRNA bands and ratio of absorbance (greater than 2) obtained at 260 nm and 280 nm. High capacity cDNA archive kit (Applied Biosystems) was used to reverse transcribe 5 μg of total RNA in a 50 μl reaction to cDNA (random primers) according to manufacturer's directions. The reverse transcription reaction was carried out at 37ºC for 120 minutes. The cDNA products were subsequently stored at -20ºC until used for estimation of gene quantification by real time PCR. Total RNA from Raji cells (Clontech) was reverse transcribed in parallel and used for construction of standard curves as described in the next section.

Real time PCR

The following pre-made FAM labeled MGB probe and primer sets used in this study were obtained from Applied Biosystems: RBM5 (Hs00172952_m1), GAPDH (4333764F), HPRT1 (4333768F), cyclophilin A or PPIA (4333763F), 18S rRNA (4352930E). Efficiencies of RBM5, HPRT1 and 18S rRNA real time PCR reactions were calculated from standard curves obtained by serialy diluting Raji cDNA. Each real time PCR reaction was done in triplicates using cDNA corresponding to 100 ng of total RNA in a 50 μl reaction also containing individual probe and primer sets and TaqMan®

Universal PCR master mix (4304437) on the ABI Prism 7700 platform (Applied Biosystems). Up- or down-regulation of RBM5 (target) with respect to housekeeping genes (reference) in presence or absence of inhibitors was calculated using the following formula (Pfaffl, 2001):

$$ratio = \frac{(E_{target})^{\Delta Ct_{target}(control-sample)}}{(E_{reference})^{\Delta Ct_{reference}(control-sample)}}$$

Efficiency of the real time PCR reaction for both target (RBM5) and reference (housekeeping gene) is calculated as E=10[-1/slope]. The value of the slope is obtained by performing standard curve over three dilution range. Both 'control' and 'sample' in the above equation represent the mean values of each condition done in triplicate. The threshold value (Ct) is defined as the PCR cycle number when the fluorescence generated by the accumulated amplicons crosses the threshold. This value is inversely proportional to the initial number of transcripts, thus higher the copy of a transcript, lower is the Ct value (Bustin, 2000).

RESULTS AND DISCUSSION

Selection of a suitable housekeeping gene for detecting induction of RBM5

As mentioned before in the introduction section, selection of a suitable housekeeping gene to detect up-regulation of RBM5 was a major hurdle. The simplified $2^{-\Delta\Delta Ct}$ method (assumes PCR amplification efficiency as two) for estimation of change in

gene expression with respect to a normalized control was not used due to different PCR reaction efficiencies of RBM5 and housekeeping genes (see next section) (Thellin et al., 1999; Livak and Schmittgen, 2001). An ideal housekeeping gene must have following characteristics: 1) no changes in the expression level of transcripts under conditions of study, 2) have real time PCR efficiency close to that of gene under study and 3) also be present in approximately the same quantity as the target gene in study for equivalent reverse transcription kinetics. Housekeeping genes commonly used to normalize RNA loading were also up-regulated in presence of VEGF-A similar to RBM5. Thus, any gene quantification calculations for RBM5 normalized to housekeeping genes showed negative or no significant induction, contradictory to the induction by VEGF-A discerned clearly by northern analysis (Chapter 2, Part I). Similar results were also obtained for GAPDH previously used in this study to normalize the quantity of total RNA in northern analysis. These disparate results might be attributed to two factors. First, the efficiency of RBM5 probe and primer set is lower as compared that of GAPDH which in turn reduces the value of numerator representing the induction of RBM5. Secondly, the amount of GAPDH mRNA is considerably higher than RBM5 mRNA as seen from the significant difference in Ct values for the same RNA sample.

In this study, five different housekeeping genes including glyceraldehyde-3-phosphate dehydrogenase (GAPDH), cyclophilin A or peptidylprolyl isomerase A (PPIA), 18S rRNA, hypoxanthine phosphoribosyl transferase 1 (HPRT1) and polymerase (RNA) II (DNA directed) polypeptide A (POLR2A) were examined. Although, the quantity of POLR2A was similar to that of RBM5 transcript (similar Ct values), it was simultaneously induced by VEGF as seen by the negative values for RBM5 induction

(figure 28A). Similar results were seen for GAPDH and PPIA transcripts, both of which are represented by a higher number of transcripts than RBM5. Two main housekeeping genes 18S rRNA and HPRT1 emerged as possible candidates to assess RBM5 gene induction. Although, ribosomal RNA is known not to vary widely under conditions changing gene expression, the amount of 18S rRNA is significantly higher than the low copy number RBM5 transcript (Schmittgen and Zakrajsek, 2000; Bustin et al., 2005). This wide discrepancy in copy number can in turn lead to introduction of high assay variability which, can be in part circumvented by accurate measurement of total RNA (Bustin et al., 2005). Assessment of both quality and quantity of total RNA isolated can be easily performed by newer techniques such as, Agilent 2100 Bioanalyser and LabChip technology, which were not available for this study (Bustin et al., 2005). Thus, HPRT1 was chosen as a housekeeping gene since it displayed a slightly lower Ct value than RBM5 and also displayed some RBM5 gene induction due to VEGF-A stimulation, although not comparable to that perceived by Northern analysis (figure 28B). It is well known that low copy number genes such as HPRT1 and RBM5 are not efficiently converted to cDNA from RNA (Karrer et al., 1995; Bustin et al., 2005). This in turn will result in faulty representation of gene up-regulation as detected by real time PCR, a trend which was observed in a few experimental sets in this study (table 7).

A)

Time of VEGF-A stimulation	Gene quantification of RBM5 (fold change) with respect to:				
	GAPDH	PPIA	HPRT1	18S rRNA	POLR2A
30 mins	1.57	-1.097	1.07	1.17	-1.56
60 mins	-1.266	-1.251	1.52	2.04	-1.398
90 mins	1.793	1.021	-	-	-2.777
120 mins	-	-	-1.42	-	-
180 mins	-	-	-	-1.94	-

B)

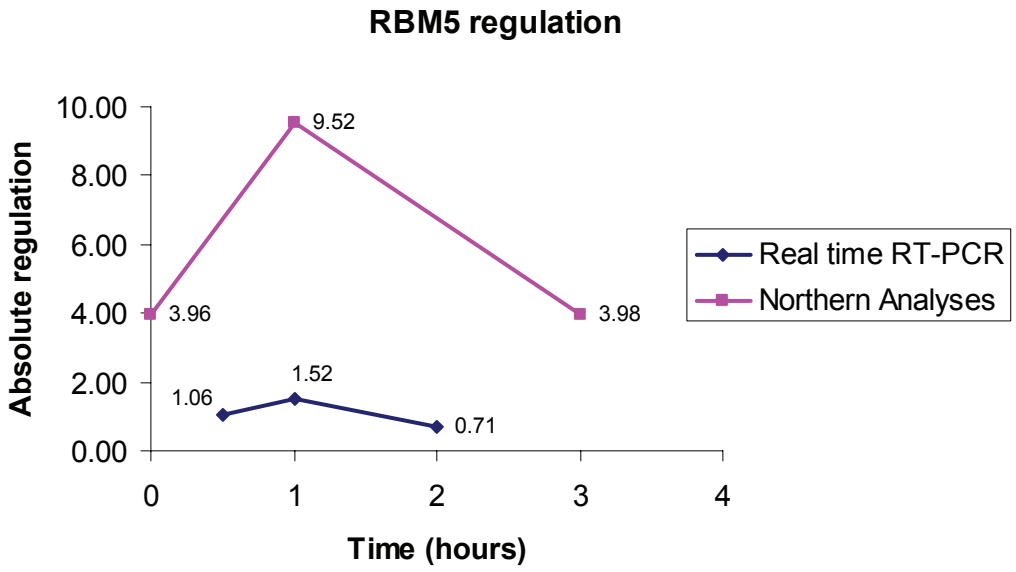

Figure 28: Calculation of VEGF-A mediated RBM5 up-regulation by real time PCR analysis. Data from individual experiments representing general trends of fold regulation of RBM5, observed with respect to various housekeeping genes examined in this study (A). Efficiencies taken into account to calculate the regulation of RBM5 with respect to various housekeeping genes for various time points of VEGF-A stimulation are: GAPDH-1.8, PPIA-1.85, 18S rRNA-1.95, and HPRT1-1.84. RBM5 efficiencies of 1.97 and 1.73 were used for calculations with respect to GAPDH/PPIA and HPRT1 due to batch to batch variations between the probe and primer sets and reverse transcription kinetics. All calculations were carried out by the formula listed in the Materials and Methods section except those for POLR2A which were calculated by the $2^{-\Delta\Delta Ct}$ method. Difference in absolute RBM5 regulation as discerned by Northern (GAPDH control) versus real time PCR (HPRT1 control) analyses is shown (B).

Efficiency calculations

As mentioned before, various parameters such as, reverse transcription efficiency, quality of RNA, copy number of the gene and efficiency of the PCR reaction determine accurate and reproducible estimation of gene regulation by real time PCR analyses. Estimation of efficiency is an essential step to determine the dynamic range of the PCR reaction for a given probe and primer set of the target/housekeeping gene. Efficiency of the PCR reaction is calculated by plotting a standard curve (log quantity of RNA vs. Ct) over a series of dilutions (figure 29). Real time PCR efficiencies were calculated for all probe and primer sets excluding POLR2A.

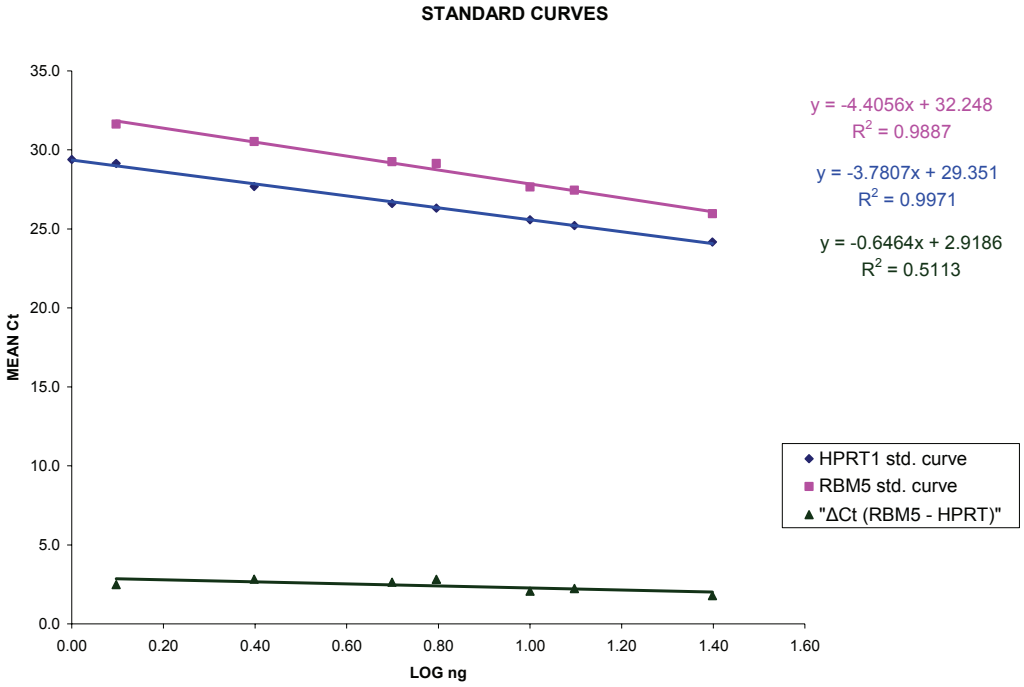

Figure 29: RBM5 and HPRT1 standard curves. Average threshold values for each individual dilution done in triplicates are plotted against the log value of cDNA in nanograms. Efficiencies (E=10[-1/slope]) for RBM5 and HPRT1 were calculated as 1.69 and 1.84, respectively. The ΔCt values for each dilution was calculated and re-plotted on the same graph using linear regression analysis. The $2^{-\Delta\Delta Ct}$ method for estimation of gene regulation can only be used if the amplification efficiencies of target and reference genes are equal and the slope is close to zero.

Estimation gene up- or down regulation by the $2^{-\Delta\Delta Ct}$ method requires the amplification efficiencies of both the target and the housekeeping genes to be equal. This is easily determined by calculating the difference between the Ct values over the same range of dilutions used for constructing standard curves. In this study however, the efficiencies of both RBM5 and HPRT1 are considerably different as discerned by the value of the slope of ΔCt curve significantly higher than zero (figure 29).

Inhibitor studies

Effect of various signaling pathways emerging from VEGF-A stimulation of endothelial cells (HUVEC) was evaluated by using two different pharmacological inhibitors targeting a single pathway wherever possible. When available inactive analogs of pharmacological inhibitors and different concentrations of carrier (DMSO) were evaluated as controls. Up-regulation is denoted by a positive value in the fold regulation column. However, since down-regulation is expressed as [1/expression ratio], the degree of inhibition can be assessed by the values in the 'Absolute gene regulation' and the '2-log regulation' columns. Threshold values for each condition for both HPRT1 and RBM5 were obtained by averaging the triplicate Ct values. Outlier Ct values differing by ±0.5 Ct units within the same condition (done in triplicate) were discarded. All values were calculated by using the Relative Expression software tool (REST) (Pfaffl et al., 2002). I used as a working hypothesis that RBM5 induction is downstream of VEGFR2 activation, which is the chief signal transducer in endothelial cells as compared to VEGFR1 (Chapter 1, Part I).

Set No.	No.	Conditions used	Avg. HPRT1 Ct	Std. error	Avg. RBM5 Ct	Std. error	E(ref)^Ct HPRT1	E(targ)^Ct RBM5	Fold regulation	Abs. gene regulation	Std. error	2-log value
1	1	60 m VEGF	27.4	0.01	27.47	0.08	-	-	-	-	-	-
	2	100 nM Wortmannin	27.19	0.04	27.41	0.1	1.134	1.035	-1.096	0.913	±0.06444	-0.132
	3	1 µM Wortmannin	26.59	0.02	26.85	0.02	1.639	1.384	-1.184	0.844	±0.03622	-0.244
	4	10 µM Wortmannin	26.28	0.02	26.03	0.09	1.968	2.119	1.077	1.077	±0.0678	0.107
2	1	0 hrs VEGF	27.12	0.01	24.58	0.05	-	-	-	-	-	-
	2	30 m VEGF	28.3	0.04	25.17	0.05	0.488	0.733	1.502	1.502	±0.06864	0.586
	3	60 m VEGF	27.18	0.01	24.94	0.09	0.961	0.827	-1.163	0.866	±0.04486	-0.217
	4	90 m VEGF	28.28	0.02	25.94	0.08	0.494	0.492	-1.005	0.995	±0.05252	-0.007
3	1	60 m VEGF	26.13	0.04	25.16	0.01	-	-	-	-	-	-
	2	20 nM PD98059	25.96	0.1	26.86	0.04	1.108	0.412	-2.691	0.372	±0.02551	-1.428
	3	200 nM PD98059	25.42	0.03	25.5	0.11	1.542	0.835	-1.846	0.542	±0.03585	-0.884
	4	200 nM Bisl	24.65	0	24.93	0.14	2.459	1.125	-2.186	0.457	±0.03568	-1.129
	5	200 nM Wortmannin	25.87	0.06	25.44	0.06	1.175	0.862	-1.363	0.734	±0.03877	-0.446
4	1	0 hrs VEGF	23.49	0.01	22.87	0.14	-	-	-	-	-	-
	2	60 m VEGF	23.66	0	22.95	0.07	0.901	0.958	1.063	1.063	±0.08962	0.089
	3	60 m VEGF+300 mg/ml CHX	23.73	0.02	22.5	0.12	0.862	1.178	1.366	1.366	±0.13683	0.45
	4	3 hrs VEGF	23.55	0.01	23.31	0.08	0.964	0.792	-1.217	0.822	±0.07049	-0.283
4	1	0 hrs VEGF	24.63	0.02	24.15	0.03	-	-	-	-	-	-
	2	60 m VEGF	24.71	0.01	24.07	0.03	0.953	1.042	1.093	1.093	±0.02545	0.129
	3	3 hrs VEGF	24.38	0.01	24.76	0.07	1.165	0.723	-1.612	0.62	±0.02503	-0.689
6	1	0 hrs VEGF	24.99	0.02	25.47	0.02	-	-	-	-	-	-
	2	60 m VEGF	25.26	0.02	25.52	0.03	0.847	0.973	1.149	1.149	±0.02897	0.2
	3	3 hrs VEGF	24.62	0.03	24.95	0	1.254	1.314	1.047	1.047	±0.02325	0.067
7	1	60 m VEGF	24.73	0.02	24.18	0.08	-	-	-	-	-	-
	2	1 µM Gö6983	25.03	0.01	25.09	0.03	0.835	0.621	-1.345	0.743	±0.03322	-0.428
	3	5 µM Gö6983	25.07	0.01	25.98	0.12	0.814	0.39	-2.086	0.479	±0.03658	-1.061

Set No.	No.	Conditions used	Avg. HPRT1 Ct	Std. error	Avg. RBM5 Ct	Std. error	E(ref)^Ct HPRT1	E(targ)^Ct RBM5	Fold regulation	Abs. gene regulation	Std. error	2-log value
8	1	0 hrs VEGF-EBM Zero	25.43	0.04	24	0.06	-	-	-	-	-	-
	2	30m VEGF-EBM Zero	25.43	0.01	23.88	0.17	0.999	1.063	1.064	1.064	±0.10468	0.09
	3	1hr VEGF-EBM Zero	26.12	0.02	24.01	0.06	0.656	0.995	1.517	1.517	±0.07787	0.601
	4	2hr VEGF-EBM Zero	24.97	0.02	24.13	0.08	1.321	0.933	-1.415	0.707	±0.03893	-0.501
9	1	0 hrs VEGF-EBM Zero	32	0.07	29.28	0.06	-	-	-	-	-	-
	2	1hr VEGF-EBM Zero	33.94	0.12	30.26	0.02	0.307	0.601	1.96	1.96	±0.17895	0.971
10	1	60 m VEGF	32.55	0.05	28.8	0.02	-	-	-	-	-	-
	2	5 µM LY294002	30.4	0.04	27.64	0.06	3.696	1.829	-2.02	0.495	±0.02415	-1.015
	3	10 µM LY294002	30.96	0.02	27.88	0.09	2.621	1.614	-1.624	0.616	±0.03682	-0.699
	4	30 µM LY294002	32.49	0.07	29.47	0.08	1.033	0.705	-1.465	0.683	±0.04703	-0.551
11	1	60 m VEGF	34.18	0.11	30.79	0.15	-	-	-	-	-	-
	2	2.5 µM LY294002	36.63	0.12	31.49	0.12	0.226	0.694	3.07	3.07	±0.42392	1.618
	3	10 µM LY294002	35.81	0.12	31.26	0.17	0.373	0.782	2.094	2.094	±0.31986	1.066
	4	50 µM LY294002	38.34	-	34.43	0.31	0.8	0.15	1.866	1.866	-	0.9
12	1	60 m VEGF	25.29	0.01	25.03	0.08	-		-	-	-	-
	2	2 µl DMSO+VEGF	26.16	0.07	25.21	0.09	0.59	0.91	1.540	1.540	±0.11503	0.623
	3	4 µl DMSO+VEGF	26.21	0.02	25.18	0.02	0.57	0.93	1.618	1.618	±0.07457	0.694
	4	16 µl DMSO+VEGF	26.22	0.00	25.72	0.06	0.57	0.70	1.219	1.220	±0.06494	0.29
13	1	60 m VEGF	25.41	0.06	26.21	0.15	-	-	-	-	-	-
	2	5 µM LY303511 + VEGF	26.73	0.02	27.30	0.05	0.45	0.57	1.265	1.265	±0.11289	0.339
	3	10 µM LY303511 + VEGF	24.27	0.01	25.01	0.02	1.996	1.87	-1.07	0.94	±0.08026	-0.10
	4	30 µM LY303511 + VEGF	29.10	0.02	30.59	0.10	0.11	0.10	-1.05	0.95	±0.09537	-0.07
14	1	60 m VEGF	23.88	0.01	23.24	0.07	-	-	-	-	-	-
	2	2.5 µM LY303511 + VEGF	24.21	0.02	23.91	0.1	0.851	0.704	-1.157	0.864	±0.05571	0.211
	3	10 µM LY303511 + VEGF	25.11	0.04	24.29	0.11	0.474	0.579	1.222	1.222	±0.08538	0.29
	4	30 µM LY303511 + VEGF	24.53	0.02	24.98	0.07	0.671	0.404	-1.662	0.602	±0.0322	-0.733
	5	18 µl DMSO + VEGF	24.19	0.02	24.08	0.06	0.825	0.644	-1.281	0.781	±0.03743	-0.357

Set No.	No.	Conditions used	Avg. HPRT1 Ct	Std. error	Avg. RBM5 Ct	Std. error	E(ref)^Ct HPRT1	E(targ)^Ct RBM5	Fold regulation	Abs. gene regulation	Std. error	2-log value
15	1	0 hr VEGF	28.74	0.03	30.61	0.03	0.19	-	-	-	-	-
	2	1 hr VEGF	28.49	0.04	30.2	0.08	1.165	1.239	1.064	1.064	±0.05579	0.09
	3	3 hrs VEGF	30.68	0.1	31.75	0.08	0.306	0.548	1.789	1.789	±0.14359	0.839
16	1	60 m VEGF	30.79	0.07	32.21	0.14	-	-	-	-	-	-
	2	5 µM SB202190 + VEGF	32.18	0.1	33.9	0.14	0.429	0.414	-1.037	0.964	±0.12346	-0.052
	3	10 µM SB202190 + VEGF	31.01	0.05	31.68	0.1	0.875	1.318	1.506	1.506	±0.15526	0.591
17	1	60 m VEGF	28.26	0.03	27.24	0.05						
	2	0.1 µM SB202190 + VEGF	27.62	0.01	27.12	0.1	1.473	1.063	-1.386	0.722	±0.04458	-0.4708
	3	1 µM SB202190 + VEGF	29.45	0.02	27.62	0.04	0.486	0.82	1.687	1.687	±0.06757	0.754
	4	5 µM SB202190 + VEGF	27.01	0.01	26.67	0.09	2.144	1.345	-1.593	0.628	±0.03587	-0.672
	5	10 µM SB202190 + VEGF	27.24	0.04	26.63	0.04	1.861	1.377	-1.351	0.74	±0.03364	-0.434
18	1	60 m VEGF	35.9	0.07	34.58	0.02	-	-	-	-	-	-
	2	5 µM L-NAME + VEGF	34.25	0.03	32.08	0.05	2.709	3.694	1.364	1.364	±0.07218	0.447
	3	10 µM L-NAME + VEGF	32.32	0.04	32.45	0.09	8.759	3.041	-2.881	0.347	±0.02315	-1.526
	4	50 µM L-NAME + VEGF	34.65	0.09	33.02	0.03	2.131	2.259	1.06	1.06	±0.07555	0.084
	5	100 µM L-NAME + VEGF	35.56	0.11	31.94	0.05	1.224	3.97	3.243	3.243	±0.26169	1.697
19	1	60 m VEGF	31.48	0.03	32.11	0.03	-	-	-	-	-	-
	2	5 µM SU5416 + VEGF	29.47	0.03	30.77	0.1	3.399	2.01	-1.691	0.591	±0.03596	-0.758
	3	20 µM SU5416 + VEGF	27.76	0.03	28.13	0.06	9.612	7.97	-1.206	0.829	±0.03749	-0.27
	4	10 µM L-NIO + VEGF	32.89	0.13	33.47	0.17	0.424	0.49	1.155	1.155	±0.13855	0.208
	5	50 µM L-NIO + VEGF	28.06	0.02	27.07	0.04	7.985	13.873	1.737	1.737	±0.06366	0.797
20	1	0 hrs VEGF	30.24	0.04	31.97	0.11	-	-	-	-	-	-
	2	60 m VEGF	31.1	0.02	32.17	0.08	0.594	0.902	1.519	1.519	±0.11566	0.603
	3	500nM SB220025	29.49	0.02	29.34	0.2	2.651	4.376	1.651	1.651	±0.18879	0.723
	4	750nM SB220025	33.17	0.05	32.1	0.04	0.283	1.035	3.653	3.653	±0.2047	1.869
	5	1 µM SB220025 + VEGF	29.43	0.04	30.5	0.03	2.751	2.395	-1.149	0.87	±0.04481	-0.2
	6	1.5 µM SB220025 + VEGF	29.18	0.03	29.61	0.05	3.196	3.797	1.188	1.188	±0.06088	0.249

Set No.	No.	Conditions used	Avg. HPRT1 Ct	Std. error	Avg. RBM5 Ct	Std. error	E(ref)^Ct HPRT1	E(targ)^Ct RBM5	Fold regulation	Abs. gene regulation	Std. error	2-log value
	7	2 µM SB220025 + VEGF	29.08	0.07	29.61	0.06	3.403	3.811	1.12	1.12	±0.07772	0.164
21	1	0 hrs VEGF	27.1	0.01	27.11	0.02	-	-	-	-	-	-
	2	60 m VEGF	26.49	0.03	26.15	0.11	1.454	1.65	1.135	1.135	±0.06788	0.182
	3	1 µM Bisl + VEGF	26.79	0.03	26.74	0.08	0.832	0.736	-1.131	0.884	±0.066	-0.177
	4	3 µM Bisl + VEGF	28.85	0.11	29.13	0.12	0.238	0.211	-1.127	0.887	±0.09454	-0.172
22	1	60 m VEGF	33.95	0.06	35.11	0.07	-	-	-	-	-	-
	2	10 µM PD98059 + VEGF	30.72	0.07	31.86	0.08	7.145	5.445	-1.312	0.762024	±0.0598	-0.39
	3	20 µM PD98059 + VEGF	32.53	0.07	34.28	0.06	2.369	1.544	1.534	0.652077	±0.04816	-0.62
	4	10 µM SU5416 + VEGF	29.03	0.02	30.93	0.11	19.94	8.855	-2.252	0.444	±0.03376	-1.17
	5	20 µM SU5416 + VEGF	33.22	0.06	34.39	0.07	1.563	1.455	-1.074	0.931	±0.06588	-0.10
23	1	0 hrs VEGF	25.38	0.02	26.62	0.09	-	-	-	-	-	-
	2	30 m VEGF	25.11	0.01	26.18	0.03	1.174	1.259	1.072	1.072	±0.05608	0.10
	3	60 m VEGF	25.42	0.01	26.62	0.11	0.977	1.001	1.024	1.024	±0.07804	0.03
24	1	0 hrs VEGF	35.36	0.07	32.84	0.1	-	-	-	-	-	-
	2	60 m VEGF	36.38	0.08	33.42	0.12	0.537	0.739	1.375	1.375	±0.14229	0.46
	3	1 µM SB220025 + VEGF	37.15	0.02	33.85	0.07	0.623	0.8	1.283	1.283	±0.11163	0.36
	4	10 µM SB220025 + VEGF	29.19	0.03	27.96	0.1	78.673	17.332	-4.539	0.22	±0.02129	-2.18
25	1	60 m VEGF	37.3	0.39	35.37	0.09	-	-	-	-	-	-
	2	100 µM Wortmannin+VEGF	36.82	0.07	35.14	0.11	1.335	1.128	-1.183	0.845	±0.21183	-0.243
	3	500 µM Wortmannin+VEGF	38.97	-	37.88	0.14	0.363	0.269	-1.346	0.743	-	-0.429
	4	10 µM L-NAME + VEGF	34.79	0.14	33.92	0.1	4.584	2.14	-2.142	0.467	±0.12128	-1.099

Table 7: Effect of various inhibitors on RBM5 gene induction by VEGF-A was evaluated by real time RT-PCR. All calculations were done by plugging in triplicate values in the Relative Expression software tool (REST) developed by Pfaffl et al., 2002. Percent CV values calculated for HPRT1 and RBM5 average Ct values are not shown. Up-regulation of RBM5 in endothelial cells by VEGF-A at various time points was calculated using the un-stimulated cells (0 hours) as control. Conversely, effect of various pharmacological inhibitors was evaluated by using the Ct values obtained from the RNA samples isolated from endothelial cells stimulated with VEGF-A for 60 minutes. Each set represents an independent experiment and each condition/sample within individual sets was carried out in separate dishes.

Treatment of HUVEC cells with a VEGFR2 inhibitor (SU5416) negatively regulated the induction of RBM5 (-1.7 fold) transcript despite its significantly lower solubility in EBM 0.5 culture medium. Regulation of RBM5 by the PI3K pathway was evaluated by using wortmannin and LY294002 and its inactive analog LY303511. RBM5 was consistently down-regulated in the presence of 0.1-1 μM wortmannin (-1.1 to -1.83 fold) but showed a slight up-regulation in the presence of 10 μM (1.07 fold) wortmannin which may be due to increased concentration of DMSO. However, no conclusive results were obtained to assess the effect of the second PI3K inhibitor LY294002, which showed an up-and down regulation in two different experimental sets, respectively. Moreover, the inactive analog of LY294002, LY303511 also displayed an overall down-regulation of RBM5 expression ratio. Similarly, evaluation of p38 MAPK in RBM5 induction by SB220025 and SB202190 was not possible due to conflicting results obtained. Although, SB202190 showed an overall down-regulation of RBM5, comparable down-regulation was not seen in the presence of SB220025.

Inhibition of both PKC by Gö6983 and Bisindolylmaleimide I HCl (-1.1 to -2.2 fold), and MAPK by PD98059 (-1.8 to -2.7 fold) significantly diminished any induction of RBM5 by VEGF-A. Unfortunately, effect of MAPK pathway on RBM5 induction by a second inhibitor U0126 and its inactive analog U0124 could not be ascertained due to extremely high HPRT1 Ct values (close to 40). Similar problems were also encountered in experiments designed to study the effect of intracellular calcium flux on induction of RBM5 using BAPTA-AM. This problem may occur if both BAPTA-AM and U0126 significantly inhibit the levels of the already low copy

number HPRT1 transcript. Additionally, amplification of low copy number genes in any given total RNA isolate by PCR is inherently difficult (Bustin et al., 2005). Surprisingly, treatment of endothelial cells with eNOS (endothelial nitric oxide synthase) inhibitors L-NIO (1.6 fold) and L-NAME (1.1 to 3.2 fold) further up-regulated the level of RBM5 transcripts as compared to that in presence of VEGF-A alone. Moreover, this observation is not false positive since, eNOS inhibitors were dissolved in basal cell culture medium and not DMSO.

Thus, in summary it appears that PKC, MAPK and PI3K pathways emerging from the activated VEGFR2 may be the up-stream regulators of RBM5. However, role of p38 MAPK and intracellular calcium could not be confirmed in this study. Additional up-regulation of RBM5 by inhibiting eNOS was another intriguing observation made in this study. It must be noted however that these results are not conclusive but do offer vital clues about possible regulation of RBM5 by VEGF-A. No doubt further studies aimed at dissecting the signal transduction pathway leading to the up-regulation of RBM5 will indeed prove exciting.

APPENDIX C

REAGENTS AND MEDIA COMPOSITIONS

TE (Tris EDTA) Buffer:
10mM Tris-HCl (pH 7.4), 1mM EDTA

Solution D:
4M guanidine thiocyanate, 25mM sodium citrate (pH 7.0), 0.5% Sarkosyl, 0.1M 2-Mercaptoethanol (added fresh)

EGM:
MCDB 131 (Sigma-Aldrich), 2% bovine fetal calf serum (Invitrogen), 1 μg/ml hydrocortisone (Sigma-Aldrich), 5 μg/ml heparin (Sigma-Aldrich), 10 ng/ml epidermal growth factor (Invitrogen), 50 units/ml penicillin, 50 μg/ml streptomycin (Invitrogen), 200 ng/ml amphotericin B (Sigma-Aldrich), 1 ng/ml basic fibroblast growth factor (Invitrogen)

EBM 0.5:
MCDB 131 (Sigma, MO), 0.5% bovine fetal calf serum (Invitrogen), 5 μg/ml heparin (Sigma), 50 units/ml penicillin, 50 μg/ml streptomycin (Invitrogen), 200 ng/ml amphotericin B (Sigma)

20X SSC:
3M NaCl, 0.3M sodium citrate, pH 7.0

Denhardt's reagent:
1 g Ficoll, 1 g polyvinylpyrrolidone, 1 g bovine serum albumin, distilled water to 50 ml

Hybridization Solution:
150 ml 20X SSC, 6 ml 0.5M EDTA, 30 ml 100X Denhardt's reagent, 12 ml 1M NaPO4 (pH 7.0), 81 ml distilled water, 60 g Dextran sulfate

5X RNA formaldehyde gel running buffer:
0.1M MOPS, 40mM sodium acetate, 5 mM EDTA in DEPC treated distilled water

Formaldehyde gel loading buffer:
50% glycerol, 1mM EDTA, 0.25% bromophenol blue, 0.25% xylene cyanol in DEPC treated water

TBS:
10mM Tris HCl (pH 7.4), 150 mM NaCl

TBST:
TBS with 0.05% Tween 20

High Salt Buffer:
50mM Tris HCl, 1M NaCl, 10mM EDTA

Pre-hybridization Solution:
300 ml 20X SSC, 12 ml 0.5M EDTA, 120 ml 100X Denhardt's reagent, 108 ml distilled water, 60 ml 1M $NaPO_4$ (pH 7.0)

FSS:
450 ml formamide, 45 ml 10% SDS, 9 ml (10 mg/ml) single stranded DNA

LB (Luria Bertani) Medium:
10 g Tryptone, 5 g yeast extract 10 g NaCl, distilled water to 1000 ml, pH 7.0

LB-Amp plates:
LB medium supplemented with 1.5% agar. Ampicillin (100 µg/ml) added after cooling to 50ºC

Phosphate Buffered Saline:
8 g NaCl, 0.2 g KCl, 1.44 g Na_2HPO_4, 0.24 g KH_2PO_4, distilled water to 1 L, pH 7.4

1X Laemmli Buffer:
50 mM Tris, pH 6.8, 10% glycerol, 2% (w/v) SDS, 0.1% (w/v) bromophenol blue, 1% 2-Mercaptoethanol (added fresh)

Lysis Buffer: (Kiledjian et al., 1999)
20 mM HEPES pH 7.6, 1.5 mM $MgCl_2$, 10 mM KCl, 1 mM DTT

BIBLIOGRAPHY

Aasheim HC, Patzke S, Hjorthaug HS, Finne EF. 2005. Characterization of a novel Eph receptor tyrosine kinase, EphA10, expressed in testis. *Biochimica et Biophysica Acta* **1723:** 1-7.

Abe M, Sato Y. 2001. cDNA microarray analysis of the gene expression profile of VEGF-activated human umbilical vein endothelial cells. *Angiogenesis* **4:** 289-98.

Abramow-Newerly M, Roy AA, Nunn C, Chidiac P. 2006. RGS proteins have a signalling complex: interactions between RGS proteins and GPCRs, effectors, and auxiliary proteins. *Cellular Signaling* **18:** 579-91.

Adams RH, Klein R. 2000. Eph receptors and ephrin ligands. essential mediators of vascular development. *Trends in Cardiovascular Medicine* **10:** 183-8.

Altschul SF, Madden TL, Schaffer AA, Zhang J, Zhang Z, Miller W, Lipman DJ. 1997. Gapped BLAST and PSI-BLAST: a new generation of protein database search programs. *Nucleic Acids Research* **25:** 3389-402.

Angel P, Karin M. 1991. The role of Jun, Fos and the AP-1 complex in cell-proliferation and transformation. *Biochimica et Biophysica Acta* **1072:** 129-57.

Aravind L, Koonin EV. 1999. G-patch: a new conserved domain in eukaryotic RNA-processing proteins and type D retroviral polyproteins. *Trends in Biochemical Sciences* **24:** 342-4.

Babic AM, Kireeva ML, Kolesnikova TV, Lau LF. 1998. CYR61, a product of a growth factor-inducible immediate early gene, promotes angiogenesis and tumor growth. *Proceedings of the National Academy of Sciences (USA)* **95:** 6355-60.

Bairoch A. 1991. PROSITE: a dictionary of sites and patterns in proteins. *Nucleic Acids Research* **19:** 2241-5.

Bonifacino JS, Traub LM. 2003. Signals for sorting of transmembrane proteins to endosomes and lysosomes. *Annual Review of Biochemistry* **72:** 395-447.

Boulikas T. 1993. Nuclear localization signals (NLS). *Critical Reviews in Eukaryotic Gene Expression* **3:** 193-227.

Boulikas T. 1996. Nuclear import of protein kinases and cyclins. *Journal of Cellular Biochemistry* **60:** 61-82.

Bowser R, Muller H, Govindan B, Novick P. 1992. Sec8p and Sec15p are components of a plasma membrane-associated 19.5S particle that may function downstream of Sec4p to control exocytosis. *The Journal of Cell Biology* **118:** 1041-56.

Brantley-Sieders D, Parker M, Chen J. 2004. Eph receptor tyrosine kinases in tumor and tumor microenvironment. *Current Pharmaceutical Design* **10:** 3431-42.

Bravo R. 1990. Genes induced during the G0/G1 transition in mouse fibroblasts. *Seminars in Cancer Biology* **1:** 37-46.

Breier G. 2000. Functions of the VEGF/VEGF receptor system in the vascular system. *Seminars in Thrombosis and Hemostasis* **26:** 553-9.

Brigstock DR. 2003. The CCN family: a new stimulus package. *The Journal of Endocrinology* **178:** 169-75.

Bubulya PA, Spector DL. 2004. "On the move"ments of nuclear components in living cells. *Experimental Cell Research* **296:** 4-11.

Bustin SA. 2000. Absolute quantification of mRNA using real-time reverse transcription polymerase chain reaction assays. *Journal of Molecular Endocrinology* **25:** 169-93.

Bustin SA, Benes V, Nolan T, Pfaffl MW. 2005. Quantitative real-time RT-PCR--a perspective. *Journal of Molecular Endocrinology* **34:** 597-601.

Burd CG, Dreyfuss G. 1994. Conserved structures and diversity of functions of RNA-binding proteins. Science. **265:** 615-21.

Cai Y, Zhang C, Nawa T, Aso T, Tanaka M, Oshiro S, Ichijo H, Kitajima S. 2000. Homocysteine-responsive ATF3 gene expression in human vascular endothelial cells: activation of c-Jun NH(2)-terminal kinase and promoter response element. *Blood* **96:** 2140-8.

Callebaut I, Mornon JP. 2005. OCRE: a novel domain made of imperfect, aromatic-rich octamer repeats. *Bioinformatics* **21:** 699-702.

Carmeliet P, Collen D. 1999. Role of vascular endothelial growth factor and vascular endothelial growth factor receptors in vascular development. *Current Topics in Microbiology and Immunology* **237:** 133-58.

Carmeliet P, Jain RK. 2000. Angiogenesis in cancer and other diseases. *Nature* **407:** 249-57.

Carmeliet P. 2004. Manipulating angiogenesis in medicine. *Journal of Internal Medicine* **255:** 538-61.

Carmo-Fonseca M, Pepperkok R, Carvalho MT, Lamond AI. 1992. Transcription-dependent colocalization of the U1, U2, U4/U6, and U5 snRNPs in coiled bodies. *The Journal of Cell Biology* **117:** 1-14.

Carr-Schmid A, Jiao X, Kiledjian M. 2006. Identification of mRNA bound to RNA binding proteins by differential display. *Methods in Molecular Biology* **317:** 299-314.

Charles CH, Simske JS, O'Brien TP, Lau LF. 1990. Pip92: a short-lived, growth factor-inducible protein in BALB/c 3T3 and PC12 cells. *Molecular and Cellular Biology* **10:** 6769-74.

Chen L, Ma S, Li B, Fink T, Zachar V, Takahashi M, Cuttichia J, Tsui LC, Ebbesen P, Liu X. 2003. Transcriptional activation of immediate-early gene ETR101 by human T-cell leukaemia virus type I Tax. *The Journal of General Virology* **84:** 3203-14.

Cheng N, Brantley DM, Chen J. 2002. The ephrins and Eph receptors in angiogenesis. *Cytokine & Growth Factor Reviews* **13:** 75-85.

Cheng ZJ, Vapaatalo H, Mervaala E. 2005. Angiotensin II and vascular inflammation. *Medical Science Monitor* **11:** RA194-205.

Chida K, Vogt PK. 1992. Nuclear translocation of viral Jun but not of cellular Jun is cell cycle dependent. *Proceedings of the National Academy of Sciences (USA)* **89:** 4290-4.

Chomczynski P, Sacchi N. 1987. Single-step method of RNA isolation by acid guanidinium thiocyanate-phenol-chloroform extraction. *Analytical Biochemistry* **162:** 156-9.

Clauss M. 2000. Molecular biology of the VEGF and the VEGF receptor family. *Seminars in Thrombosis and Hemostasis* **26:** 561-9.

Cochran BH, Reffel AC, Stiles CD. 1983. Molecular cloning of gene sequences regulated by platelet-derived growth factor. *Cell* **33:** 939-47

Coleman MP, Ambrose HJ, Carrel L, Nemeth AH, Willard HF, Davies KE. 1996. A novel gene, DXS8237E, lies within 20 kb upstream of UBE1 in Xp11.23 and has a different X inactivation status. *Genomics* **31:** 135-8.

Connolly DT, Heuvelman DM, Nelson R, Olander JV, Eppley BL, Delfino JJ, Siegel NR, Leimgruber RM, Feder J. 1989. Tumor vascular permeability factor

stimulates endothelial cell growth and angiogenesis. *The Journal of Clinical Investigation* **84:** 1470-8.

Cunningham SA, Waxham MN, Arrate PM, Brock TA. 1995. Interaction of the Flt-1 tyrosine kinase receptor with the p85 subunit of phosphatidylinositol 3-kinase. Mapping of a novel site involved in binding. *The Journal of Biological Chemistry* **270:** 20254-7.

Dang CV, Lee WM. 1988. Identification of the human c-myc protein nuclear translocation signal. *Molecular and Cellular Biology* **8:** 4048-54.

Davis S, Yancopoulos GD. 1999. The angiopoietins: Yin and Yang in angiogenesis. *Current Topics in Microbiology and Immunology* **237:** 173-85.

Diatchenko L, Lukyanov S, Lau YF, Siebert PD. 1999. Suppression subtractive hybridization: a versatile method for identifying differentially expressed genes. *Methods in Enzymology* **303:** 349-80.

Dignam JD, Lebovitz RM, Roeder RG. 1983. Accurate transcription initiation by RNA polymerase II in a soluble extract from isolated mammalian nuclei. *Nucleic Acids Research* **11:** 1475-89.

Dingwall C, Laskey RA. 1991. Nuclear targeting sequences--a consensus? *Trends in Biochemical Sciences* **16:** 478-81.

Dodelet VC, Pasquale EB. 2000. Eph receptors and ephrin ligands: embryogenesis to tumorigenesis. *Oncogene* **19:** 5614-9.

Drabkin HA, West JD, Hotfilder M, Heng YM, Erickson P, Calvo R, Dalmau J, Gemmill RM, Sablitzky F. 1999. DEF-3(g16/NY-LU-12), an RNA binding protein from the 3p21.3 homozygous deletion region in SCLC. *Oncogene* **18:** 2589-97.

Druey KM, Blumer KJ, Kang VH, Kehrl JH. 1996. Inhibition of G-protein-mediated MAP kinase activation by a new mammalian gene family. *Nature* **379:** 742-6.

Dvorak HF, Nagy JA, Feng D, Brown LF, Dvorak AM. 1999. Vascular permeability factor/vascular endothelial growth factor and the significance of microvascular hyperpermeability in angiogenesis. *Current Topics in Microbiology and Immunology* **237:** 97-132.

Edamatsu H, Kaziro Y, Itoh H. 2000. LUCA15, a putative tumour suppressor gene encoding an RNA-binding nuclear protein, is down-regulated in ras-transformed Rat-1 cells. *Genes to Cells* **5:** 849-58.

Edwards DR. and Mahadevan LC. 1992. Protein synthesis inhibitors differentially superinduce c-fos and c-jun by three distinct mechanisms: lack of evidence for labile repressors. *The EMBO Journal* **11:** 2415-2424,

Efrat S, Kaempfer R. 1984. Control of biologically active interleukin 2 messenger RNA formation in induced human lymphocytes. *Proceedings of the National Academy of Sciences (USA)* **81:** 2601-5.

Eklund L, Olsen BR. 2006. Tie receptors and their angiopoietin ligands are context-dependent regulators of vascular remodeling. *Experimental Cell Research* **312:** 630-41.

Eriksson U, Alitalo K. 1999. Structure, expression and receptor-binding properties of novel vascular endothelial growth factors. *Current Topics in Microbiology and Immunology* **237:** 41-57.

Fang D and Kerppola T. 2004. Ubiquitin-mediated fluorescence complementation reveals that Jun ubiquitinated by Itch/AIP4 is localized to lysosomes. *Proceedings of the National Academy of Sciences (USA)* **101:** 14782-14787.

Farrell RE Jr. 1998. *RNA Methodologies*, 2nd ed. San Diego: Academic Press.

Ferrara N, Davis-Smyth T. 1997. The biology of vascular endothelial growth factor. *Endocrine Reviews* **18:** 4-25.

Ferrara N. 1999. Vascular endothelial growth factor: molecular and biological aspects. *Current Topics in Microbiology and Immunology* **237:** 1-30.

Ferrara N. 2005. VEGF as a therapeutic target in cancer. *Oncology* **69:** 11-6.

Gale NW, Yancopoulos GD. 1999. Growth factors acting via endothelial cell-specific receptor tyrosine kinases: VEGFs, angiopoietins, and ephrins in vascular development. *Genes & Development* **13:** 1055-66.

Gately S, Li WW. 2004. Multiple roles of COX-2 in tumor angiogenesis: a target for antiangiogenic therapy. *Seminars in Oncology* **31:** 2-11.

Gelinas DS, Bernatchez PN, Rollin S, Bazan NG, Sirois MG. 2002. Immediate and delayed VEGF-mediated NO synthesis in endothelial cells: role of PI3K, PKC and PLC pathways. *British Journal of Pharmacology* **137:** 1021-30.

Gerber HP, McMurtrey A, Kowalski J, Yan M, Keyt BA, Dixit V, Ferrara N. 1998. Vascular endothelial growth factor regulates endothelial cell survival through the phosphatidylinositol 3'-kinase/Akt signal transduction pathway. Requirement for Flk-1/KDR activation. *The Journal of Biological Chemistry* **273:** 30336-43.

Ghetti A, Pinol-Roma S, Michael WM, Morandi C, Dreyfuss G. 1992. hnRNP I, the polypyrimidine tract-binding protein: distinct nuclear localization and association with hnRNAs. *Nucleic Acids Research* **20:** 3671-8.

Gill SK, Bhattacharya M, Ferguson SS, Rylett RJ. 2003. Identification of a novel nuclear localization signal common to 69- and 82-kDa human choline acetyltransferase. *The Journal of Biological Chemistry* **278:** 20217-24.

Gille H, Kowalski J, Yu L, Chen H, Pisabarro MT, Davis-Smyth T, Ferrara N. 2000. A repressor sequence in the juxtamembrane domain of Flt-1 (VEGFR-1) constitutively inhibits vascular endothelial growth factor-dependent phosphatidylinositol 3'-kinase activation and endothelial cell migration. *The EMBO Journal* **19:** 4064-73.

Gille H, Kowalski J, Li B, LeCouter J, Moffat B, Zioncheck TF, Pelletier N, Ferrara N. 2001. Analysis of biological effects and signaling properties of Flt-1 (VEGFR-1) and KDR (VEGFR-2). A reassessment using novel receptor-specific vascular endothelial growth factor mutants. *The Journal of Biological Chemistry* **276:** 3222-30.

Greenberg ME, Ziff EB. 1984. Stimulation of 3T3 cells induces transcription of the c-fos proto-oncogene. *Nature* **311:** 433-8.

Greenberg ME, Hermanowski AL, Ziff EB. 1986. Effect of protein synthesis inhibitors on growth factor activation of c-fos, c-myc, and actin gene transcription. *Molecular and Cellular Biology* **6:** 1050-7.

Hahn MA, Marsh DJ. 2005. Identification of a functional bipartite nuclear localization signal in the tumor suppressor parafibromin. *Oncogene* **24:** 6241-8.

Hai T, Wolfgang CD, Marsee DK, Allen AE, Sivaprasad U. 1999. ATF3 and stress responses. *Gene Expression* **7:** 321-35.

Hai T, Hartman MG. 2001. The molecular biology and nomenclature of the activating transcription factor/cAMP responsive element binding family of transcription factors: activating transcription factor proteins and homeostasis. *Gene* **273(1):** 1-11.

Hashimoto G, Inoki I, Fujii Y, Aoki T, Ikeda E, Okada Y. 2002. Matrix metalloproteinases cleave connective tissue growth factor and reactivate angiogenic activity of vascular endothelial growth factor 165. *The Journal of Biological Chemistry* **277:** 36288-95.

Heil M, Clauss M, Suzuki K, Buschmann IR, Willuweit A, Fischer S, Schaper W. 2000. Vascular endothelial growth factor (VEGF) stimulates monocyte migration

through endothelial monolayers via increased integrin expression. *European Journal of Cell Biology* **79:** 850-7.

Heroult M, Schaffner F, Augustin HG. 2006. Eph receptor and ephrin ligand-mediated interactions during angiogenesis and tumor progression. *Experimental Cell Research* **312:** 642-50.

Holmes DI, Zachary I. 2004. Placental growth factor induces FosB and c-Fos gene expression via Flt-1 receptors. *FEBS Letters* **557:** 93-8.

Hsu SC, TerBush D, Abraham M, Guo W. 2004. The exocyst complex in polarized exocytosis. *International Review of Cytology* 233: 243-65.

Huang L, Sankar S, Lin C, Kontos CD, Schroff AD, Cha EH, Feng SM, Li SF, Yu Z, Van Etten RL, Blanar MA, Peters KG. 1999. HCPTPA, a protein tyrosine phosphatase that regulates vascular endothelial growth factor receptor-mediated signal transduction and biological activity. *The Journal of Biological Chemistry* **274:** 38183-8.

Huang S, Mills L, Mian B, Tellez C, McCarty M, Yang XD, Gudas JM, Bar-Eli M. 2002. Fully humanized neutralizing antibodies to interleukin-8 (ABX-IL8) inhibit angiogenesis, tumor growth, and metastasis of human melanoma. *The American Journal of Pathology* **161:** 125-34.

Iniguez MA, Rodriguez A, Volpert OV, Fresno M, Redondo JM. 2003. Cyclooxygenase-2: a therapeutic target in angiogenesis. *Trends in Molecular Medicine* **9:** 73-8.

Jaen C, Doupnik CA. 2005. Neuronal Kir3.1/Kir3.2a channels coupled to serotonin 1A and muscarinic m2 receptors are differentially modulated by the "short" RGS3 isoform. *Neuropharmacology* **49:** 465-76.

Jans DA, Briggs LJ, Gustin SE, Jans P, Ford S, Young IG. 1997. A functional bipartite nuclear localisation signal in the cytokine interleukin-5. *FEBS Letters* **406(3):** 315-20.

Joseph LJ, Le Beau MM, Jamieson GA Jr, Acharya S, Shows TB, Rowley JD, Sukhatme VP. 1988. Molecular cloning, sequencing, and mapping of EGR2, a human early growth response gene encoding a protein with "zinc-binding finger" structure. *Proceedings of the National Academy of Sciences (USA)* **85:** 7164-8.

Jośko J. and Mazurek M. 2004. Transcription factors having impact on vascular endothelial growth factor (VEGF) gene expression in angiogenesis. *Medical Science Monitor* **10(4):** 89-98.

Kalderon D, Roberts BL, Richardson WD, Smith AE. 1984. A short amino acid sequence able to specify nuclear location. *Cell* **39:** 499-509.

Karkkainen MJ, Petrova TV. 2000. Vascular endothelial growth factor receptors in the regulation of angiogenesis and lymphangiogenesis. *Oncogene* **19:** 5598-605.

Karkkainen MJ, Makinen T, Alitalo K. 2002. Lymphatic endothelium: a new frontier of metastasis research. *Nature Cell Biology* **4:** 2-5.

Karrer EE, Lincoln JE, Hogenhout S, Bennett AB, Bostock RM, Martineau B, Lucas WJ, Gilchrist DG, Alexander D. 1995. In situ isolation of mRNA from individual plant cells: creation of cell-specific cDNA libraries. *Proceedings of the National Academy of Sciences (USA)* **92:** 3814-8.

Kau TR, Silver PA. 2003. Nuclear transport as a target for cell growth. *Drug Discovery Today* **8:** 78-85.

Keyse SM, Emslie EA. 1992. Oxidative stress and heat shock induce a human gene encoding a protein-tyrosine phosphatase. *Nature* **359:** 644-7.

Kiledjian M, Day N, Trifillis P. 1999. Purification and RNA binding properties of the polycytidylate-binding proteins alphaCP1 and alphaCP2. *Methods* **17:** 84-91.

Kim R, Sandler SJ, Goldman S, Yokota H, Clark AJ, Kim S. 1998. Overexpression of archaeal proteins in *Escherichia coli*. *Biotechnology Letters* **20**: 207-210.

Kliche S, Waltenberger J. 2001. VEGF receptor signaling and endothelial function. *IUBMB Life* **52:** 61-6.

Knecht E and Salvador N. 2005. Chaperone-mediated autophagy. In *Lysosomes*, (ed. P. Saftig), pp 181-193. Texas: Landes Bioscience.

Koch AE, Polverini PJ, Kunkel SL, Harlow LA, DiPietro LA, Elner VM, Elner SG, Strieter RM. 1992. Interleukin-8 as a macrophage-derived mediator of angiogenesis. *Science* **258:** 1798-801.

Koh GY, Kim I, Kwak HJ, Yun MJ, Leem JC. 2002. Biomedical significance of endothelial cell specific growth factor, angiopoietin. *Experimental & Molecular Medicine* **34:** 1-11.

Kok K, Naylor SL, Buys CH. 1997. Deletions of the short arm of chromosome 3 in solid tumors and the search for suppressor genes. *Advances in Cancer Research* **71:** 27-92.

Kopito RR. 2000. Aggresomes, inclusion bodies and protein aggregation. *Trends in Cell Biology* **10:** 524-30.

Kothapalli R, Yoder SJ, Mane S, Loughran TP Jr. 2002. Microarray results: how accurate are they? *BMC Bioinformatics* **3:**22.

Kreft M, Milisav I, Potokar M, Zorec R. 2004. Automated high through-put colocalization analysis of multichannel confocal images. *Computer Methods and Programs in Biomedicine* **74:** 63-7.

Kruijer W, Cooper JA, Hunter T, Verma IM. 1985. Platelet-derived growth factor induces rapid but transient expression of the c-fos gene and protein. Nature **312:** 711-6.

Laemmli UK. 1970. Cleavage of structural proteins during the assembly of the head of bacteriophage T4. Nature **227:** 680-5.

Lamond AI, Spector DL. 2003. Nuclear speckles: a model for nuclear organelles. *Nature Reviews Molecular Cell Biology* **4(8):** 605-12.

Lau LF, Nathans D. 1987. Expression of a set of growth-related immediate early genes in BALB/c 3T3 cells: coordinate regulation with c-fos or c-myc. *Proceedings of the National Academy of Sciences (USA)* **84:** 1182-6.

Lerman MI, Minna JD. 2000. The 630-kb lung cancer homozygous deletion region on human chromosome 3p21.3: identification and evaluation of the resident candidate tumor suppressor genes. The International Lung Cancer Chromosome 3p21.3 Tumor Suppressor Gene Consortium. *Cancer Research* **60:** 6116-33.

Leask A, Abraham DJ. 2003. The role of connective tissue growth factor, a multifunctional matricellular protein, in fibroblast biology. *Biochemistry and Cell Biology* **81:** 355-63.

Lee WS, Hsu CY, Wang PL, Huang CY, Chang CH, Yuan CJ. 2004. Identification and characterization of the nuclear import and export signals of the mammalian Ste20-like protein kinase 3. *FEBS Letters* **572:** 41-5.

Letunic I, Copley RR, Pils B, Pinkert S, Schultz J, Bork P. 2006. SMART 5: domains in the context of genomes and networks. *Nucleic Acids Research* **34:** D257-60.

Liu D, Jia H, Holmes DI, Stannard A, Zachary I. 2003. Vascular endothelial growth factor-regulated gene expression in endothelial cells: KDR-mediated induction of Egr3 and the related nuclear receptors Nur77, Nurr1, and Nor1. *Arteriosclerosis, Thrombosis, and Vascular Biology* **23:** 2002-7

Livak KJ, Schmittgen TD. 2001. Analysis of relative gene expression data using real-time quantitative PCR and the 2(-Delta Delta C(T)) Method. *Methods* **25:** 402-8.

Luo JC, Shibuya M. 2001. A variant of nuclear localization signal of bipartite-type is required for the nuclear translocation of hypoxia inducible factors (1alpha, 2alpha and 3alpha). *Oncogene* **20:** 1435-44.

Lu Q, Sun EE, Klein RS, Flanagan JG. 2001. Ephrin-B reverse signaling is mediated by a novel PDZ-RGS protein and selectively inhibits G protein-coupled chemoattraction. *Cell* **105:** 69-79.

Mahadevan LC, Edwards DR. 1991. Signalling and superinduction. *Nature* **349:** 747-8.

Maisonpierre PC, Suri C, Jones PF, Bartunkova S, Wiegand SJ, Radziejewski C, Compton D, McClain J, Aldrich TH, Papadopoulos N, Daly TJ, Davis S, Sato TN, Yancopoulos GD. 1997. Angiopoietin-2, a natural antagonist for Tie2 that disrupts in vivo angiogenesis. *Science* **277:** 55-60.

Manders EMM, Verbeek FJ, Aten JA. 1993. Measurement of co-localization of objects in dual-colour confocal images. *Journal of Microscopy* **169:** 375–382.

Masckauchan TN, Kitajewski J. 2006. Wnt/Frizzled signaling in the vasculature: new angiogenic factors in sight. *Physiology* **21:** 181-8.

Matsushima-Nishiu M, Unoki M, Ono K, Tsunoda T, Minaguchi T, Kuramoto H, Nishida M, Satoh T, Tanaka T, Nakamura Y. 2001. Growth and gene expression profile analyses of endometrial cancer cells expressing exogenous PTEN. *Cancer Research* **61:** 3741-9.

Matsumoto M, Minami M, Takeda K, Sakao Y, Akira S. 1996. Ectopic expression of CHOP (GADD153) induces apoptosis in M1 myeloblastic leukemia cells. *FEBS Letters* **395:** 143-7.

Matsumoto T, Claesson-Welsh L. 2001. VEGF receptor signal transduction. *Science's STKE* **2001:** RE21.

Meadows KN, Bryant P, Pumiglia K. 2001. Vascular endothelial growth factor induction of the angiogenic phenotype requires Ras activation. *The Journal of Biological Chemistry* **276:** 49289-98.

Michael WM, Eder PS, Dreyfuss G. 1997. The K nuclear shuttling domain: a novel signal for nuclear import and nuclear export in the hnRNP K protein. *The EMBO Journal* **16:** 3587-98.

Miller J, McLachlan AD, Klug A. 1985. Repetitive zinc-binding domains in the protein transcription factor IIIA from Xenopus oocytes. *The EMBO Journal* **4:** 1609-14.

Mintz PJ, Spector DL. 2000. Compartmentalization of RNA processing factors within nuclear speckles. *Journal of Structural Biology* **129:** 241-51.

Misteli T. 2000. Cell biology of transcription and pre-mRNA splicing: nuclear architecture meets nuclear function. *Journal of Cell Science* **113:** 1841-9.

Mitchell RL, Zokas L, Schreiber RD, Verma IM. 1985. Rapid induction of the expression of proto-oncogene fos during human monocytic differentiation. *Cell* **40:** 209-17.

Mizukami Y, Jo WS, Duerr EM, Gala M, Li J, Zhang X, Zimmer MA, Iliopoulos O, Zukerberg LR, Kohgo Y, Lynch MP, Rueda BR, Chung DC. 2005. Induction of interleukin-8 preserves the angiogenic response in HIF-1alpha-deficient colon cancer cells. *Nature Medicine* **11:** 992-7.

Moll T, Tebb G, Surana U, Robitsch H, Nasmyth K. 1991. The role of phosphorylation and the CDC28 protein kinase in cell cycle-regulated nuclear import of the S. cerevisiae transcription factor SWI5. *Cell* **66:** 743-58.

Moore MS. 1998. Ran and nuclear transport. *The Journal of Biological Chemistry* **273:** 22857-60.

Mourtada-Maarabouni M, Sutherland LC, Williams GT. 2002. Candidate tumour suppressor LUCA-15 can regulate multiple apoptotic pathways. *Apoptosis* **7:** 421-32.

Mourtada-Maarabouni M, Sutherland LC, Meredith JM, Williams GT. 2003. Simultaneous acceleration of the cell cycle and suppression of apoptosis by splice variant delta-6 of the candidate tumour suppressor LUCA-15/RBM5. *Genes to Cells* **8:**109-19.

Mourtada-Maarabouni M, Keen J, Clark J, Cooper CS, Williams GT. 2006. Candidate tumor suppressor LUCA-15/RBM5/H37 modulates expression of apoptosis and cell cycle genes. *Experimental Cell Research* **312:** 1745-52.

Mukhopadhyay D, Zeng H, Bhattacharya R. 2004. Complexity in the vascular permeability factor/vascular endothelial growth factor (VPF/VEGF)-receptors signaling. *Molecular and Cellular Biochemistry* **264:** 51-61.

Nakai K, Horton P. 1999. PSORT: a program for detecting sorting signals in proteins and predicting their subcellular localization. *Trends in biochemical sciences* **24:** 34-6.

Naylor SL, Johnson BE, Minna JD, Sakaguchi AY. 1987. Loss of heterozygosity of chromosome 3p markers in small-cell lung cancer. *Nature* **329:** 451-4.

Novick P, Schekman R. 1979. Secretion and cell-surface growth are blocked in a temperature-sensitive mutant of Saccharomyces cerevisiae. *Proceedings of the National Academy of Sciences (USA)* **76:** 1858-62.

Neufeld G, Cohen T, Gengrinovitch S, Poltorak Z. 1999. Vascular endothelial growth factor (VEGF) and its receptors. *The FASEB Journal* **13:** 9-22.

Oh JJ, Grosshans DR, Wong SG, Slamon DJ. 1999. Identification of differentially expressed genes associated with HER-2/neu overexpression in human breast cancer cells. *Nucleic Acids Research* **27:** 4008-17.

Oh JJ, West AR, Fishbein MC, Slamon DJ. 2002. A candidate tumor suppressor gene, H37, from the human lung cancer tumor suppressor locus 3p21.3. *Cancer Research* **62:** 3207-13.

Oh JJ, Razfar A, Delgado I, Reed RA, Malkina A, Boctor B, Slamon DJ. 2006. 3p21.3 tumor suppressor gene H37/Luca15/RBM5 inhibits growth of human lung cancer cells through cell cycle arrest and apoptosis. *Cancer Research* **66:** 3419-27.

Olofsson B, Pajusola K, Kaipainen A, von Euler G, Joukov V, Saksela O, Orpana A, Pettersson RF, Alitalo K, Eriksson U. 1996. Vascular endothelial growth factor B, a novel growth factor for endothelial cells. *Proceedings of the National Academy of Sciences (USA)* **93:** 2576-81.

Oyadomari S, Mori M. 2004. Roles of CHOP/GADD153 in endoplasmic reticulum stress. *Cell Death and Differentiation* **11:** 381-9.

Papetti M, Herman IM. 2002. Mechanisms of normal and tumor-derived angiogenesis. *American Journal of Physiology. Cell physiology* **282:** C947-70.

Parker LH, Schmidt M, Jin SW, Gray AM, Beis D, Pham T, Frantz G, Palmieri S, Hillan K, Stainier DY, De Sauvage FJ, Ye W. 2004. The endothelial-cell-derived secreted factor Egfl7 regulates vascular tube formation. *Nature* **428:** 754-8.

Partanen J, Dumont DJ. 1999. Functions of Tie1 and Tie2 receptor tyrosine kinases in vascular development. *Current Topics in Microbiology and Immunology* **237:** 159-72.

Patrignani P, Tacconelli S, Sciulli MG, Capone ML. 2005. New insights into COX-2 biology and inhibition. *Brain Research Reviews* **48:** 352-9.

Pemberton LF, Paschal BM. 2005. Mechanisms of receptor-mediated nuclear import and nuclear export. *Traffic* **6:** 187-98.

Perbal B. 2004. CCN proteins: multifunctional signalling regulators. *Lancet* **363:** 62-4.

Pfaffl MW. 2001. A new mathematical model for relative quantification in real-time RT-PCR. *Nucleic Acids Research* **29:** E45.

Pfaffl MW, Horgan GW and Dempfle L. 2002. Relative Expression Software Tool (*REST©)* for group wise comparison and statistical analysis of relative expression results in real-time PCR. *Nucleic Acids Research* **30:** E36

Phair RD, Misteli T. 2000. High mobility of proteins in the mammalian cell nucleus. *Nature* **404:** 604-9.

Pollard VW, Michael WM, Nakielny S, Siomi MC, Wang F, Dreyfuss G. 1996. A novel receptor-mediated nuclear protein import pathway. *Cell* **86:** 985-94.

Poltorak Z, Cohen T, Sivan R, Kandelis Y, Spira G, Vlodavsky I, Keshet E, Neufeld G. 1997. VEGF145, a secreted vascular endothelial growth factor isoform that binds to extracellular matrix. *The Journal of Biological Chemistry* **272:** 7151-8.

Pontecorvi A, Tata JR, Phyillaier M, Robbins J. 1988. Selective degradation of mRNA: the role of short-lived proteins in differential destabilization of insulin-induced creatine phosphokinase and myosin heavy chain mRNAs during rat skeletal muscle L6 cell differentiation. *The EMBO Journal* **7:** 1489-95.

Poon IK, Jans DA. 2005. Regulation of nuclear transport: central role in development and transformation? *Traffic* **6:** 173-86.

Ratcliffe KE, Tao Q, Yavuz B, Stoletov KV, Spring SC, Terman BI. 2002. Sck is expressed in endothelial cells and participates in vascular endothelial growth factor-induced signaling. *Oncogene* **21:** 6307-16.

Reiss Y, Machein MR, Plate KH. 2005. The role of angiopoietins during angiogenesis in gliomas. *Brain Pathology* **15:** 311-7.

Ribatti D, Vacca A, Presta M. 2000. The discovery of angiogenic factors: a historical review. *General Pharmacology* **35:** 227-31.

Riddle EL, Schwartzman RA, Bond M, Insel PA. 2005. Multi-tasking RGS proteins in the heart: the next therapeutic target? *Circulation Research* **96:** 401-11.

Rintala-Maki ND, Sutherland LC. 2004a. LUCA-15/RBM5, a putative tumour suppressor, enhances multiple receptor-initiated death signals. *Apoptosis* **9(4):** 475-84.

Rintala-Maki ND, Abrasonis V, Burd M, Sutherland LC. 2004b. Genetic instability of RBM5/LUCA-15/H37 in MCF-7 breast carcinoma sublines may affect susceptibility to apoptosis. *Cell Biochemistry and Function* **22:** 307-13.

Ristimaki A. 2004. Cyclooxygenase 2: from inflammation to carcinogenesis. *Novartis Foundation Symposium* **256:** 215-21.

Robbins J, Dilworth SM, Laskey RA, Dingwall C. 1991. Two interdependent basic domains in nucleoplasmin nuclear targeting sequence: identification of a class of bipartite nuclear targeting sequence. *Cell* **64:** 615-23.

Robinson DR, Wu YM, Lin SF. 2000. The protein tyrosine kinase family of the human genome. *Oncogene* **19:** 5548-57.

Rodgers ND, Jiao X, Kiledjian M. 2002. Identifying mRNAs bound by RNA-binding proteins using affinity purification and differential display. *Methods* **26:**115-22.

Romanelli MG, Morandi C. 2002. Importin alpha binds to an unusual bipartite nuclear localization signal in the heterogeneous ribonucleoprotein type I. *European Journal of Biochemistry* **269:** 2727-34.

Ron D, Habener JF. 1992. CHOP, a novel developmentally regulated nuclear protein that dimerizes with transcription factors C/EBP and LAP and functions as a dominant-negative inhibitor of gene transcription. *Genes & Development* **6:** 439-53.

Rosenkilde MM, Schwartz TW. 2004. The chemokine system - a major regulator of angiogenesis in health and disease. *Acta Pathologica, Microbiologica, et Immunologica Scandinavica* **112:** 481-95.

Rosenfeld R, Margalit H. 1993. Zinc fingers: conserved properties that can distinguish between spurious and actual DNA-binding motifs. *Journal of Biomolecular Structure & Dynamics* **11:** 557-70.

Roux PP and Blenis J. 2004. ERK and p38 MAPK-Activated Protein Kinases: a Family of Protein Kinases with Diverse Biological Functions. *Microbiology and Molecular Biology Reviews* **68:** 320-344.

Rouzer CA, Marnett LJ. 2005. Structural and functional differences between cyclooxygenases: fatty acid oxygenases with a critical role in cell signaling. *Biochemical and Biophysical Research Communications* **338:** 34-44.

Saitoh N, Spahr CS, Patterson SD, Bubulya P, Neuwald AF, Spector DL. 2004. Proteomic analysis of interchromatin granule clusters. *Molecular Biology of the Cell* **15:** 3876-90.

Sambrook J, Fritsch EF, Maniatis T. 1989. *Molecular Cloning: A Laboratory Manual*, 2nd ed. New York: Cold Spring Harbor Laboratory Press.

Sanchez-Perez I, Martinez-Gomariz M, Williams D, Keyse SM, Perona R. 2000. CL100/MKP-1 modulates JNK activation and apoptosis in response to cisplatin. *Oncogene* **19:**5142-52.

Saaristo A, Karpanen T, Alitalo K. 2000. Mechanisms of angiogenesis and their use in the inhibition of tumor growth and metastasis. *Oncogene* **19:** 6122-9.

Sassone-Corsi P, Visvader J, Ferland L, Mellon PL, Verma IM. 1988. Induction of proto-oncogene fos transcription through the adenylate cyclase pathway: characterization of a cAMP-responsive element. *Genes & Development* **2:** 1529-38.

Sassone-Corsi P. 1994. Goals for signal transduction pathways: linking up with transcriptional regulation. *The EMBO Journal* **13:** 4717-28.

Sato TN, Qin Y, Kozak CA, Audus KL. 1993. Tie-1 and tie-2 define another class of putative receptor tyrosine kinase genes expressed in early embryonic vascular system. *Proceedings of the National Academy of Sciences (USA)* **90:** 9355-8.

Sato Y. 2001a. Current understanding of the biology of vascular endothelium. *Cell Structure and Function* **26:** 9-10.

Sato Y. 2001b. Role of ETS family transcription factors in vascular development and angiogenesis. *Cell Structure and Function* **26:** 19-24.

Scanlan MJ, Gordan JD, Williamson B, Stockert E, Bander NH, Jongeneel V, Gure AO, Jager D, Jager E, Knuth A, Chen YT, Old LJ. 1999. Antigens recognized by autologous antibody in patients with renal-cell carcinoma. *International Journal of Cancer* **83:** 456-64.

Schlessinger J. 2000. New roles for Src kinases in control of cell survival and angiogenesis. *Cell* **100:** 293-6.

Schneider A, Fischer A, Weber D, von Ahsen O, Scheek S, Kruger C, Rossner M, Klaussner B, Faucheron N, Kammandel B, Goetz B, Herrmann O, Bach A, Schwaninger M. 2004. Restriction-mediated differential display (RMDD) identifies pip92 as a pro-apoptotic gene product induced during focal cerebral ischemia. *Journal of Cerebral Blood Flow and Metabolism* **24:** 224-36.

Schmittgen TD, Zakrajsek BA. 2000. Effect of experimental treatment on housekeeping gene expression: validation by real-time, quantitative RT-PCR. *Journal of Biochemical and Biophysical Methods* **46:** 69-81.

Schultz J, Milpetz F, Bork P, Ponting CP. 1998. SMART, a simple modular architecture research tool: identification of signaling domains. *Proceedings of the National Academy of Sciences (USA)* **95:** 5857-64.

Shalaby F, Rossant J, Yamaguchi TP, Gertsenstein M, Wu XF, Breitman ML, Schuh AC. 1995. Failure of blood-island formation and vasculogenesis in Flk-1-deficient mice. *Nature* **376:** 62-6.

Shaulsky G, Goldfinger N, Ben-Ze'ev A, Rotter V. 1990. Nuclear accumulation of p53 protein is mediated by several nuclear localization signals and plays a role in tumorigenesis. *Molecular and Cellular Biology* **10:** 6565-77.

Shav-Tal Y, Blechman J, Darzacq X, Montagna C, Dye BT, Patton JG, Singer RH, Zipori D. 2005. Dynamic sorting of nuclear components into distinct nucleolar caps during transcriptional inhibition. *Molecular Biology of the Cell* **16:** 2395-413.

Shibuya M. 2001. Structure and function of VEGF/VEGF-receptor system involved in angiogenesis. *Cell Structure and Function* **26:** 25-35.

Shibuya M, Claesson-Welsh L. 2006. Signal transduction by VEGF receptors in regulation of angiogenesis and lymphangiogenesis. *Experimental Cell Research* **312:** 549-60.

Shopland LS, Johnson CV, Lawrence JB. 2002. Evidence that all SC-35 domains contain mRNAs and that transcripts can be structurally constrained within these domains. *Journal of Structural Biology* **140:** 131-9.

Singh BB, Patel HH, Roepman R, Schick D, Ferreira PA. 1999. The zinc finger cluster domain of RanBP2 is a specific docking site for the nuclear export factor, exportin-1. *The Journal of Biological Chemistry* **274:** 37370-8.

Slack DN, Seternes OM, Gabrielsen M, Keyse SM. 2001. Distinct binding determinants for ERK2/p38alpha and JNK map kinases mediate catalytic activation and substrate selectivity of map kinase phosphatase-1. *The Journal of Biological Chemistry* **276:** 16491-500.

Smith KP, Moen PT, Wydner KL, Coleman JR, Lawrence JB. 1999. Processing of endogenous pre-mRNAs in association with SC-35 domains is gene specific. *The Journal of Cell Biology* **144:** 617-29.

Sohaskey ML, Ferrell JE Jr. 2002. Activation of p42 mitogen-activated protein kinase (MAPK), but not c-Jun NH(2)-terminal kinase, induces phosphorylation and stabilization of MAPK phosphatase XCL100 in Xenopus oocytes. *Molecular Biology of the Cell* **13:** 454-68.

Soncin F, Mattot V, Lionneton F, Spruyt N, Lepretre F, Begue A, Stehelin D. 2003. VE-statin, an endothelial repressor of smooth muscle cell migration. *The EMBO Journal* **22:** 5700-11.

Spector DL, Fu XD, Maniatis T. 1991 Associations between distinct pre-mRNA splicing components and the cell nucleus. *The EMBO Journal* **10:** 3467-81.

Spector DL. 2001. Nuclear domains. *Journal of Cell Science* **114:** 2891-3.

Spector DL. 2003. The dynamics of chromosome organization and gene regulation. *Annual review of biochemistry* **72:** 573-608.

Subramaniam M, Schmidt LJ, Crutchfield CE 3rd, Getz MJ. 1989. Negative regulation of serum-responsive enhancer elements. *Nature* **340:** 64-6.

Sung YJ, Conti J, Currie JR, Brown WT, Denman RB. 2000. RNAs that interact with the fragile X syndrome RNA binding protein FMRP. *Biochemical and Biophysical Research Communications* **275:** 973-80.

Surh YJ, Kundu JK. 2005. Signal transduction network leading to COX-2 induction: a road map in search of cancer chemopreventives. *Archives of Pharmacal Research* **28:** 1-15.

Sutherland LC, Edwards SE, Cable HC, Poirier GG, Miller BA, Cooper CS, Williams GT. 2000. LUCA-15-encoded sequence variants regulate CD95-mediated apoptosis. *Oncogene* **19:** 3774-81.

Sutherland LC, Rintala-Maki ND, White RD, Morin CD. 2005. RNA binding motif (RBM) proteins: a novel family of apoptosis modulators? *Journal of cellular biochemistry* **94:** 5-24.

Suzuma K, Naruse K, Suzuma I, Takahara N, Ueki K, Aiello LP, King GL. 2000. Vascular endothelial growth factor induces expression of connective tissue growth factor via KDR, Flt1, and phosphatidylinositol 3-kinase-akt-dependent pathways in retinal vascular cells. *The Journal of Biological Chemistry* **275:** 40725-31.

Taipale J, Makinen T, Arighi E, Kukk E, Karkkainen M, Alitalo K. 1999. Vascular endothelial growth factor receptor-3. *Current Topics in Microbiology and Immunology* **237:** 85-96.

Takahashi H, Shibuya M. 2005. The vascular endothelial growth factor (VEGF)/VEGF receptor system and its role under physiological and pathological conditions. *Clinical Science* **109:** 227-41.

Thellin O, Zorzi W, Lakaye B, De Borman B, Coumans B, Hennen G, Grisar T, Igout A, Heinen E. 1999. Housekeeping genes as internal standards: use and limits. *Journal of Biotechnology* **75:** 291-5.

Thiselton DL, McDowall J, Brandau O, Ramser J, d'Esposito F, Bhattacharya SS, Ross MT, Hardcastle AJ, Meindl A. 2002. An integrated, functionally annotated gene map of the DXS8026-ELK1 interval on human Xp11.3-Xp11.23: potential hotspot for neurogenetic disorders. *Genomics* **79:** 560-72.

Tichopad A, Pecen L, Pfaffl MW. 2006. Distribution-insensitive cluster analysis in SAS on real-time PCR gene expression data of steadily expressed genes. *Computer Methods and Programs in Biomedicine* **82:** 44-50.

Timmer T, Terpstra P, van den Berg A, Veldhuis PM, Ter Elst A, Voutsinas G, Hulsbeek MM, Draaijers TG, Looman MW, Kok K, Naylor SL, Buys CH. 1999a. A comparison of genomic structures and expression patterns of two closely related flanking genes in a critical lung cancer region at 3p21.3. *European Journal of Human Genetics* **7:** 478-86.

Timmer T, Terpstra P, van den Berg A, Veldhuis PM, Ter Elst A, van der Veen AY, Kok K, Naylor SL, Buys CH. 1999b. An evolutionary rearrangement of the Xp11.3-11.23 region in 3p21.3, a region frequently deleted in a variety of cancers. *Genomics* **60:** 238-40.

Tovey SC, Willars GB. 2004. Single-cell imaging of intracellular Ca2+ and phospholipase C activity reveals that RGS 2, 3, and 4 differentially regulate signaling via the Galphaq/11-linked muscarinic M3 receptor. *Molecular Pharmacology* **66:** 1453-64.

Treisman R. 1995. Journey to the surface of the cell: Fos regulation and the SRE. *The EMBO Journal* **14:** 4905–13.

Trifillis P, Day N, Kiledjian M. 1999. Finding the right RNA: identification of cellular mRNA substrates for RNA-binding proteins. *RNA* **5:** 1071-82.

Tsukahara M, Suemori H, Noguchi S, Ji ZS, Tsunoo H. 2000. Novel nucleolar protein, midnolin, is expressed in the mesencephalon during mouse development. *Gene* **254:** 45-55.

Unoki M, Nakamura Y. 2003. EGR2 induces apoptosis in various cancer cell lines by direct transactivation of BNIP3L and BAK. *Oncogene* **22:** 2172-85.

van den Berg A, Hulsbeek MF, de Jong D, Kok K, Veldhuis PM, Roche J, Buys CH. 1996. Major role for a 3p21 region and lack of involvement of the t(3;8) breakpoint region in the development of renal cell carcinoma suggested by loss of heterozygosity analysis. *Genes, Chromosomes & Cancer* **15:** 64-72.

Vearing CJ, Lackmann M. 2005. "Eph receptor signalling; dimerisation just isn't enough". *Growth Factors* **23:** 67-76.

Veikkola T, Karkkainen M, Claesson-Welsh L, Alitalo K. 2000. Regulation of angiogenesis via vascular endothelial growth factor receptors. *Cancer Research* **60:** 203-12.

von der Kammer H, Demiralay C, Andresen B, Albrecht C, Mayhaus M, Nitsch RM. 2001. Regulation of gene expression by muscarinic acetylcholine receptors. *Biochemical Society Symposium* **67:** 131-40.

Wall R, Briskin M, Carter C, Govan H, Taylor A, Kincade P. 1986. A labile inhibitor blocks immunoglobulin kappa-light-chain-gene transcription in a pre-B leukemic cell line. *Proceedings of the National Academy of Sciences (USA)* **83:** 295-8.

Wei MH, Latif F, Bader S, Kashuba V, Chen JY, Duh FM, Sekido Y, Lee CC, Geil L, Kuzmin I, Zabarovsky E, Klein G, Zbar B, Minna JD, Lerman MI. 1996. Construction of a 600-kilobase cosmid clone contig and generation of a transcriptional map surrounding the lung cancer tumor suppressor gene (TSG) locus on human chromosome 3p21.3: progress toward the isolation of a lung cancer TSG. *Cancer Research* **56:** 1487-92.

Wek RC, Jiang HY, Anthony TG. 2006. Coping with stress: eIF2 kinases and translational control. *Biochemical Society Transactions* **34:** 7-11.

Welch K, Franke J, Kohler M, Macara IG. 1999. RanBP3 contains an unusual nuclear localization signal that is imported preferentially by importin-alpha3. *Molecular and Cellular Biology* **19:** 8400-11.

Welling DB, Lasak JM, Akhmametyeva E, Ghaheri B, Chang LS. 2002. cDNA microarray analysis of vestibular schwannomas. *Otology & Neurotology* **23:** 736-48.

Wilson T, Treisman R. 1988. Removal of poly(A) and consequent degradation of c-fos mRNA facilitated by 3' AU-rich sequences. *Nature* **336:** 396-9.

Wu KK, Liou JY, Cieslik K. 2005. Transcriptional Control of COX-2 via C/EBPbeta. *Arteriosclerosis, Thrombosis, and Vascular Biology* **25:** 679-85.

Wu LW, Mayo LD, Dunbar JD, Kessler KM, Baerwald MR, Jaffe EA, Wang D, Warren RS, Donner DB. 2000. Utilization of distinct signaling pathways by receptors for vascular endothelial cell growth factor and other mitogens in the induction of endothelial cell proliferation. *The Journal of Biological Chemistry* **275:** 5096-103.

Yan C, Boyd DD. 2006. ATF3 Regulates the Stability of p53: A Link to Cancer. *Cell Cycle* **5:** 926-9.

Yancopoulos GD, Davis S, Gale NW, Rudge JS, Wiegand SJ, Holash J. 2000. Vascular-specific growth factors and blood vessel formation. *Nature* **407:** 242-8.

Yeaman C, Grindstaff KK, Wright JR, Nelson WJ. 2001. Sec6/8 complexes on trans-Golgi network and plasma membrane regulate late stages of exocytosis in mammalian cells. *The Journal of Cell Biology* **155:** 593-604.

Yeaman C, Grindstaff KK, Nelson WJ. 2004. Mechanism of recruiting Sec6/8 (exocyst) complex to the apical junctional complex during polarization of epithelial cells. *Journal of Cell Science* **117:** 559-70.

Yu Y, Sato JD. 1999. MAP kinases, phosphatidylinositol 3-kinase, and p70 S6 kinase mediate the mitogenic response of human endothelial cells to vascular endothelial growth factor. *Journal of Cellular Physiology* **178:** 235-46.

Zachary I. 1998. Vascular endothelial growth factor: how it transmits its signal. *Experimental Nephrology* **6:** 480-7.

Zachary I, Gliki G. 2001. Signaling transduction mechanisms mediating biological actions of the vascular endothelial growth factor family. *Cardiovascular Research* **49:** 568-81.

Zacksenhaus E, Bremner R, Phillips RA, Gallie BL. 1993. A bipartite nuclear localization signal in the retinoblastoma gene product and its importance for biological activity. *Molecular and Cellular Biology* **13:** 4588-99.

Zdobnov EM, Apweiler R. 2001. InterProScan--an integration platform for the signature-recognition methods in InterPro. *Bioinformatics* **17:** 847-8.